Environmental and genetic factors controlling the selection of the T cell repertoire.

Patricio Artusa

Department of Physiology, McGill University, Montreal

A thesis submitted to McGill University in partial fulfillment of the requirements of the degree of Doctor of Philosophy.

Table of Contents

Abstract

The immune system is responsible for defense against pathogens and cancer. T cells are at the heart of the mechanisms that protect us by discriminating self from foreign peptides on major histocompatibility molecules (MHC) expressed by antigen presenting cells, enacting downstream effector functions, and forming immunological memory. Altered T cell homeostasis due to aging, chronic disease or environmental factors such as vitamin D deficiency are associated with increased prevalence of infections, cancers, and autoimmune diseases. Many of these are partially attributed to defects in T cell development in the thymus. Thymocytes generate their antigen receptor (T cell receptor, TCR) through expression and recombination of TCR genes. Random nucleotide additions into TCR gene junctions by terminal deoxynucleotidyl transferase (TdT) account for ~95% of TCR diversity. However, a functional consequence due to the loss of TdT activity has not been established. TCRs have variable reactivities for pMHC with some incapable of binding at all and others being overly self-reactive. This is addressed by selection events through interactions with self-pMHC expressing thymic epithelial cells (TECs). Highly self-reactive thymocytes undergo apoptosis in a process called negative selection after strong TCR signaling in interactions with medullary TECs (mTECs) expressing tissue restricted antigens (TRAs) representative of most organs in the body. TRA expression in mTECs is driven by the transcription factor autoimmune regulator (AIRE) and AIRE deficiency in humans results multi-organ autoimmunity. As a result, regulation of thymic development and the links with autoimmunity have undergone rigorous investigation. However, several questions remain regarding thymic development and the establishment of an effective T cell repertoire. Vitamin D deficiency is associated with increased incidence of autoimmune conditions, yet its role in the thymus has been mostly overlooked. TCR reactivity for pMHC heavily influences T cell effector function but its

relationship with TCR sequence is poorly characterized. Both gaps in our knowledge were addressed in this thesis. Active vitamin D signaling in the thymus, including in mTECs, was verified in mice. Importantly, treatment with the biologically active form of vitamin D, 1,25-dihydroxyvitamin D (1,25D), induced Aire and TRA expression. We also found that Aire interacts with the vitamin D receptor (Vdr) and acts as a Vdr coactivator. We addressed the effect of the absence of 1,25D signaling on thymic function using Cyp27b1 knockout (KO) mice, which lack the enzyme necessary to generate 1,25D. KO mice had a 50% reduction in thymic cellularity and reduced splenic T cell numbers. In the thymus of KO mice, there were reduced $Aire^+$ cells, reduced TRA expression, and impaired negative selection of thymocytes. Single cell RNA sequencing of sorted TECs revealed altered TEC differentiation in the absence of 1,25D and a phenotype consistent with premature thymic aging, which is associated with impaired naïve T cell production and autoimmunity. Together, these data provide evidence for the importance of vitamin D in the establishment of a self-tolerant repertoire. Lastly, previous data suggested that TCRs generated in the absence of TdT may be highly self-reactive. Using TdT KO mice, we found that $CD4^+$ T cell differentiation was altered and biased towards follicular helper T cells, which were previously shown to be induced from T cells bearing highly reactive TCRs. This suggests two functions for TdT, to improve pathogen detection and to generate TCRs with lower pMHC reactivity predisposed towards non-Tfh responses. Overall, these findings enhance our understanding of how critical events occurring in the thymus generate an effective, self-tolerant T cell repertoire able to respond to diverse threats by revealing a previously unknown role for vitamin D in T cell development and linking TCR sequences to functional outcomes.

Résumé

Le système immunitaire est responsable de la défense contre les agents pathogènes et le cancer. Les lymphocytes T (LT) nous protègent, en discriminant le soi des peptides étrangers présentés par les molécules du complexe majeur d'histocompatibilité (CMH) exprimées à la surface des cellules présentatrices d'antigène. L'altération de l'homéostasie des LT due au vieillissement, aux maladies chroniques ou à des facteurs environnementaux telle que la carence en vitamine D est associée à une prévalence accrue d'infections, de cancers et de maladies auto-immunes. Les thymocytes génèrent leur récepteur antigénique (récepteur des LT, TCR) par l'expression et la recombinaison des gènes TCR. Les additions aléatoires de nucléotides au niveau des zones de jonctions des gènes TCR par la terminal déoxynucléotidyl transferase (TdT) participent à ~95% de la diversité des TCR. Les TCR ont des réactivités variables pour les complexes pCMH, certains sont incapables de se lier alors que d'autres sont trop auto-réactifs. Ceci est résolu par une sélection d'interactions avec des cellules épithéliales thymiques (TEC) exprimant le peptide du soi-pCMH. Les thymocytes hautement auto-réactifs subissent une apoptose, après une forte signalisation TCR lors d'interactions avec des TEC médullaires (mTEC) exprimant des antigènes spécifiques de tissus périphériques (TRA). L'expression des TRA dans les mTEC est régulée par le facteur de transcription AIRE (autoimmune regulator) et un déficit en AIRE entraîne un syndrome polyendocrinien auto-immun. En conséquence, la régulation du développement thymique et les liens avec l'auto-immunité ont fait l'objet d'investigations rigoureuse. La carence en vitamine D est associée à une incidence accrue de maladies auto-immunes, mais son rôle dans le thymus a été largement négligé. La réactivité du TCR pour le pMCH influence fortement la fonction effectrice des LT, mais sa relation avec la séquence du TCR est mal caractérisée. Ces deux lacunes ont été abordées dans cette thèse.

La signalisation active de la vitamine D dans le thymus et dans les mTEC, a été vérifiée chez la souris. Le traitement avec la forme biologiquement active de la vitamine D, la 1,25-dihydroxyvitamine D (1,25D), induit l'expression de Aire et des TRA. Nous avons constaté que Aire interagit avec le récepteur de la vitamine D et agit comme un co-activateur de celui-ci. En utilisant des souris Cyp27b1 knockout (KO), qui sont dépourvues de l'enzyme nécessaire pour générer la 1,25D nous avons observé une réduction du nombre de cellules dans le thymus de 50% et aussi de LT spléniques, ainsi que des cellules exprimant Aire. De plus, l'expression des TRA diminue et la sélection négative des thymocytes est altérée. Le séquençage d'ARN de cellule unique de TEC a révélé une altération de la différenciation en TEC en l'absence de 1,25D et un phénotype compatible avec un vieillissement thymique prématuré, qui est associé à une altération de la production de cellules T naïves et à une auto-immunité. Ces données mettent en évidence l'importance de la vitamine D dans l'établissement d'un répertoire auto-tolérant. Enfin, des données antérieures suggéraient que les TCR générés en l'absence de TdT pouvaient être hautement auto-réactifs. Avec les souris TdT KO, la différenciation des LT CD4+ était altérée et biaisée en faveur des LT auxiliaires folliculaires, qui ont précédemment été démontré d'être induits à partir de LT porteurs de TCR hautement réactifs. Cela suggère deux fonctions pour la TdT: améliorer la détection des agents pathogènes et générer des TCR avec une réactivité pCMH plus faible prédisposés aux réponses non-Tfh. Pour conclure, ces découvertes améliorent notre compréhension des évènements critiques dans le thymus qui génèrent un répertoire de LT efficaces et auto-tolérants, capable de répondre à diverses menaces, en révélant un nouveau rôle de la vitamine D dans le développement des LT et en reliant les séquences des TCR à des résultats fonctionnels.

Acknowledgments

I wouldn’t be the person or scientist I am today without the help of my friends, family, colleagues, and mentors. I want to thank my supervisor, Dr. White, for being a pleasure to work with and for steadying the ship throughout my Ph.D. studies. Likewise, I appreciate the training I received during my time in Dr. Mandl’s lab.

My studies would not have been the same without the lifelong friendships made throughout my studies. I want to thank Parvaneh Sarmadi, Camille Barbier, Yuki Sato, Mariana Márquez Machorro, and Miguel Romero Sepúlveda for making every day in the lab interesting and fun, and for all the fun times we had outside the lab. Thank you, Camille and Yuki, for proof reading the French abstract! I want to thank the other White lab members as well for their support and help with my project. My numerous other friends made at McGill and Montreal over the years are not forgotten, and all the good times we had over the years will stay with me forever.

As cliché as it sounds, my Ph.D. has been filled with its shares of ups and downs. However, this journey started well before my graduate studies. I would like to think that I am completely original, but my parents being scientists likely guided my interests and career path. Therefore, I want to thank them for exposing the world of science to me and encouraging me. Gracias mami por haberme empujado así pude mejorar y por todo tu apoyo durante los años.

Contribution to Original Knowledge

Vitamin D deficiency is a risk factor for several human autoimmune diseases. However, the benefit of therapeutic vitamin D supplementation is unclear, suggesting that it may be more important prior to the onset of disease. Autoimmunity arises from a lack of T cell tolerance to self, which is first generated in the thymus, an organ that is most active in the early stages of life. We hypothesized that vitamin D signaling contributed to the establishment of central tolerance. Our data contribute to this gap in the field by demonstrating that:

1. Thymic epithelial cells, thymic B cells, and thymic dendritic cells express the vitamin D receptor (Vdr).
2. Cyp27b1 expression is widespread in the thymus, suggesting that the availability of biologically active vitamin D (1,25D) is locally regulated.
3. Vitamin D signaling is active in the thymus, notably in $Aire^{+}$ medullary thymic epithelial cells (mTECs).
4. 1,25D-treatment stimulates the expression of Aire mRNA and protein, and Aire-dependent tissue restricted antigen gene expression.
5. The Vdr and Aire are cofactors, and Aire is a coactivator of Vdr-dependent transcription.
6. mTEC differentiation is skewed towards $CCL21^{+}$ $mTEC^{lo}$ cells, and $Aire^{+}$ mTEC frequencies are vastly reduced in *Cyp27b1* knockout mice.
7. *Cyp27b1* knockout mice have systemic lymphopenia.
8. Thymic involution is accelerated in the absence of 1,25D.

Significance: These data for the first time demonstrate that vitamin D signaling is active in multiple thymic cell types and regulates the differentiation and function of $Aire^{+}$ mTECs, which are essential to tolerize T cells to self. Maintaining vitamin D sufficiency during childhood may be more important than previously thought for reducing autoimmune risk.

Reduced T cell receptor (TCR) repertoire diversity is associated with increased risk of infection, autoimmunity, and certain cancers. TCR diversification occurs in the thymus through two main mechanisms. The first is the somatic recombination of TCR genes. The second is the addition of non-templated nucleotides into the complementarity determining region 3 (CDR3) of the TCR

by terminal deoxynucleotidyl transferase (TdT). Importantly, the CDR3 domain contacts the peptide and confers ligand-specificity. However, general defects in pathogen detection in TdT KO mice, which have ~90% reduced repertoire diversity, have not been observed, suggesting another role for TdT. Data from a previous study suggested that the TdT deficient repertoire was enriched for T cells with higher pMHC reactivity, and TCR reactivity for peptide-MHC influences cell fate decisions during $CD4^+$ T cell differentiation. However, how TCR sequences correlate with ligand specificity and reactivity, and T cell function, is unclear. We addressed this gap in the literature by investigating whether CDR3 sequence diversification by TdT was a mechanism to diversity effector T cell responses. We found that:

1. Germinal center follicular helper (GC-Tfh) T cell differentiation was increased in TdT KO mice in response to genetically diverse pathogens in a TCR-intrinsic manner, indicating it is a general property of the repertoire.
2. T helper 2 (Th2) and Th17 differentiation were altered in TdT KO mice in response to the fungus, *Cryptococcus neoformans*, but not the parasite Heligmosomoides polygyrus, indicating biases in some antigen-specific populations of T cells with germline-encoded TCRs.
3. The increased GC-Tfh cell differentiation in TdT KO mice has both T cell and B cell intrinsic components.
4. Control of viral replication during persistent lymphocytic choriomeningitis virus infection in T cell specific TdT KO chimeras was impaired relative to wildtype and full KO chimeras.

Significance: T cells with TCRs containing short CDR3 sequences are biased towards GC-Tfh differentiation, correlating a structural component of the TCR with T cell effector function.

Author Contributions

All manuscripts were written by **P.A.**, with supervision from J.H.W. All experiments in this thesis, excluding those from chapter 2, figure 3, were conceived by **P.A.** with guidance from J.H.W. (Chapters 2-3), and J.M (Chapter 4).

Chapter 2:

- M.E.L. prepared and cultured thymic slices (making this project possible), and sorted and cultured TECs.
- C.B. did the initial thymic slice qPCR experiments, performed additional qPCR experiments throughout the project, performed pilot coactivation and co-IP experiments, and contributed intellectually throughout the project in terms of planning and data interpretation.
- Importantly, B.M. performed all ChIP assays and related optimization experiments.
- R.S.T. performed co-IP experiments and designed the plasmids.
- S.K. performed the coactivation assay and designed figure 3A.
- A.I. performed bioinformatics to identify the presence of a VDRE in the *Rnase1* gene in a mouse ChIP-seq study performed in gut epithelial cells.
- H.M. provided intellectual guidance and contributed materials throughout the project.
- **P.A**. and J.H.W. designed, planned, and interpreted all the results. J.H.W. recognized the significance of the presence of LXXLL motifs in Aire.
- **P.A.** performed most qPCR experiments, all imaging and flow cytometry experiments, and analysis of published scRNAseq data.

Chapter 3:

- L.N.Y. bred *Cyp27b1* knockout mice and did all tissue harvests, including some *very* early mornings.
- C.B. performed some qPCR experiments, assisted greatly with the setup and sample prep for scRNAseq, and contributed intellectually to experiment design and data interpretation.
- H.D. provided code and expertise for initial scRNAseq analyses with Seurat.
- Y.A.H. helped with imaging experiments and CCL21 image analysis.
- A.I. Prepared DEGs from sequencing data.
- M.E.L. contributed intellectually to experimental design.
- I.R. and D.G. contributed resources for the project.
- H.M. provided intellectual guidance and contributed materials throughout the project.
- **P.A**. and J.H.W. designed, planned, and interpreted all the results.
- **P.A.** performed most imaging and qPCR experiments, all flow cytometry experiments, sample preparation for scRNAseq, and all downstream scRNAseq analyses (RNA velocity, heatmaps, UMAPs, cell cycle analysis, etc.).

Chapter 4:

- C.S. and D.R. helped with *Cryptococcus neoformans* harvests.
- **P.A.** and J.M. designed, planned, and interpreted all the results.
- **P.A.** performed all the experiments.

List of Abbreviations

1,25D–1a,25-dihydroxyvitamin D
25D–25-hydroxyvitamin D
4SP–CD4 single positive
8SP–CD8 single positive
Abs–Antibodies
AIRE–Autoimmune regulator
AMP–Antimicrobial peptide
APC –Antigen presenting cell
APECED–Autoimmune polyendocrinopathy candidiasis ectodermal dystrophy
ASL–Airway surface liquid
Bcl-6–B cell lymphoma 6
BCR–B cell receptor
Brd4–Bromodomain-containing protein
C. neoformans–Cryptococcus neoformans
CAMP–Cathelicidin antimicrobial peptide
CARD–Caspase-activation and recruitment domain
CCL21–Chemokine ligand 21
CCR7–Chemokine receptor 7
CD80–Cluster of differentiation 80
CD–Crohn's disease
CDR3–Complementarity determining region 3
ChIP–Chromatin immunoprecipitation
ChIP-seq–Chromatin immunoprecipitation sequencing
CK5–Cytokeratin 5
CK8–Cytokeratin 8
CLP–Common lymphoid precursor
CMJ–Cortico-medullary junction
CMP–Common myeloid precursor
cTEC–Cortical thymic epithelial cell
CYP24A1–gene encoding vitamin D 24-hydroxylase
CYP27B1–gene encoding 25-hydroxyvitamin D 1α-hydroxylase
CYP2R1–gene encoding vitamin D 25-hydroxylase
DAMP–Damage associated molecular pattern
DBD–DNA-binding domain
DBP–Vitamin D-binding protein
DC–Dendritic cell
DN–Double negative
DP–Double positive
E.coli–Escherichia coli
EAE–Experimental autoimmune encephalomyelitis
ETP–Early T-lineage precursors
FDA–Food and Drug Administration
FDC–Follicular dendritic cell
Fgf21–Fibroblast growth factor 21
Fgf7–Fibroblast growth factor 7 (KGF)
FoxN1–Forkhead box N1
FoxP3–Forkhead box P3
GATA-3–GATA binding protein 3
GC-Germinal center
GC-Tfh–Germinal center follicular helper T
H. polygyrus–Heligmosomoides polygyrus
H3K4–Histone 3 lysine 4
HEK293–Human embryonic kidney 293 cells
HEL–Hen egg lysozyme
HIV–Human immunodeficiency virus
HLA-I/II–Human leukocyte antigen I/II
HSC–Hematopoietic stem cell
Hsp65–Heat shock protein 65
HSV–Herpes simplex virus
IBD–Inflammatory bowel disease
IFNγ–Interferon gamma
Igf1–Insulin-like growth factor 1
ILC–Innate lymphoid cell
Il–Interleukin
IPA–Ingenuity pathway analysis
IRF–Interferon regulatory factor
iTreg–induced regulatory T cell
IU–International units
jTEC–Junctional thymic epithelial cell
KLH–Keyhole limpet hemocyanin
LBD–Ligand binding domain
LCMV–Lymphocytic choriomeningitis virus
Lifr–Leukemia inhibitory factor receptor
LIP–Lymphopenia-induced proliferation

LPS–Lipopolysaccharide
LTβ–Lymphotoxin beta
LTi–Lymphoid tissue inducer
LXXLL–Leucine, any AA, any AA, leucine, leucine
M.Tb–*Mycobacterium tuberculosis*
MAPK–Mitogen-activated protein kinase
MEP–Erythroid/megakaryocytic precursor
MFI-Mean fluorescence intensity
MHC-I/II–Major histocompatibility complex I/II
MPP–Multipotent progenitor
MS–Multiple sclerosis
mTEC–Medullary thymic epithelial cell
mTOR–Mammalian target of rapamycin
NF-κB–Nuclear factor kappa B
NHEJ–Non-homologous end joining
NK–Natural killer
NKT–Natural killer T
NLS–Nuclear localization signal
NOD–Non-obese diabetic
nTreg–Natural regulatory T cell
OVA–Ovalbumin
P.aeruginosa–Pseudomonas aeruginosa
PAMP–Pathogen associated molecular pattern
PBMC–Peripheral blood mononuclear cell
PD-1–Programmed death 1
pDC–Plasmacytoid dendritic cell
Pdpn–Podoplanin
PHD–Plant-homeodomain
pMHC–peptide major histocompatibility complex
PMSF–Phenylmethylsufonyl fluoride
PRR–Pattern recognition receptor
p-TEFb–Positive transcription elongation factor
RAG–Recombination-activating gene
RANK–Receptor activator of nuclear factor of kappa B
RCT–Randomized controlled trial
RFI–Relative fluorescence intensity
RoRγt–Retinoic acid receptor-related orphan receptor gamma t
RSS–Recombination signal sequences
RT–Room temperature
RXR–Retinoid X receptor
SAND–Sp100, Aire-1, NucP41/75, Deaf-1
Sca-1–Stem cells antigen-1
scRNAseq–Single cell RNA sequencing
SLE–Systemic lupus erythematosus
SLO–Secondary lymphoid organ
SNP–Single nucleotide polymorphism
SWM–Sperm whale myoglobin
T1D–Type 1 diabetes
TAC-TEC–Transit amplifying cells-thymic epithelial cells
T-bet–T-box transcription factor 21
Tb–Tuberculosis
TCR–T cell receptor
TdT–Terminal deoxynucleotidyl transferase
TEC–Thymic epithelial cell
Tfh–Follicular helper T
TGF–Transforming growth factor
Th–T helper
TLR–Toll-like receptor
TNFα–Tumor necrosis factor alpha
TRA–Tissue-restricted antigen
Treg–Regulatory T cell
UMAP–Uniform manifold approximation and projection
UVB–Ultraviolet B
VDJ–Variable, diversity, joining
VDRE–Vitamin D response element
VDR–Vitamin D receptor
VSV–Vesicular stomatitis virus
Xid–X-linked immunodeficiency

Chapter 1: Literature Review

Introduction to the immune system

The immune system consists of a complex network of hematopoietic cells that survey the body and eliminate dead and malignant cells, and foreign threats such as viruses, bacteria, and parasites. As evidence for the critical role of the immune system, genetic or acquired immune deficiencies are often fatal if untreated due to recurrent severe infections, cancer, or autoimmunity [1, 2]. The origin of immune cells can be traced back to the bone marrow and hematopoietic stem cell (HSC) precursors. However, prior to formation of the bone marrow during gestation, waves of immune cells are first derived from the yolk sac and fetal liver [3]. The first hematopoietic cells can be detected as early as 3–4 weeks of gestation and are derived from the mesoderm of the yolk sac. Migration of these cells through the circulation to the liver at 5–6 weeks of gestation represents the transition to the next wave of hematopoietic cell output and an increase in the output of nucleated cells. Major immune organs including the bone marrow, thymus, spleen, and lymph nodes are generated from these cells starting at 6–8 weeks of gestation and are done developing by 11–12 weeks of gestation [3].

The process of blood cell development in the bone marrow, or hematopoiesis, involves the progressive differentiation of HSCs (Figure 1)[4]. HSCs are long-lived cells with self-renewal and differentiation potential. *In vitro* differentiation experiments and adoptive transfer of HSCs into recipients with a depleted bone marrow niche decisively support their role as the progenitor population of the immune system [5]. HSCs give rise to a sequence of multipotent progenitor (MPP) cells with varying self-renewal capacities that ultimately give rise to cells committed to erythroid/megakaryocytic (MEP), myeloid (CMP), or lymphoid lineages (CLP) [4]. MPP

commitment to downstream lineages occurs through the sequential loss of lineage differentiation potential starting with the loss of erythroid/megakaryocytic potential, then myeloid potential, finally becoming CLPs [4]. Ultimately, MEPs give rise to erythrocytes and platelets and CMPs give rise to neutrophils, eosinophils, basophils, monocytes, macrophages, and dendritic cells. CLPs develop into natural killer (NK) and B cells in the bone marrow or migrate to the thymus to further differentiate into one of various T cell lineages including innate-like natural killer T (NKT) cells, γδ T cells, and conventional αβ T cells. Together, mature hematopoietic cells coordinate to form the innate and adaptive arms of the immune system, which provide multiple layers of protection to be discussed below.

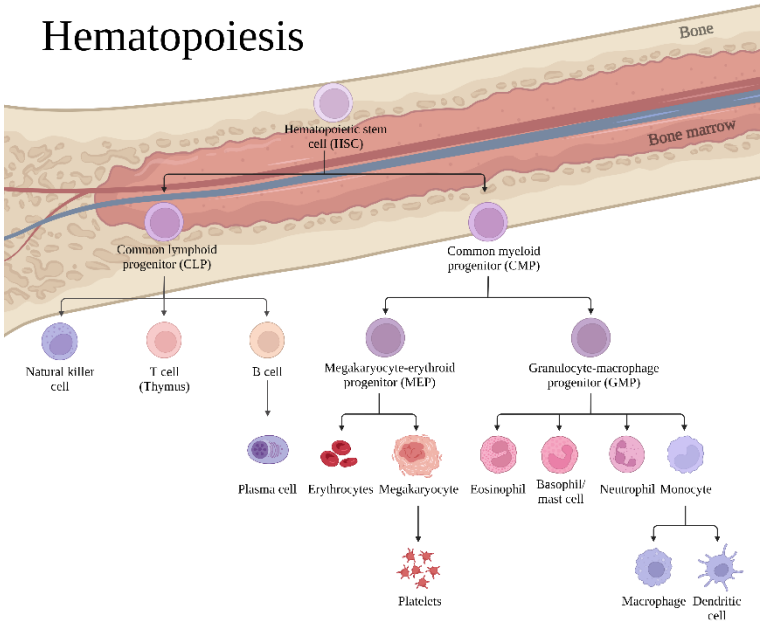

Figure 1. Overview of hematopoiesis. Self-renewing HSCs found in the bone marrow niche give rise to all hematopoietic (blood) cells through progressive differentiation and loss of alternative differentiation potential. Progeny cells can be generally grouped into lymphoid lineages (left), myeloid lineages (right), and red blood cells (middle). *Figure made in BioRender.*

Innate immunity

In conjunction with physical barriers like the skin and mucosal surfaces, the cellular components of the innate immune system act as the first line of defense against invading pathogens [6]. Innate immune cells include monocytes, dendritic cells (DCs), macrophages, neutrophils,

eosinophils, basophils, mast cells, NK cells, and innate lymphoid cells (ILCs). Furthermore, some non-hematopoietic cells such as epithelial cells also have innate immune functions and contribute significantly to host protection [7]. Phagocytes, as the name implies, are cells that engulf microbes and kill them intracellularly. This includes macrophages, neutrophils, and DCs. Macrophages are a long-lived sentinel population established during initial waves of hematopoiesis during embryogenesis and are supported by *de novo* differentiation of circulating monocytes in adults [8]. Neutrophils are a population of short-lived circulating first-responders, which also contain cytolytic granules used to kill extracellular microbes. Eosinophils and mast cells are involved in anti-parasite immune responses and together with basophils initiate allergic responses. ILCs are functionally diverse tissue-resident cells that contribute to immunity via the secretion of cytokines tailored to the threat encountered [9]. Finally, NK cells are important for anti-viral and anti-tumor activity because of direct killing via cytolytic granules and through the production of interferon γ (IFNγ). IFNγ can activate and recruit other immune cells such as macrophages, ILCs, and T and B cells, which are components of the adaptive immune system [10].

DCs are professional antigen presenting cells (APCs) that are critical for stimulating antigen-specific T cell responses. While other immune cells and epithelial cells have APC functionality, DCs are optimized to generate peptides derived from proteins of phagocytosed microbes and present them on the cell surface. Antigens are presented by DCs on major histocompatibility class II (MHC-II) or MHC-I molecules (human leukocyte antigen-I or II in humans, HLA-I/II), and provide other important signals including costimulatory signals and cytokines [6]. Antigen-specific recognition of these peptides by T cells in conjunction with co-stimulation and cytokine signaling stimulates a wave of epitope-specific immunity by T cells. This helps eradicate the threat,

and later forms immunological memory, enabling more efficient pathogen clearance upon future encounters [11].

Pathogen recognition and initiation of inflammatory responses by innate immune cells mainly depends on the detection by pattern recognition receptors (PRRs) of microbial peptides with common motifs known as pathogen associated molecular patterns (PAMPs) [12]. Detection of damage associated molecular patterns (DAMPs) released from dying cells is another mechanism by which innate immune cells sense danger and trigger an inflammatory response. Signaling of membrane-bound or intracellular PRRs triggers a variety of downstream signaling pathways via the recruitment of one or many adapter molecules, resulting in transcriptional changes and the production of pro-inflammatory cytokines. This stimulates effector responses to combat infection, as well as antimicrobial peptide (AMP) production [12].

AMPs are a group of small, secreted proteins that kill or inhibit the growth of viruses, fungi, parasites, and bacteria. AMPs are grouped into membrane acting or non-membrane acting peptides. Non-membrane acting AMPs inhibit microbial growth by acting on protein and nucleic acid synthesis, enzyme activity, or cell wall synthesis [13]. AMPs can also prevent viral entry into host cells by preventing viral attachment and membrane fusion, in addition to destruction of the viral envelope directly and inhibition of viral replication [14, 15]. Many AMPs are positively charged, allowing them to bind and disrupt negatively charged bacterial cell membranes, leading to bacterial lysis [13]. In addition to their direct effects microbial growth, certain AMPs have immunoregulatory functions such as induction of chemokine expression by macrophages [16].

The most extensively studied group of PRRs, called toll-like receptors (TLRs), are a group of membrane-bound proteins that recognize lipids and nucleic acids in addition to PAMPs and DAMPs [12]. Downstream responses to TLR signaling are mediated by mitogen-activated protein

kinases (MAPKs)[17], and transcription factors nuclear factor kappa B (NF-κB) [18], and interferon regulator factors (IRFs) [17]. TLR signaling through NF-κB induces the expression of pro-inflammatory cytokines including interleukin 1 (IL-1), IL-6, and tumor necrosis factor alpha (TNFα). IL-1 has pleiotropic effects, including inducing fever, stimulating lymphocyte and neutrophil proliferation, boosting antigen-specific antibody production, and stimulating the production of IL-6 and TNFα (as well as itself)[19]. Like IL-1, IL-6 and TNFα have numerous functions critical for the host response to acute infection, notably including tissue repair and remodeling after the resolution of infection, and cell signaling leading to apoptosis, respectively [20]. Engagement of TLRs also induces upregulation of chemokines, cytokines that control the migration and recruitment of cells, as well as cytokine receptors, and MHC molecules. TLR signaling collectively results in enhanced phagocytosis of microbes, antigen presentation, and activation and recruitment of lymphocytes to the site of infection [12].

Adaptive immunity

The adaptive immune system is made up of populations of T cells and B cells. After activation, they generate antigen-specific immunity via direct cytotoxic killing, cytokine secretion, or secretion of antibodies. The profile of cytokines produced by a subset of activated T cells is tailored to the type of pathogen encountered, promoting the activation and recruitment of other immune cells beneficial for pathogen elimination [11]. As mentioned above briefly, immunological memory is formed after pathogen clearance. During the contraction of the immune response, specialized memory cells remain and retain the capability to rapidly secrete cytokines or neutralizing antibodies in response to pathogen renewed pathogen threat. Importantly, this is the principle upon which vaccination is based, and therefore represents an essential targetable mechanism for preserving human health [21].

Antigen recognition is exquisitely sensitive and is mediated by binding of unique cell surface T cell receptors (TCR) to 8–12 amino-acid-long peptides bound to MHC-I or MHC-II molecules (pMHC) on the surface of APCs. B cells use their B cell receptors (BCR) to recognize antigen directly, without the need for MHC-I or MHC-II, and produce antibodies in response to activation, which either neutralize pathogens or tag them for destruction by phagocytes or the complement system [22].

T cells can be segregated into two major subsets, distinguished by their expression of the cell surface proteins CD4 and CD8. Naïve T cells are antigen-inexperienced cells lacking the effector functions associated with an active immune response. These cells continuously recirculate through the blood and lymph, and surveil pMHC expressing cells in secondary lymphoid organs (SLOs) for signs of infection [23]. SLOs consist of the spleen and lymph nodes, and naïve T cell survival is crucially dependent on access to these organs. In SLOs, naïve T cells receive survival cues in the form of IL-7, secreted primarily by fibroblastic reticular cells, and through tonic sub-threshold TCR signaling via interactions with self-pMHC expressing DCs [23]. T cells and B cells are segregated into distinct zones within SLOs. Groups of T cells bearing TCRs with the same specificity are called T cell clones. Notably, reductions in naïve T cell numbers (lymphopenia) result in the rapid clonal expansion in SLOs of naïve T cells in a process called lymphopenia induced proliferation (LIP), which is in part due to the decreased competition for access to IL-7 and clonal competition for specific self-pMHC [23]. Interestingly, naïve T cells undergoing LIP adopt a phenotype similar to antigen-experienced cells, and in some cases can acquire effector functions including increased cytokine production and cytotoxicity [24].

Activated $CD4^+$ T cells are also known as helper T (Th) cells and cooperate with innate and adaptive immune cells via the secretion of pro- or anti-inflammatory cytokines, resulting in

mobilization, activation, and modulation of effector functions [25]. $CD8^+$ T cells are a cytotoxic subset that kill tumor cells or cells infected by intracellular pathogens. As mentioned, the flavor of the $CD4^+$ T cell response is tailored to the type of threat the host is facing. This is possible due to the differentiation of $CD4^+$ T cells into distinct Th subsets with unique functions after activation [25]. The signals that regulate Th cell activation and differentiation are finely regulated and include TCR signaling during antigen specific interactions with APCs in combination with costimulation and cytokine signaling. A number of different Th programs have been described, including Th1, Th2, Th17, follicular helper T (Tfh), or induced regulatory T cells (iTreg)[25, 26]. Differentiation of these subsets, maintenance of subset identity, and suppression of alternative programs are regulated by master transcriptional regulators including T-box transcription factor 21 (T-bet, Th1), GATA binding protein 3 (GATA-3, Th2), retinoic acid receptor-related orphan receptor gamma t (RoRγt, Th17), B cell lymphoma 6 (Bcl-6, Tfh), and Forkhead box P3 (FoxP3, Treg).

Th1 cells secrete IFNγ and provide support for anti-intracellular pathogen and anti-tumor immunity [26]. Th2 cells secrete IL-4, IL-5, and IL-13 and mediate anti-helminth immunity, promote tissue repair, and play an important role during allergies [26]. Initial models of Th differentiation described a paradigm of Th1 vs. Th2 cells where IL-4 and IL-2 polarizing signals favored Th2 differentiation whereas sequestration of IL-4 and the addition of IL-12 promoted Th1 differentiation [26]. This was expanded upon by revealing that TCR signal strength also played a role in cell fate decisions. TCR signal strength is a product of TCR avidity for its pMHC ligand in addition to TCR and pMHC cell surface density. Fundamentally, TCR avidity is a term to describe the multimeric reactivity for pMHC, where monomeric pMHC affinity is directly dictated by TCR sequence. Studies analyzing the effects of TCR signal strength found that strong TCR signals favored Th1 differentiation and weak signals favored Th2 differentiation [27].

IL-17 producing Th17 cells were later described as a distinct Th subset with roles in clearing of extracellular pathogens and mucosal immunity. Th17 polarization is mediated by TGFβ signaling in combination with IL-6. The effect of TCR signaling strength in Th17 differentiation remains controversial, however. iTregs are a suppressive population and have a similar differentiation program to Th17 cells, as they also require TGFβ and IL-6. However, their differentiation was shown decisively to be favored by weak TCR signals. Tfh cells are the most recently described subset and are important regulators of B cell maturation during immune responses and antibody production. Tfh cells upregulate CXCR5 during their differentiation, which allows them to migrate to the border of the T-B zone in SLOs. Unlike other Th subsets, Tfh differentiation is more fluid, with less well-defined lineage determining signals [28]. It has been demonstrated that strong TCR signals favor the formation of germinal center (GC) Tfh cells (GC-Tfh), whereas weak persistent TCR signaling generates Tfh cells residing at the T-B border [29]. Furthermore, the dominant cytokine milieu promotes the formation of Tfh cells taking on functional characteristics of other Th subsets.

Distinct effector subsets play essential roles in the immune response to diverse threats, including in the pathogenesis or suppression of autoimmune diseases [30, 31]. Viral clearance and host survival of mice infected with lymphocytic choriomeningitis virus (LCMV) is dependent upon LCMV-triggered reprogramming of virus-specific Th2 cells to a Th1-like phenotype [30]. Mice infected with the intestinal parasite Schistosoma mansoni had severe morbidity and mortality in the absence of a significant Th2 response in CD154 KO mice, despite unaltered Th1 cell frequencies [31]. Therefore, the precise orchestration of T cell differentiation is essential for clearance of pathogens, as well as cancer cells [32]. Strategies to modify effector subsets in humans may be beneficial as therapeutic options. For example, promoting anti-tumor or anti-viral Th1 and

Th17 responses during chronic infections, and suppressing the presence of immunosuppressive Tregs. In contrast, promoting Treg formation or maintenance and inhibiting Th1 and Th17 responses may be beneficial in conditions of autoimmunity.

Stromal crosstalk with the immune system

Stromal cells refers to a heterogenous group non-hematopoietic structural cells present throughout the body. This includes epithelial cells, endothelial cells, fibroblasts, etc. Among their various organ-specific functions, stromal cells contribute to immune responses in multiple capacities. They directly participate to the secretion of cytokines and in the maintenance of immune cell homeostasis [7]. In addition to IL-7 production, stromal cells in SLOs called follicular dendritic cells (FDCs) present antigen to B cells [33]. The coordinated expansion of the stromal network during the immune response is also important, as it creates space for rapidly proliferating B and T cells [34]. In the thymus, stromal cells play an important role in the production of naïve T cells. First, thymic epithelial cells (TECs) are major producers of IL-7, which is needed for thymocyte survival and proliferation. Second, interactions with TECs are responsible for MHC-restriction of thymocytes, such that immature T cells bearing TCRs incapable to bind to pMHC undergo death by neglect. Finally, as will be discussed below, interactions with a subset of TECs are essential for the deletion of many autoreactive T cell clones. Overall, in addition to their innate immune functions, stromal cells are important players in adaptive immune cell maturation, homeostasis, and effector functions.

Vitamin D

Introduction to vitamin D and the immune system

Vitamin D is best known for its role in the prevention and treatment of nutritional rickets in children, which is due to defects in bone growth [35]. The effects of vitamin D on bone growth are indirect with this regard, as it regulates calcium and phosphorus absorption in the gut and therefore the homeostasis of these metabolites. Numerous studies have identified extra-skeletal effects of vitamin D which include in reproduction, skin differentiation, muscle function, and immune system function [35]. The association between vitamin D and the immune system dates to the 1800's, when sunlight was recognized to be beneficial for tuberculosis (TB) patients. The association between vitamin D and TB susceptibility was made decades later, in the 1980's. Since then, vitamin D insufficiency and deficiency has been linked with susceptibility to infections and autoimmune disease by various randomized controlled trials (RCTs) [36-42]. The following subsections will go over vitamin D synthesis and signaling and the known roles of vitamin D signaling in the immune system.

Vitamin D production

Vitamin D can be obtained both from food and from adequate sunlight exposure and exists in two forms, vitamin D_2 and vitamin D_3. While both can cure rickets and are nearly identical in their absorption and mechanisms of action, vitamin D_3 increases the level of the major circulating metabolite of vitamin D, 25-hydroxyvitamin D (25D), more than vitamin D_2 and maintains its levels for a longer time [43]. 25D is used as a read out of vitamin D status, but there is disagreement between groups as to what serum concentration of 25D qualifies as vitamin D deficiency. The Institute of Medicine committee struck by the NIH to review dietary reference intakes for vitamin

D and calcium proposed that blood 25D concentration ≥ 50 nmol/L (20 ng/mL) was considered healthy, 30–50 nmol/L (12–20 ng/mL) as vitamin D insufficiency, and < 30 nmol/L (12 ng/mL) as vitamin D deficient [44]. However, the Institute of Medicine proposals were controversial and the US Endocrine Society subsequently defined vitamin D deficiency as 25D < 30nmol/L (12ng/mL) [45]. The daily recommended intake of vitamin D is 20 µg/day (800 international units, IU) for those 4 years and older, according to the United States Food and Drug Administration (FDA).

Vitamin D_3 can be produced in the skin from 7-dehydrocholesterol when UV-B light (280–320nm) is able to break the B ring, forming pre-vitamin D_3, which isomerizes to vitamin D_3 in a heat-sensitive reaction [43]. Vitamin D_3 is naturally found in animal products, notably fatty fish (14.2–34 µg/serving), whereas vitamin D_2 is present in fungi such as mushrooms (variable, up to 9.2 µg/serving) [43]. Vitamin D_2 is derived from the fungal steroid ergosterol, which is produced by a similar biosynthetic pathway as cholesterol. Vitamin D_2 differs from vitamin D_3 by an extra methyl group and a double bond in the secosteroid side chain. Many countries fortify foods with vitamin D in order to combat vitamin D insufficiency and rickets. For example, in Canada, this includes milk (up to 1µg/100 mL) and margarine (13.25 µg/100g), among other foods [46]. Circulating vitamin D and its metabolites are mainly bound to vitamin D binding protein (DBP).

To become biologically active vitamin D_3 or D_2 must undergo sequential hydroxylation events [43]. 25-hydroxylation of vitamin D to 25D occurs in the liver and is catalyzed primarily by CYP2R1, although other cytochrome P450 enzymes like CYP27A1 also possess 25-hydroxylation activity. 1α hydroxylation of 25D to form 1α, 25-dihydroxyvitamin D_3 (1,25D) is catalyzed by the enzyme encoded by *CYP27B1*. Historically, 1α hydroxylation of 25D was thought to solely occur in the kidney, under the control of calcium regulatory signals such as parathyroid hormone.

However, emerging evidence over the last 40 years has shown that CYP27B1 is expressed in tissues and cells with functions unrelated to calcium homeostasis [47]. The largest group of cells shown to express CYP27B1 are epithelial cells [47]. Interestingly, epidermal keratinocytes express more CYP27B1 than kidney cells and could in theory account for all circulating 1,25D [47]. However, most, or all of 1,25D produced in the epidermis signals and is metabolized locally suggesting that CYP27B1 expression in the epidermis is necessary for local demand of 1,25D [48]. Other extra-renal sites of CYP27B1 expression include bone, placenta, endocrine glands, brain, liver, endothelia, and various cells of the immune system including macrophages, monocytes, DCs, T cells and B cells [47]. Importantly, CYP27B1 expression in immune cells is independent of calcium homeostatic inputs [49]. Notably, *CYP27B1* is induced downstream of signaling through PRRs and by cytokines produced by T cells.

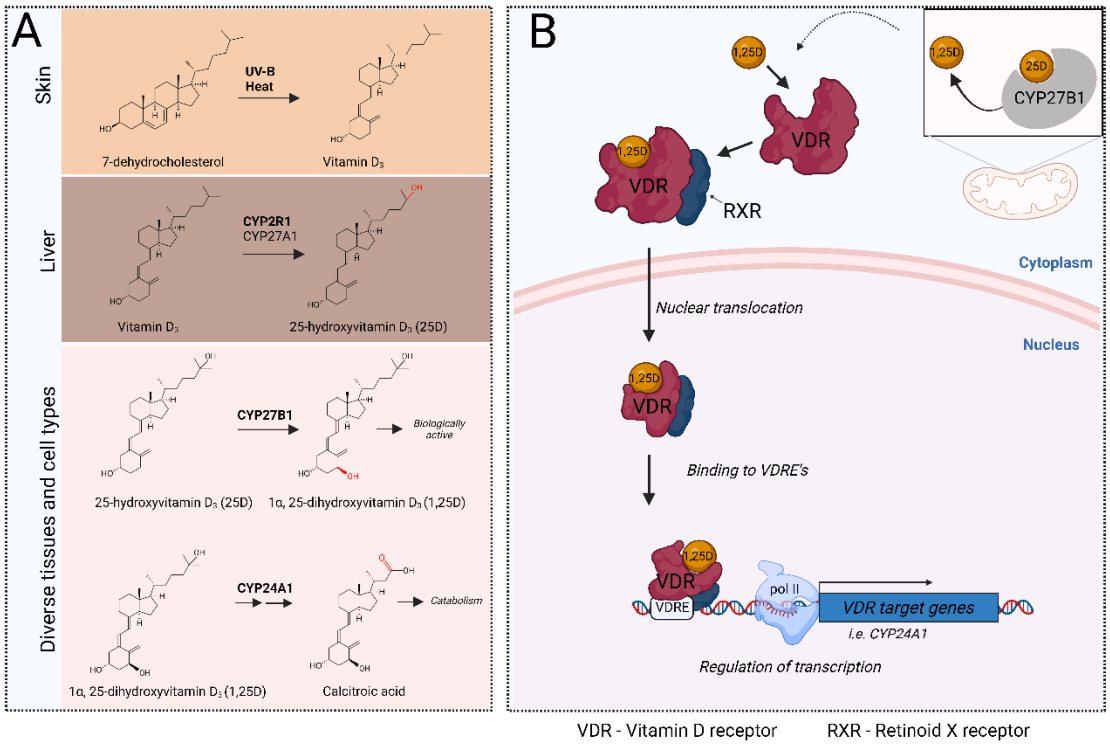

Figure 2: Overview of vitamin D biosynthesis and signaling. A. Sufficient UV-B radiation induces breakage of the B-ring of cholesterol precursor 7-dehydrocholesterol, which is found in the skin. The cleavage product isomerizes to vitamin D_3 in a heat sensitive manner to produce vitamin D3.

Vitamin D_3 is first 25-hydroxylated largely in the liver by 25-hydroxylase enzymes (CYP2R1 or CYP27A1) to generate 25-hydroxyvitamin D_3 (25D), the major circulating metabolite of vitamin D. 25D is 1a hydroxylated in a controlled manner in the kidney or other tissues by the unique 1a-hydroxylase enzyme (CYP27B1) to generate the biologically active form of vitamin D, 1a-25-dihydroxyvitamin D_3 (1,25D). Catabolism of 25D and 1,25D is initiated by 24-hydroxylation catalyzed by CYP24A1, whose gene expression is induced by 1,25D signaling in a negative feedback loop. **B.** Intracrine or blood-derived 1,25D binds to the vitamin D receptor (VDR), triggering association with retinoid X receptors (RXRs) and nuclear translocation, followed by binding to vitamin D response elements (VDRE) to regulate gene transcription. *Figure made in BioRender.*

Activated macrophages are a major source of circulating 1,25D in the context of sarcoidosis, which in extreme cases can lead to hypercalcemia [50]. Sarcoidosis a highly inflammatory disease, in which CYP27B1 activity is regulated by inflammatory and pathogen derived signals including lipopolysaccharide (LPS), IFNγ, and TNFα, but not calcium-related signals [51]. DCs and T cells upregulate CYP27B1 when activated, and 1,25D signaling in these cell types induces a more tolerogenic T cell phenotype [52]. Therefore, the tight regulation of local 1,25D production in immune cells appears to be an important mechanism to modify the immune response. The function of locally produced 1,25D is likely non-redundant with circulating kidney-derived 1,25D. One study examined IgE responses to OVA challenge in global *Cyp27b1* KO mice, and in strains lacking *Cyp27b1* in either T or B cells. The authors found that OVA-specific IgE was elevated in global and T cell-specific *Cyp27b1* KO mice relative to controls, but not in B cell-specific KO mice [53]. Therefore, local 1,25D production by T cells appears to be important to suppress hyper IgE responses in this system.

Vitamin D signaling

Many of the physiological effects of vitamin D signaling can be understood through its capacity to regulate gene transcription. The genomic actions of vitamin D signaling are mediated through binding of 1,25D to the vitamin D receptor (VDR) [43]. The VDR is a ligand-regulated transcription factor and a member of the nuclear receptor superfamily. It is most highly expressed in metabolic tissues but can be found in lower amounts in nearly all human tissues [54], consistent with the pleiotropic functions of vitamin D signaling. The VDR contains a DNA binding domain (DBD) that allows it to contact specific sequences of DNA and a ligand binding domain (LBD)

that is critical for 1,25D-regulated gene transcription [55]. Despite being a transcription factor, the VDR is found in the cytoplasm in addition to the nucleus. Photobleaching experiments using VDR-GFP fusion proteins demonstrated that both liganded and unliganded VDR proteins constantly shuttle between the nucleus and cytoplasm, and that introduction of 1,25D vastly increased the nuclear transport of the VDR while slowing export [56]. Once in the nucleus, the DBD of the VDR recognizes specific direct repeats of hexameric sequences called vitamin D response elements (VDREs). Its affinity as a monomer for these motifs is insufficient for the formation of a stable protein-DNA complex [55]. This is resolved by dimerization of the VDR with related retinoid x receptors (RXR's). Together, VDR/RXR complexes bind stably to VDRE's. Gene expression is then regulated by 1,25D-dependent recruitment of co-activator complexes that are essential for hormone-dependent transactivation of adjacent target genes. The hormone dependence of this recruitment occurs because 1,25D binding induces a conformational change in the largely α-helical receptor LBD, leading to the formation of a hydrophobic cleft on the LBD surface [57]. This cleft is recognized by specific hydrophobic LXXLL motifs (where L is leucine) on coactivators. One of the most strongly induced VDR target gene is *CYP24A1*, which encodes the enzyme (24-hydroxylase, CYP24A1) responsible for negative regulation of vitamin D signaling [43]. CYP24A1 catalyzes the hydroxylation of 1,25D (and 25D) at the 24 position of the cholesterol side chain that strongly reduces affinity for the VDR and initiates the catabolic degradation of the sidechain. CYP24A1 expression is exquisitely sensitive to the presence of 1,25D, making it an excellent readout of active vitamin D signaling.

While 1,25D primarily signals through the VDR, some VDR-independent activity of 1,25D has been reported, such as inhibition of nitric oxide production in cultured Vdr KO osteoblasts [58]. Additionally, the Vdr can regulate gene expression in the absence of 1,25D [59]. Complete

inactivation of the Vdr leads to rickets and alopecia [60]. Notably, whereas mutations in *CYP27B1* cause rickets, alopecia is absent in patients lacking 1α-hydroxylase activity [60]. Intriguingly, people with certain mutations in the *VDR* develop alopecia without any rachitic symptoms [61, 62]. These mutations do not affect ligand binding, but do disrupt the 1,25D-independent association of the VDR with the so-called hairless transcriptional repressor, whose regulation is required for normal hair cycling [63]. In this regard, both *Vdr* and *Cyp27b1* mouse KO strains are models of rickets arising from loss of vitamin D signaling. However, like humans, only the *Vdr* KO strain presents with alopecia [64]. In addition, chromatin immunoprecipitation followed by high-throughput sequencing (ChIP-seq) studies investigating the genome-wide binding of the receptor found considerable Vdr bound to DNA in the absence of 1,25D, depending on the cell type studied, again supporting a role for 1,25D-independent activity [65]. As expected though, introduction of 1,25D greatly increased the number of distinct Vdr binding sites by 2–10-fold, again depending on the cell type [65]. The precise mechanisms of such 1,25D-independent function of the VDR are still under investigation.

Vitamin D deficiency

A meta-analysis of global vitamin D status from 2000 to 2022 of 7.9 million pooled participants found that 15.7% of people had serum concentrations of 25D lower than 30 nmol/L and would be considered as severely vitamin D deficient [66]. Furthermore, among various other factors associated with prevalence of vitamin D deficiency, people living in higher latitudes were notably more at risk of becoming vitamin D deficient. UV-B intensity affects the rate of vitamin D_3 formation in the skin, therefore, insufficient sunlight during the winter months of many countries (a period known as vitamin D winter) leads to insufficient cutaneous vitamin D synthesis [67]. Regions, such as northern Finland, are in vitamin D winter year-round, whereas regions near

the equator have sufficient surface UV-B penetration year-round. However, conservative dress, sun avoidance and darker skin tones often found in such regions can also prevent the acquisition of significant vitamin D from sun exposure. The consequences of vitamin D deficiency are widespread and the skeletal effects, including rickets in children and osteomalacia (soft bone) in adults, are well documented [35].

The extra-skeletal consequences of vitamin D deficiency are implicated in psoriasis, skin cancer, muscle strength, inflammatory bowel disease, and all major autoimmune diseases [35]. Intriguingly, the incidence of autoimmune diseases such as type 1 diabetes (T1D) and multiple sclerosis (MS) are associated with latitude [68]. A study of white army recruits in the United States (US) found that low vitamin D status (25D < 50 nmol/L) at the time of recruitment resulted in an almost twofold increased risk of later onset of MS [69]. Maternal vitamin D deficiency (25D < 30 nmol/L) in Finnish women was associated with a 1.9-fold increased risk of developing MS in the offspring [70]. Furthermore, genetic variants predisposing to lower circulating 25D levels were also correlated with increased MS risk in multiple studies [71]. Mutations in the coding region of *CYP2R1* were associated with decreased circulating 25D levels and a 1.4-fold increased risk of developing MS [72]. A meta-analysis of US and Swedish cohort studies analyzing the effect of single nucleotide polymorphisms (SNPs) associated with decreased 25D levels on MS risk also concluded that decreased 25D was a risk factor for MS [42].

Similar studies have been performed analyzing T1D risk in various populations. In a study identifying 310 T1D cases (613 controls), non-Hispanic US military personnel, but not Hispanic or non-Hispanic black personnel, with 25D levels > 100nmol/L had a 44% lower risk of T1D whereas those in the bottom 20% of 25D status had the highest risk of developing T1D [73]. A series of retrospective studies found that vitamin D supplementation in the first year of life reduced

the risk of developing T1D later in life. A large study tracking a cohort of 10,366 children born in northern Finland over the course of 30 years found that vitamin D supplementation was associated with decreased incidence of T1D [74]. Specifically, the risk for regular versus no supplementation was 0.12, and children who took the recommended dose (2,000 IU per day) had a relative risk of 0.22 compared to those that received less than the recommended amount. Children suspected of having rickets had a 3.0 relative risk of developing T1D. Importantly, many studies can be difficult to interpret due to sun exposure in control cohorts. However, this was not a confounding factor in this study due to year-round vitamin D winter in northern Finland.

Despite the availability of data suggesting that vitamin D sufficiency should prevent autoimmune diseases, the therapeutic benefit of vitamin D supplementation remains inconclusive due to intervention trials being limited in power or placebo wings being poorly controlled due to variable sunlight exposure. However, clinical studies, such as the Finnish cohort study above, analyzing the benefit of supplementation early in life tend to support the notion that vitamin D status during this critical period is an important determinant of the risk of future onset of autoimmunity.

Vitamin D signaling in immune cells

The effects of vitamin D signaling in the immune system have been studied extensively. These range from stimulation of antibacterial and antiviral immunity to suppression of autoimmune adaptive immune responses [35]. Observations that airway surface liquid (ASL) antimicrobial activity varied depending on the season (higher in the summer versus winter months) was consistent with a role for vitamin D in antimicrobial responses [75]. Strikingly, vitamin D supplementation masked the seasonal variability in the antimicrobial activity of ASL. Furthermore, results from a RCT demonstrated that vitamin D supplementation for 90 days increased the

antimicrobial activity of ASL [75]. This activity was ascribed to the production of the antimicrobial peptide CAMP (cathelicidin antimicrobial peptide), as antibody blockade of CAMP abrogated the antimicrobial efficacy of ASL [76]. AMPs can be broadly classified into cathelicidins and defensins. Importantly, VDRE's adjacent to the transcription start site of *CAMP* and *DEFB2/DEFB4/HBD2* (β-defensin 2) have been described [77, 78]. In neutrophils, CAMP was strongly inducible by 1,25D, whereas 1,25D stimulated IL-1β-induced *DEFB2* expression [78]. Furthermore, a small RCT of vitamin D supplementation in 27 Crohn's Disease (CD) patients found that circulating levels of CAMP were significantly increased in the treatment group versus placebo [79]. Stromal cells contribute to antimicrobial responses, and 1,25D stimulated antimicrobial activity in cultured human, but not mouse, epithelial cells against *Escherichia coli* (E. coli), and the lung pathogen *Pseudomonas aeruginosa* (P. aeruginosa)[80].

Regulation of antimicrobial responses by 1,25D is multi-layered and includes stimulation of PRR expression and autophagy, in addition to induced antimicrobial peptide production. Stimulation of monocytic cells and keratinocytes with 1,25D strongly induced *CD14* gene expression, the co-receptor of TLR4 [81]. It also induced the expression of the gene encoding the PRR NOD2/CARD15, supporting a role for 1,25D in barrier immunity [82]. Autophagy is a key process of immunity that bridges the innate and adaptive immune system. Its roles include helping to clear intracellular pathogens by enhancing antigen presentation and regulation of cytokine production [83]. Vitamin D can activate autophagy in numerous cell types including keratinocytes, hepatocytes, and endothelial cells in response to cellular damage and oxidative stress [84]. In the immune system, 1,25D induces autophagy in macrophages by inhibiting branched chain amino acid-dependent activation of the regulatory kinase mammalian target of rapamycin (mTOR)[85], which is a key inhibitor of autophagy. Vitamin D also plays an important function in the immune

system by modulating cytokine production in both innate and adaptive immune cells. In macrophages, 1,25D stimulates the production of IL-1β and chemokines including CCL3, CCL4, CCL8, IL-8/CXCL8 [86]. Co-culture experiments of *Mycobacterium tuberculosis (M.tb)*-infected macrophages with primary human airway epithelial cells demonstrated that 1,25D-dependent induction of IL-1β enhanced the survival of infected macrophages [49]. These data collectively suggest that vitamin D signaling positively regulates anti-microbial responses of first responders to infection, which includes macrophages, neutrophils, and stromal cells.

However, with the exception of the pro-inflammatory anti-microbial responses discussed here, vitamin D generally functions to dampen the immune response. In *M.tb*.-infected human peripheral blood mononuclear cells (PBMCs), 1,25D suppressed the production of pro-inflammatory cytokines IL-6, TNFα, and IFNγ in a dose-dependent manner [87]. LPS-induced IL-6 and TNFα production in human and murine monocytes/macrophages was also suppressed by 1,25D [88]. In NK cells, 1,25D in combination with dexamethasone enhanced the expression IL-10 and induced a regulatory phenotype [89]. Intracrine production of 1,25D by DCs induces a tolerogenic phenotype, characterized by IL-10 production, decreased IL-12 and IL-23 production, and decreased expression of MHC-II and co-stimulatory molecules including CD40, CD83, and CD86 [90]. This, in turn, has significant effects on lymphocyte phenotypes including reduction of B cell proliferation and antibody production and altered Th differentiation away from Th1 and Th17 phenotypes and towards Th2 and Treg subtypes. Aside from the regulation of Th differentiation imposed by DCs, 1,25D signaling in T cells also intrinsically affects their phenotypes.

TCR triggering with co-stimulation results in upregulation of the VDR [91]. In humans, 1,25D signaling through the VDR results in enhanced expression of the VDRE containing gene

PLCG1, which encodes PLC-γ1, a central component of the TCR signaling cascade [92]. Therefore, 1,25D signaling in human cells contributes to T cell priming in addition to its other effects. IL-2 is fundamental to the differentiation and proliferation of both $CD4^+$ and $CD8^+$ T cells. Importantly, 1,25D signaling through the VDR attenuates *IL2* transcription and may function as a part of a negative feedback loop in cases of excessive T cell activation [93, 94]. The role of vitamin D signaling in Th differentiation is well documented. Th2 cells contribute to allergic hypersensitivity and vitamin D deficiency is a risk factor of asthma, allergic rhinitis, and wheezing [95]. In a mouse model of allergic airway hypersensitivity to chicken egg ovalbumin (OVA), mice fed a vitamin D deficient diet had increased T cell dependent antibody titers associated with enhanced Th2 responses [96]. $CD4^+$ T cells cultured in the presence of Th17 inducing cytokines (TGF-β1 and IL-6) and TCR stimulation resulted in double the amount of Th17 cells in Vdr KO versus wild-type cultures [97]. Conversely, treatment with 100nM 1,25D reduced the frequency of Th17 cells by half. These data are supported by results from an *in vivo* model of inflammatory bowel disease (IBD) where donor T cells adoptively transferred into recombination-activating gene (RAG) KO recipient mice, which lack B and T cells, initiate inflammation in the gut due to pathogenic T cell responses. Transfer of naïve Vdr KO or wildtype T cells to RAG KO mice resulted in enhanced frequencies of Th17 cells in the recipients of Vdr KO cells and worsened IBD severity [97]. The signals that drive Th17 and iTreg differentiation overlap in part, thereby often leading to concomitant analysis of this differentiation axis. While the frequency of naturally occurring Tregs in the circulation or in SLOs is unaltered in Vdr KO versus wild-type mice, polarization of Vdr KO iTregs using TGF-β1 and TCR stimulation is significantly impaired relative to controls. Therefore, reduced Treg generation in the context of vitamin D deficiency is likely to negatively impact the pathogenesis of the disease. 1,25D treatment has been demonstrated

to slow the progression of experimental autoimmune encephalomyelitis (EAE), a mouse model of MS that results in ascending paralysis [98]. Notably, the pathogenesis of EAE is driven by inappropriate Th17 and Th1 cells responses to injected myelin basic protein, which is expressed by neuronal cells and is the target of the ensuing autoimmune attack. Selective deletion of the Vdr in T cells abrogated the benefit of 1,25D in EAE pathogenesis [99]. The benefit of 1,25D during EAE may be due to its effects on both Th1 and Th17 differentiation and function, since 1,25D was shown to inhibit Th1 differentiation and IFNγ production [100, 101].

Investigation of the relationships between vitamin D signaling and autoimmunity are not limited to models of MS. Dietary intake of 1,25D in mice prevented or abrogated symptoms associated with two models of murine arthritis [102]. Mutation of the *Fas* gene, which regulates apoptosis in many cells including T cells, in the mouse strain MRL results in uncontrolled lymphoproliferation and autoimmunity, mimicking human systemic lupus erythematosus (SLE)[103]. Dietary intake of 1,25D in combination with intraperitoneal injection of 1,25D every other day inhibited the formation of dermatologic lesions, necrosis of the ear, and scab formation in MRL mice [104]. Non obese diabetic (NOD) mice are the most used model of human type 1 diabetes (T1D) due to their genetic predisposition to spontaneously develop T1D [105]. Results of studies examining the role of vitamin D in autoimmune diabetes development in NOD mice are conflicting. An early study in 1994 found that the incidence of disease in 1,25D-treated female NOD mice was 8% compared to 56% in the control group [106]. Another study investigating the effect of vitamin D deficiency in NOD mice found that 35% of male and 66% of female mice that were fed a no vitamin D diet for the first 100 days of life were diabetic after 250 days, compared to 15% and 45% of control mice, respectively [107]. Surprisingly, Vdr-deficient NOD mice developed diabetes at the same rate as control NOD mice [108]. More investigation of this complex

phenotype is thus merited, potentially into the 1,25D-extrinsic role of the Vdr in the onset and pathogenesis of autoimmune diabetes. It is important to note that vitamin D signaling in pancreatic beta cells, the target of autoreactive cells in T1D, is important for beta cell proliferation and survival [109]. This may further add to the complexity of the phenotypes observed in studies of vitamin D in models of diabetes. Collectively, impaired 1,25D signaling is implicated in the pathogenesis of several autoinflammatory models of disease, mirroring clinical observations made in humans. However, the therapeutic benefit and optimal window of 1,25D supplementation in the treatment and prevention of human autoimmune diseases is still a topic of investigation.

Introduction to thymic development

The thymus is a bi-lobed organ with outer cortical regions and inner medullary regions resting below the sternum. It is the site of naïve conventional T cell, invariant natural killer T cell (iNKT), and γδ T cell production. Its functions are essential for protective immunity as shown by defects in thymic organogenesis, such as through mutations the master regulator of thymic epithelial cell generation, FoxN1, which result in severe combined immunodeficiency in humans and murine KO models [110]. Furthermore, more subtle defects in thymic processes range in consequences from overt autoimmunity including T1D and MS, to increased risk of cancers and infections. T cell effector functions depend on the specificity of their TCR to recognize peptides bound on MHC molecules.

Importantly, conventional T cells generate their (αβ) TCRs and undergo MHC restriction in the thymus. This is coupled with selection events through interactions with multiple levels of thymic APCs that filter out thymocytes bearing undesirable TCRs. Thymocyte development is supported by a network of phenotypically diverse stromal and hematopoietic cells that provide essential instructions through chemotactic cues and direct interactions regulating thymocyte

selection and survival. These include epithelial cells, fibroblasts, DCs, macrophages, and tissue resident B cells.

Conventional T cell development

Circulating CLPs generated in the bone marrow enter the thymus through blood vessels near the cortico-medullary junction (CMJ) and migrate to the cortex where they undergo T cell lineage commitment through the progressive loss of potential towards other lineages including γδ T cell, iNKT cells, macrophages, DCs, and even granulocytes. B cell potential has been shown to be lost even prior to entering the thymus [111]. While CLPs initially retain the potential to develop into multiple cell types, the microenvironment of the thymus strongly favors the production of conventional T cells, largely due to notch signaling following engagement of delta-like ligand 4 expressed by cTECs [112, 113]. Thymocyte development can be broadly segregated into four stages, defined by the expression of CD4 and CD8 molecules ($CD4^-$ $CD8^-$ double negative (DN), $CD4^+$ $CD8^+$ double positive (DP), $CD4^+$ $CD8^-$ single positive (4SP), and $CD4^-$ $CD8^+$ single positive (8SP)). DN thymocytes are further segregated into DN1–4 categories and lose non-T cell lineage commitment potential by the DN3 stage, where TCR gene expression and other important transcription factors necessary for T cell development are turned on [114].

The remainder of thymocyte development is guided by events that foster the production of T cells bearing a functional TCR. The TCR on conventional T cells is a heterodimer made up of TCR β and TCR α chains (αβ TCR). Individual TCR chains are encoded by an arrangement of constant (C) regions and variable (V), diversity (D), and joining (J) TCR genes that undergo somatic recombination in a process known as V(D)J recombination [115]. Notably, TCRα chains are encoded only by V-J gene segments (70 and 61 gene segments for humans) whereas TCRβ chains are encoded by V-D-J genes (52, 2, and 13 gene segments for humans) [116]. Therefore,

V(D)J recombination is an important source of germline encoded receptor diversity. V(D)J recombination is initiated at V-J junctions by nicks in chromosomal DNA, catalyzed by RAG recombinase (RAG), at specific recombination signal sequences (RSS) that flank each V, D, and J gene segment [117]. Hairpins are formed at these double stranded breaks, which are opened by the Artemis/DNA-PKcs to generate palindromic sequences. At this stage, the DNA polymerase terminal deoxynucleotidyl transferase (TdT) adds up to 5 non-templated nucleotides (N-region nucleotides) to each 3'-OH end [118]. Unpaired nucleotides are then trimmed, and template dependent polymerases fill in missing nucleotides before DNA repair by non-homologous end joining (NHEJ)[119]. Then, V-DJ recombination proceeds after the formation of DJ segments. Amazingly, the estimated potential diversity yielded by V(D)J recombination exceeds 10^{15} unique receptors where TdT is estimated to generate 90–95% of this diversity [120]. After TCRβ chain recombination, DN thymocytes express an invariant α chain to form the pre-TCR complex. They then undergo an important developmental checkpoint after cell surface expression of the pre-TCR in a process called β selection [121]. Successful signaling through the pre-TCR complex ensures αβ T cell lineage commitment, restricts further *Tcrb* gene rearrangement, and initiates a proliferative burst [121].

At this point, DN4 thymocytes upregulate CD4 and CD8 to become DP thymocytes and the pre-TCR is replaced by mature αβ TCR molecules after TCRα V-J recombination. DP thymocytes then face a series of critical checkpoints based on reactivity towards self-pMHC complexes expressed on thymic APCs. Unlike B cells, which recognize native antigen, T cells only recognize antigen when bound to MHC-I or MHC-II molecules. The process of MHC-restriction occurs during a stage of thymic development known as positive selection [113]. During positive selection, DP thymocytes interact with cortical thymic epithelial cells (cTECs) presenting

self-peptides on MHC-I and MHC-II molecules. Interestingly, cTECs are uniquely poised to support positive selection due to their ability to generate 'private' positively selecting ligands through unconventional proteasomal processing machinery termed the thymoproteasome [122]. The majority of thymocytes bear TCRs with insufficient reactivity to recognize pMHC expressed on cTECs, resulting in thymocyte apoptosis, also called death by neglect. Another important maturational step is the commitment to either the $CD4^+$ or $CD8^+$ lineage. Multiple models have been proposed to explain the signaling events that distinguish $CD4^+$ and $CD8^+$ T cell lineage commitment. The current most accepted model posits that DP thymocytes downregulate CD8 to 'audition' for the CD4 lineage and only switch to $CD8^+$ $CD4^-$ expression if CD4-dependent TCR signaling is lost [123]. Positively selected thymocytes upregulate CCR7 to follow CCL21 and CCL19 chemotactic cues secreted in the thymic medulla, where they undergo further selection events. In the medulla, thymocytes are culled based on their reactivity for self-pMHC expressed by medullary thymic epithelial cells (mTECs), DCs, and resident thymic B cells [114]. Cells with high self-pMHC reactivity undergo apoptosis in a process called negative selection and those with intermediate reactivity are diverted into the regulatory T cell (Treg) lineage. Therefore, thymocytes with low to intermediate TCR reactivity ultimately survive to become mature 4SP or 8SP thymocytes and after undergoing final maturation steps leave the thymus to circulate in the periphery.

Negative selection and autoimmune regulator (AIRE)

The result of dysregulation of negative selection is a combination of autoimmunity and autoinflammatory disorders [124, 125]. Effective negative selection of autoreactive thymocytes is critically dependent on the presentation of essentially an entire body worth of self-antigens so as to not allow specific clones to escape to the periphery. Therefore, the cells of the thymus must take

on the incredible task of curating and presenting these tissue restricted antigen (TRA). Part of this is resolved by the shuttling of peripheral antigen to the thymus by plasmacytoid DCs (pDCs)[126]. However, the majority of TRA are expressed ectopically in the thymus largely due to the action of the transcription factor autoimmune regulator (AIRE)[127]. AIRE is highly expressed by mTECs, but more recent studies have revealed expression in thymic B cells [128]. In support of its essential role, certain mutations in *AIRE* in humans results in autoimmune polyendocrinopathy candidiasis ectodermal dystrophy (APECED), which is characterized by multi organ autoimmunity and recurrent fungal infections [129]. In addition, numerous mouse models have demonstrated the essential role AIRE and AIRE-dependent TRA expression plays in the prevention of autoimmunity. Aire KO mice, first generated in 2002, were found to have multi organ autoimmune infiltrates [130]. TEC specific deletion of *AIRE*-dependent TRAs such as *Ins2* would rapidly result in pancreas specific autoimmunity [127]. The revelation of the important role of AIRE prompted countless studies analyzing its mechanism of action, how it is regulated, and which cells are precursors of $AIRE^{+}$ mTECs.

AIRE contains a caspase-activation and recruitment domain (CARD), a nuclear localization signal (NLS), a SAND domain (named after a range of proteins **S**p100, **A**ire-1, **N**ucP41/75, and **D**eaf-1) for binding DNA phosphate groups, and two plant-homeodomain (PHD) fingers (Figure 3)[127]. Notably, the SAND domain of AIRE lacks important DNA-binding residues (KDWK motif), suggesting that it is recruited to DNA by its interaction partners [131]. Furthermore, the PHD1 finger of AIRE binds to unmethylated H3K4, which generally marks transcriptionally repressed loci, suggesting that AIRE may be recruited to regions with inactive chromatin to exert its effects [132]. Furthermore, TRA expression is not completely abolished in *Aire* KO mice but is variably reduced for *Aire*-dependent genes. This suggests that AIRE may

serve to amplify gene expression rather than to induce it. Several additional lines of evidence suggest that AIRE does not appear to be a classical transcription factor with a site-specific binding domain. AIRE influences the expression of thousands of genes with distinct modes of regulation and controls the expression of large numbers of genes when transfected into numerous different cell types [133].

TRA expression in mTECs at the population level is stochastic and individual TRAs are only detected in 1–3% of mTECs at a given time, demonstrating a sort of 'randomness' to TRA expression [134]. In addition, TRA transcription in TECs depends on distinct cofactors and initiation from transcriptional start sites that are distinct from those used in peripheral expression[135]. AIRE appears to exist in multimolecular complexes with proteins involved in initiation and post-initiation transcriptional events in regions dense with AIRE target genes [127]. This explains why AIRE staining appears punctate by immunofluorescent microscopy [136]. Based on all this evidence, it has been postulated that other factors may serve to recruit AIRE to TRA genes [133]. Both human and murine AIRE contains four LXXLL motifs, where L stands for leucine and X for any amino acid [127, 137]. This motif is part of an amphipathic α-helix, which binds to hydrophobic clefts formed in agonist-bound nuclear receptors. Therefore, a potential mechanism of AIRE recruitment may be through interactions with nuclear receptors that recruit it to target genes, a hypothesis investigated below.

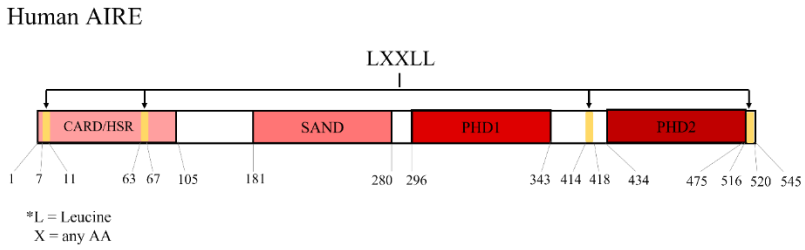

Figure 3. Domain structure of human AIRE. AIRE contains SAND domain, two PHD fingers, and a CARD domain. Notably, four LXXLL motifs are present, which bind to hydrophobic motifs in ligand-bound nuclear receptors. *Figure made in BioRender.*

Transcriptional regulation occurs at the level of chromatin through several post-translational modifications, including acetylation/deacetylation and methylation/demethylation of histone lysine residues [138]. This results in positive or negative regulation of chromatin accessibility. Regulation also occurs through access to DNA regulatory elements and of direct regulation of the transcriptional machinery [138]. Transcription factors may regulate initiation of transcription, elongation, or both. Transcriptional regulation occurs by binding of transcription factors to specific DNA motifs located in distal enhancer or proximal promoter regions. This leads to recruitment of co-regulatory proteins which prepare the chromatin landscape for transcriptional initiation. Transcription factors also recruit the mediator complex, which acts as a functional bridge between a transcription factor and the pre-initiation complex and RNA polymerase II. Often transcription is initiated for ~10–60 bp before RNA polymerase is stalled by pause factors [139]. Recruitment of elongation factors such as the positive transcription elongation factor (p-TEFb) is necessary to release the stalled polymerase.

Investigation of the mechanism by which Aire regulates transcription has found that it functions to release paused transcription via recruitment of p-TEFb [140, 141]. Aire is tethered to p-TEFb by bromodomain-containing protein (Brd4) via its CARD domain [142]. Despite current advancements, it remains unclear how the seemingly stochastic expression of relatively few TRAs per mTEC is sufficient to tolerize the T cell repertoire to self-antigen. Due to AIRE's central role in adaptive immunity, further investigations are merited to carefully define the pathways mediating the recruitment of AIRE to its targets and the regulation of its activity.

Thymic organogenesis and epithelial cell development

The thymus and parathyroid glands are derived from the third pharyngeal pouch during embryogenesis, which can be detected by E9.5 in mice [143]. Patterning into the thymus and

parathyroids occurs at E11.5, followed by migration of the primordia and detachment into distinct tissues [143]. The initial expression of transcription factors and subsequent signaling pathways that regulate thymic morphogenesis also occurs at E11.5, however, it is still to be determined how these factors cooperate to coordinate organogenesis. Further development and organization into the typical 3D structure of the adult thymus is dependent on the colonization of the thymus by lymphoid progenitor cells at E11–12 and the interplay between thymocytes and TECs [144]. Thymic cellularity notably increases in the post-natal period, beginning at 6–8 days, peaking at 4 weeks [145]. This expansion is temporally associated with the proliferation of $CD45^-$ thymic stromal cells, including TECs [145]. The exact order of TEC differentiation is disputed, but it is generally accepted that cTECs and mTECs are derived from a common precursor[146]. For example, mTECs were shown to have previously expressed cTEC specific genes, including *beta5t* [147]. Cytokeratin 5 (CK5) staining by immunofluorescent microscopy is used as a marker of mTECs, and co-staining with cytokeratin 8 (CK8), which labels both cTECs and mTECs, allows for visualization of cortical and medullary compartments [148]. mTECs have been more intensively investigated than cTECs, leading to the identification of a number of phenotypically and functionally distinct subtypes. Analysis of mTECs by flow cytometry using a combination of MHC-II and the costimulatory molecule, CD80, identify two mTEC subsets termed $mTEC^{lo}$ and $mTEC^{hi}$. $mTEC^{hi}$ cells, which are $CD80^+$ and $MHC\text{-}II^{hi}$, also highly express Aire. $mTEC^{lo}$ cells ($CD80^-$ $MHC\text{-}II^{hi/lo}$) appear to represent a more diverse group of mTECs including terminally differentiated 'Post-Aire' cells that have downregulated CD80 and MHC-II, $MHC\text{-}II^{hi}$ CD80- $mTEC^{hi}$ precursors, and CCL21 expressing $mTEC^{lo}$ [149]. The signals that drive Aire expression and $mTEC^{hi}$ maturation have also been studied in detail. In the embryonic thymus, lymphotoxin beta (LTβ) provided by lymphoid tissue inducer (LTi) cells and NF-κB signals driven through

receptor activator of NF-κB (RANK) and CD40 on mTECs are essential for organogenesis and TEC proliferation [150]. In adult thymi, LTβ signaling remains important for $CCL21^+$ mTECs but is dispensable for $AIRE^+$ mTEC maturation [150]. However, RANKL signals provided by positively selected thymocytes are essential for mTEC maturation in adult thymi.

Our knowledge of TEC subpopulations was enormously expanded by single cell RNA sequencing (scRNAseq) studies. For example, transit amplifying cells (TAC-TECs), which are proliferating cells enriched for S and G2M phase genes, were identified to be precursors of $AIRE^+$ and $CCL21^+$ TECs [151]. Minor populations of cells that had been observed histologically but were difficult to study were also identified, including keratinocyte like Hassall's corpuscles and lung like ciliated cells [152]. Furthermore, thymic tuft cells, microfold mTECs, thyroid mTEC, and others have been discovered [153, 154]. These cells, coined 'mimetic' cells, express the lineage driving transcription factors of their peripheral counterparts while retaining a strong mTEC gene signature [154]. Thus, these cells present TRAs mirroring their peripheral self. Their origin and precise roles in central tolerance are currently being investigated but it has been speculated that they may serve to preserve tolerance to a series of important peripheral cell types.

Age-related thymic involution

Aging affects T cell repertoire diversity and effectiveness through both thymic and peripheral mechanisms. In the periphery, repeated exposure to antigen over time results in the accumulation of memory T cells while decreasing the diversity of naïve T cells [155]. The thymus is the most rapidly aging organ in the body and is characterized by persistent involution of the organ starting during childhood with concomitant reductions in the production of naïve T cells throughout life [156]. Thymic involution is thought to have both hematopoietic and stromal components. Decreased bone marrow output over time contributes to reductions in T cell precursors entering

the thymus. While likely contributing to the thymic phenotype, changes in the thymic stroma are likely the primary mechanism by which involution occurs [157]. Several lines of evidence have demonstrated this experimentally. Irradiation of young and aged mice to ablate hematopoietic, but not stromal cells, and reconstitution with early T-lineage precursors (ETPs) from young mice resulted in impaired thymopoiesis in the aged, but not young, recipients [158]. Fetal thymic transplants into the kidney capsules of young or aged mice resulted in similar thymopoiesis, strongly suggesting that thymic extrinsic factors such as reduced ETPs or other signaling pathways in aged mice are not responsible for thymopoiesis [159]. Furthermore, alterations in the thymic expression of transcription factors such as forkhead box N1 (FoxN1), growth and longevity factors like fibroblast growth factor 21 (Fgf21), and various other signaling pathways involved in stromal cell proliferation and development have been identified to have a causative function in thymic involution [156]. For example, administration of exogenous FoxN1 greatly boosts thymic regeneration, rescues age-dependent involution, and naïve T cell output [160]. However, it is unclear what physiological changes during aging orchestrate the concerted downregulation of pro-thymic factors and upregulation of pro-involution ones.

What makes an effective T cell repertoire?

The role of T cells in immunity is fundamentally based on the capacity of their TCR to detect foreign, or transformed self, peptides in the context of MHC. Therefore, an effective T cell repertoire is one with sufficient diversity to detect all potential threats and lacking overly self-reactive clones. The importance of repertoire diversity is illustrated by several experimental findings from mice, and from genetic disorders in humans. A case of reversion of the X-linked immunodeficiency (Xid) mutation in a single T cell progenitor resulted in the generation of 2.5 x 10^4 distinct TCRs [161]. Stimulation of their T cells with mitogens or two antigens demonstrated

impaired proliferation relative to control T cells [161]. Nevertheless, this individual was protected from major infections in early life, indicating the presence of some redundancy in this limited repertoire [162]. Insertion of a TCRβ transgene prevents the expression of endogenous TCRβ genes, resulting in repertoire diversity of approximately 4 x 10^5 attributable to TCRα subunits. OT-1 TCRβ transgenic mice, which recognize OVA-8p antigen, were unable to reject bone marrow from F1 mice, indicating holes in their T cell repertoire [163]. A 50% reduction in repertoire diversity occurs in mice lacking TCR Vβ5, 8, 9, 11, 12, and 13. These mice were unable to respond to sperm whale myoglobin or myelin basic protein presented on MHC-II [164].

Additional *in vivo* data in the form of polyclonal $CD8^+$ T cell responses to the immunodominant herpes simplex virus (HSV) gB-8p epitope have been informative. In a polyclonal repertoire, the $CD8^+$ T cell response is dominated by T cells specific for HSV gB-8p, and genetic deletion of this epitope from the virus resulted in a 70% decrease in the CD8+ T cell response [165]. 60–65% of $CD8^+$ T cells responding to HSV gB-8p express TCR Vβ10 chains [166]. HSV infection of mice lacking TCR Vβ10 chains results in a 60% reduced T cell response to the virus [166]. These results indicate two things: $CD8^+$ T cell responses to the immunodominant epitope of HSV are poorly compensated for by other clones, and there are important structural components of the TCR that can strongly affect the magnitude of the T cell response to a pathogen. Bm8 mice have increased TCR diversity for HSV gB-8p relative to co-isogenic mice, due to alterations in MHC-I alleles, resulting in increased resistance to HSV infection [165]. TdT deficient mice, which have 90–95% reduced repertoire diversity, surprisingly do not display obvious signs of defects in pathogen detection and generating protective immune responses [120]. Neither *in vitro* or *in vivo* challenge with keyhole limpet hemocyanin (KLH) or sperm whale myoglobin (SWM) peptides altered T cell proliferation in TdT deficient mice [167]. *In vitro*

measurement of cytotoxic T cell responses via chromium release assay from TdT deficient and control mice infected with the LCMV WE strain were indistinguishable [167]. Helper T cell-dependent antibody titers in control versus TdT deficient mice infected with vesicular stomatitis virus (VSV) were also unchanged, indicating the presence of functional antigen specific Th cells [167]. Another study found that $CD8^+$ T cell responses to influenza A and vaccinia virus were reduced by 30% in TdT deficient mice, but an effect on pathogen control was not investigated in this study [168]. Despite generating 90% of repertoire diversity, it does not appear that N-region nucleotide additions catalyzed by TdT markedly affect pathogen detection or responsiveness. An interesting observation, however, is that the TdT deficient T cell repertoire appears to be enriched for TCRs more efficiently able to bind self-pMHC [169], raising the possibility that N-nucleotide additions may function to broaden the diversity of TCR reactivities for antigen.

The immune response can be categorized into acute and chronic phases, depending on whether the pathogen is cleared or persists after infection [170]. Acute phase T cell responses are dominated by T cells with high TCR reactivities [171, 172]. During chronic infections, T cells undergo antigen-mediated exhaustion due to chronic stimulation through the TCR [173]. This may primarily affect T cells with more highly reactive TCRs. Notably, pathogen resistance in TdT deficient mice was only investigated in infectious models causing acute infection. Furthermore, Th differentiation is heavily influenced by TCR reactivity for pMHC, but Th functionality was only indirectly assessed in TdT deficient mice. Therefore, N-nucleotide additions into the TCR catalyzed by TdT could affect the immune response to infection in two ways. First, by generating TCRs with decreased pMHC reactivity potentially needed during chronic infections when T cells bearing more highly reactive TCRs are functionally exhausted. Secondly, by creating a broader range of TCR reactivities in the repertoire to diversify Th effector responses. However,

experimental data to support that the TdT-deficient T cell repertoire is of higher pMHC reactivity is lacking. In addition, it is not understood how TdT-encoded TCRs may benefit the host during chronic infections. Although these examples of reductions in repertoire diversity occurred through rare genetic disorders or specific genetic manipulations in mice, reductions of T cell repertoire diversity occur in humans during infection with human immunodeficiency virus (HIV), treatment with highly active antiretroviral therapy, bone marrow transplantation, T cell leukemia, and aging [162].

The previous section mostly discussed T cell responses in specific cases of reduced repertoire diversity and factors affecting the size of the repertoire. Another critical facet of an effective T cell repertoire is the prevention of autoimmunity via both thymic and peripheral mechanisms. This is central to generating an effective T cell repertoire. Prevention of autoimmunity is regulated by central tolerance generated in the thymus and peripheral tolerance through multiple mechanisms. The peripheral mechanisms include suppression of inappropriate autoinflammatory responses by Treg cells, the *de novo* differentiation of peripheral Tregs during an immune response, and enforcement of T cell anergy in the presence of suprathreshold TCR triggering in the absence of co-stimulation and cytokines [174]. Much is known about the role of vitamin D signaling in the context of T cell activation and effector functions. However, our knowledge of 1,25D signaling in the thymus is limited, especially with regards to conventional T cell development, and its potential functions in the process of central tolerance are completely unknown. Exploration of the effect vitamin D may have on the induction central tolerance is of particular interest, given that the thymus is most active in early life. Additionally, vitamin D deficiency is clearly associated with increased risk of autoimmunity, but the therapeutic benefit of 1,25D in humans with ongoing

disease is unclear. It may be that vitamin D signaling, in the context of autoimmunity, is more relevant prior to the onset disease, which is typically in younger individuals.

Introduction (Hypothesis and Aims)

An effective T cell repertoire is self-tolerant but able to respond vigorously to pathogens and cancer cells. The magnitude and breadth of T cell responses are related to the size and diversity of the T cell repertoire, which is generated in the thymus and maintained in the periphery. Thymic development and the selection of the T cell repertoire are dependent on both genetic and environmental factors, including stress, nutrition, infections, and certain mutations. Vitamin D deficiency in infants and children, the period when thymic activity is highest, is a risk factor for autoimmune diseases, including type 1 diabetes and multiple sclerosis. However, the potential role(s) of vitamin D signaling in thymic central tolerance have not been reported. Reduced T cell repertoire diversity due to chemotherapy, bone marrow transplantation, or genetic mutations results in increased susceptibility to cancers, autoimmunity, and infection. TCR sequence diversity is generated in the thymus and T cell effector functions are in part regulated by the strength of TCR signaling, which depends on its sequence. **We hypothesized** that (1) vitamin D signaling in the thymus would regulate the process of central tolerance, and that (2) TCR diversification in the thymus may be a mechanism to broaden TCR reactivities and thus $CD4^+$ effector response diversity.

These hypotheses were investigated in this thesis with the following aims:

Aim 1: Investigate whether vitamin D signaling is active in the thymus and assess its potential functional relationship with Aire.

Aim 2: Investigate how the absence of 1,25D impacts thymic development, Aire expression and function.

Aim 3: Investigate whether T cell repertoire diversity impacts $CD4^+$ T cell differentiation.

Chapter 2: Aire is a coactivator of the vitamin D receptor

Patricio Artusa*, Marie-Ève Lebel†, Camille Barbier*, Babak Memari*, Reyhaneh Salehi-Tabar*, Sophia Karabatsos*, Aiten Ismailova*, Heather J. Melichar†, John H. White*

**Department of Physiology, McGill University, Montreal QC, Canada. †Département de Médecine, Université de Montréal and Maisonneuve-Rosemont Hospital Research Center, Montreal QC, Canada.*

Abstract

Vitamin D deficiency is associated with the development of autoimmunity, which arises from defects in T cell tolerance to self-antigens. Interactions of developing T cells with medullary thymic epithelial cells (mTECs), which express tissue restricted antigens (TRAs), are essential for the establishment of central tolerance. However, vitamin D signaling in the thymus is poorly characterized. We find that stromal and hematopoietic cells in the mouse thymus express the vitamin D receptor (Vdr) and Cyp27b1, the enzyme that produces hormonal 1,25-dihydroxyvitamin D (1,25D). Treatment of cultured thymic slices with 1,25D enhances expression of the critical mTEC transcription factor Aire, its colocalization with the Vdr, and enhances TRA gene expression. Moreover, the Vdr interacts with Aire in a 1,25D-dependent manner and recruits Aire to DNA at vitamin D response elements, where it acts as a Vdr coactivator. These data link vitamin D signaling directly to critical transcriptional events necessary for central tolerance.

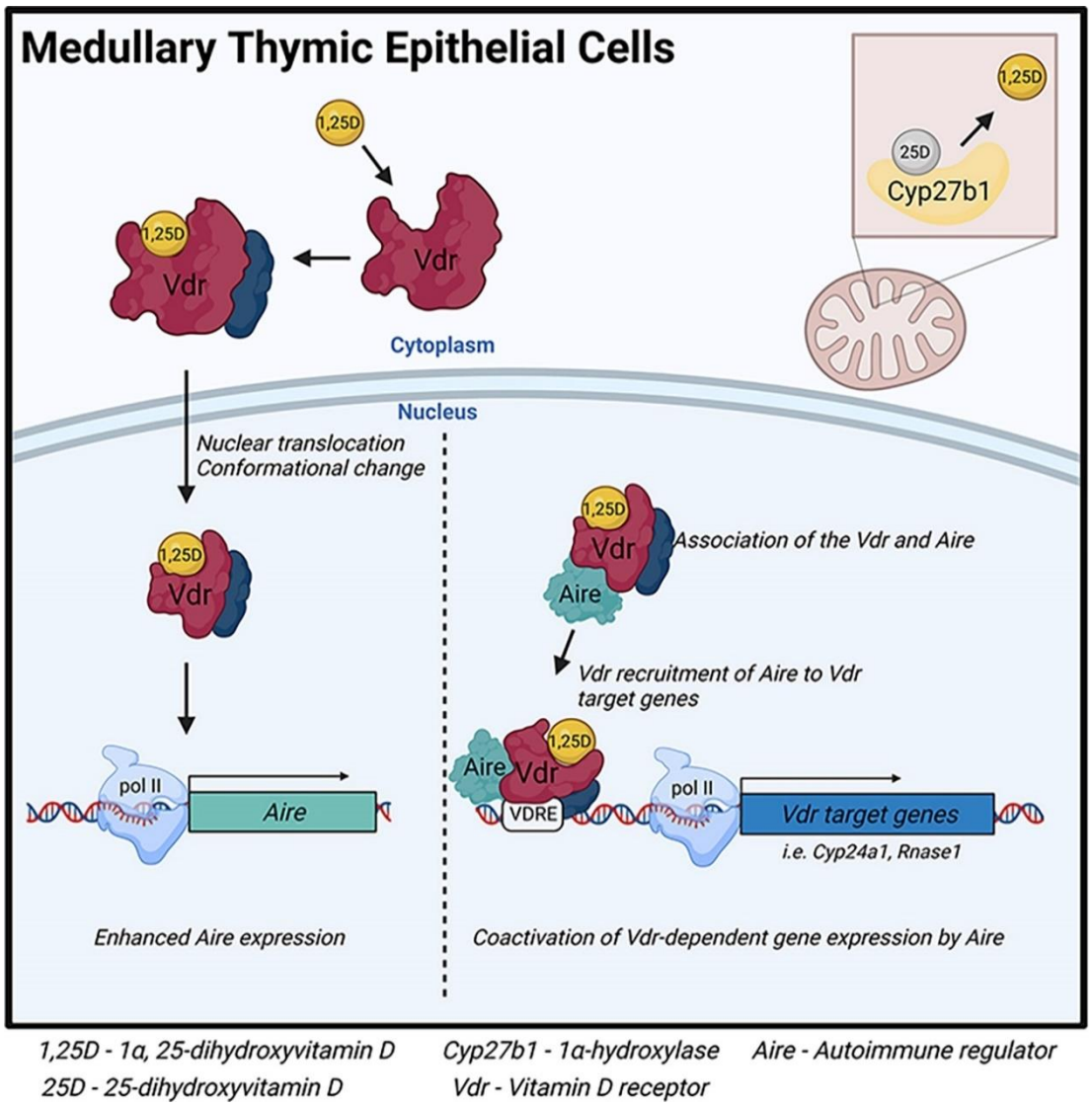

Key points

- The vitamin D receptor is expressed in Aire^{+} medullary thymic epithelial cells.
- Thymic vitamin D signaling stimulates Aire expression and Aire-dependent gene transcription.
- Aire interacts with the Vdr and is a coactivator of Vdr-dependent transcription.

Introduction

Vitamin D signaling is widespread, including in cells of the innate and adaptive immune system [1]. While vitamin D can be obtained from diet, supplements, or cutaneous exposure to adequate UV-B irradiation [1], vitamin D-poor diets, sun avoidance, and conservative dress lead to widespread vitamin D deficiency [2]. Profound deficiency in children causes rickets, a diagnosis associated with increased risk of diseases unrelated to poor calcium status [3], including autoimmune disorders [1, 4]. Vitamin D is activated by primarily hepatic 25-hydroxylation followed by peripheral 1α-hydroxylation catalyzed by Cyp27b1 to generate 1,25-dihydroxyvitamin D (1,25D). 1,25D binds to the vitamin D receptor (Vdr), a nuclear receptor and ligand-regulated transcription factor [1], which binds to cognate vitamin D response elements (VDREs). In the periphery, 1,25D attenuates T cell activation and proliferation and suppresses T cell-driven inflammation while enhancing suppressive Treg cells [5]. However, the links between vitamin D deficiency in infancy and childhood and subsequent risk of autoimmunity suggest that vitamin D signaling also contributes to thymic central tolerance.

Central tolerance is established by elimination of developing thymocytes with overly self-reactive antigen receptors via negative selection or diversion towards immunoregulatory lineages [6]. Transcription of tissue-restricted antigen (TRA) genes in medullary thymic epithelial cells (mTECs) is critical for central tolerance. The transcription factor autoimmune regulator (Aire) is necessary for expression of most TRAs [7] and its loss in humans causes APECED (autoimmune polyendocrinopathy-candidiasis-ectodermal dystrophy), characterized by multi-organ autoimmunity [7]. Very little is known about the role of 1,25D in thymic development, cellularity, and function. One study provided evidence that invariant NKT (iNKT) cells fail to mature in the thymus of *Vdr*-null mice [8]. However, the molecular mechanisms of thymic Vdr action have not

been addressed. We show that Vdr signaling is active in thymic hematopoietic and stromal cells, including mTECs, and that 1,25D induces Aire and TRA expression. Moreover, Aire is recruited to Vdr target genes and acts as a coactivator. This implicates 1,25D signaling in transcriptional events necessary for central tolerance.

Materials and Methods

Mice

6–10-week-old male or female C57BL/6J mice (Jackson Laboratory) were maintained in a specific pathogen-free environment at the Maisonneuve-Rosemont Hospital Research Center. All animal protocols were approved by the local Animal Care Committee in accordance with the Canadian Council on Animal Care guidelines.

Thymic slice preparation and culture

Thymic slices were prepared as described [9]. Harvested thymi were placed into a 4% low-melt agarose solution < 40 °C. After solidification, 500 µm thick sections were prepared. Slices (3–10/condition) were cultured in 6-well plates and treated with RPMI containing 100nM of 1,25D or 1 µL of vehicle (100% EtOH), for up to 24 hours at 37 °C (5% CO_2).

Preparation of single cell suspensions

Tissue was cut into 1 mm pieces and digested in RPMI 1640 (Wisent) containing 10% FBS (Millipore Sigma) (R10) and Collagenase D (250 µg/mL;Sigma), Papain (250 µg/mL;Worthington Bioc.), and DNase I (200 µg/mL;Sigma) for 30 min at 37 °C with shaking. Cells were further released by pipetting up and down. Digestion buffer was freshly prepared for each experiment.

Flow Cytometry

2–5x10^6 cells were incubated with fixable viability dye diluted in PBS at 4 °C for 20 min. Cells were washed and resuspended with PBS containing 1% FBS, 2 mM EDTA (FACS buffer), fluorophore conjugated antibodies (Abs), and FC block (Supplemental Table 1), and incubated for 30 min at 4 °C. For intracellular proteins, cells were fixed and permeabilized using the FoxP3 Fix/Perm Kit (Thermo Fisher) for 30 min at room temperature (RT). Cells were then resuspended in 1X Perm/Wash buffer containing fluorophore-conjugated Abs and incubated for 30 min at 4 °C. Cells and UltraComp ebeads (Thermo Fisher) were used for compensation controls. Samples were acquired on a LSR Fortessa (BD Biosciences) and analyzed by FlowJo (BD Biosciences). Gating is as follows (See Supplemental Fig 3): $mTEC^{hi}$ ($EpCAM^+$, UEA-$1^{+/-}$, $Ly51^-$, MHC-II^{hi}, $CD80^+$), $mTEC^{lo}$ ($EpCAM^+$, UEA-$1^{+/-}$, $Ly51^-$, MHC-$II^{+/-}$, $CD80^-$), cTECs ($EpCAM^+$, $Ly51^+$), B cells ($CD45^+$, $CD19^+$, MHC-II^+, $CD11c^-$), DCs ($CD45^+$, $CD11c^+$, MHC-II^+, $CD19^-$), and thymocytes ($CD45^+$, TCR$\beta^{+/-}$, MHC-II^-, $CD19^-$, $CD11c^-$).

Cell sorting

TECs were enriched by positively selecting for $EpCAM^+$ cells by MACS (Miltenyi Biotec). Flow cytometric staining was performed as described above. Total TECs ($EpCAM^+$, $CD45^-$) or mTECs ($EpCAM^+$, $CD45^-$, UEA-1^+, $Ly51^-$) were sorted with a BD FACSAria Fusion into cold FACS buffer.

Immunofluorescence (IF) microscopy

Samples were fixed with 4% PFA and incubated with sucrose (Bioshop) solutions (10–30%) for ~8 hr each and embedded using base molds (Fisherscientific) containing O.C.T. compound (Fisherscientific), frozen on dry ice, and stored at -80 °C. 5–20 µm sections were obtained with a Leica CM3050 S Cryostat and Superfrost Plus slides (Fisherscientific). A hydrophobic barrier was applied (Millipore Sigma) and slides were blocked with PBS containing 2% BSA (w/v), 0.3% Triton X-100, 1% FBS, and 10% goat serum (Blocking buffer) for 1 hr at RT. Slides were incubated in a humidified chamber with primary Abs diluted in blocking buffer (Supplemental Table 1) overnight at 4 °C, secondary Abs conjugated to fluorophores diluted in blocking buffer for 1 hr at RT, fluorophore conjugated primary Abs for 1 hr at RT, and DAPI diluted in PBS for 5 min at RT. Slides were washed 3x with 100 µM Tris buffer between each step, mounted with Fluoromount 4G (Thermo Fisher) and cover slips (No. 1.5;Fisher scientific), and imaged with a Zeiss LSM710 confocal microscope with 20–100X objectives. Images were analyzed with FIJI (ImageJ). For colocalization analysis, images were acquired with the same settings and JaCoP was used on split channels without prior contrast changes and automatic thresholds to quantify overlap.

Gene expression

$5x10^6$ cells were lysed and RNA extracted using FavorPrep Total RNA Mini Kit (Favorgen) and quantified with a NanoDrop 2000c (Thermo Fisher). 500ng of RNA was converted to cDNA using AdvanTech 5X master mix. Oligo sequences (available upon request) were designed with Primer3 and primer specificity was verified by BLAST. 10 ng of cDNA was used per qPCR reaction and BlasTaq 2X qPCR MasterMix (abm). qPCR reactions and melting curves were done with a

LightCycler 96 (Roche). Gene expression was normalized to 18S. Fold changes for thymic slices were calculated by comparing gene expression between treatment conditions from individual mice.

Plasmids

VDR expression vector pcDNA 3.1-VDR was generated by inserting the human VDR cDNA as a BamH1-Xho1 fragment. AIRE cDNA expression vector (pGMV3-Aire-myc) was from Sino Biological Inc. (HG17322-UT). The 1,25D-responsive *luciferase* reporter plasmid *pVDRE2*-pGL4.24 was constructed by insertion of tandem 31 bp oligos containing consensus VDREs upstream of the minimal promoter of pGL4.24 (Promega). Cells were transfected using CalFectin transfection reagent (SL100478; Signagen).

Immunoprecipitation (IP) and Western analysis

Cells were lysed with 20 mmol/L Tris, pH 7.5, 100 mmol/L NaCl, 0.5% Nonidet P-40, 0.5 mmol/L EDTA, 0.5 mmol/L phenylmethylsulfonyl fluoride (PMSF). For co-IP assays, 4 ng of AIRE Ab (Supplemental Table 1) was pre-bound for 2 hrs to Dynabeads protein A, washed with lysis buffer, added to the lysate, and IP-ed overnight. Beads were washed 5x with washing buffer (20 mmol/L Tris, pH 7.5, 200 mmol/L NaCl, 1% Nonidet P-40, 0.5 mmol/L EDTA, 0.5 mmol/L PMSF) and processed for Western blotting.

Chromatin immunoprecipitation (ChIP)

Sorted mTECs cells were prepared as described above. ChIP assays were performed as described [10]. After fixation, cells were recovered in 1% IGEPAL, 20 mM Tris-pH 8, 0.5 mM EDTA, 100 mM NaCl + RNase, pelleted at 6,000 rpm, resuspended in 1% SDS, NaCl 50 mM, 20 mM Tris-pH 8 + RNase, sonicated to obtain fragments < 500 bp, vortexed, and centrifuged at 10,000 rpm

for 10 minutes at 4 ℃. 1% of each sample was stored at -20 °C for input controls. The rest was divided into IgG control and IP tests. A protease inhibitor cocktail and 1 µL of Dynabeads-Protein-G (#10003D) per 2 µg of Ab was added and samples were incubated overnight at 4 ℃. The supernatant was removed while samples were on a magnet and Proteinase-K and 1% IGEPAL buffer was added to each sample, including inputs, and shaken at 1,000 rpm for 2 hr at 45 °C. Crosslinking was reversed at 65 °C for 4 hrs. The supernatant was removed while samples were on a magnet and the FavorPrep GEL/PCR purification mini kit (Favorgen) was used to collect DNA.

Luciferase reporter assay

HEK293 cells were cultured in DMEM with heat-inactivated FBS and Normacin and transfected when 60% confluent [luciferase expression vector only (+/- 1,25D 100 nM), luciferase + VDR expression vector + increasing amounts of AIRE (+/- 1,25D 100 nM; 0–100 ng AIRE)]. Plates were incubated for 4–5 hr prior to incubation overnight with 1,25D (100 nM). 200uL of Glo Lysis Buffer (Promega, Wisconsin) was added and plates were left for 5 min on the shaker. 100uL of each lysate and Luciferase substrate were transferred to a round-bottom tube and luminescence was immediately read with a luminometer.

Human scRNAseq data analysis

Raw data (GSM4466784/5) was analyzed with Seurat and filtered by unique feature counts and mitochondrial genes. Samples were integrated, scaled, and normalized. Dimensionality reduction was conducted using the first 20 principal components. UMAPs were constructed and clusters were identified using the shared nearest neighbor algorithm (res. = 0.5).

Statistical analyses

Statistics were calculated using GraphPad Prism version 8 with parametric unpaired t tests, and non-parametric tests or parametric paired t tests for thymic slice data. Statistical significance is indicated by p-values *p < 0.05, **p < 0.01, ***p < 0.001.

Results and Discussion

While the Vdr is expressed in thymocytes and thymic iNKT cells [8, 11], receptor function in other important cell types, notably TECs, has not been examined. The *Vdr* and *Cyp27b1* mRNAs are expressed in mature mouse mTECs at higher levels than in thymocytes and iNKT cells (Supplemental Figures 1A,B), and RNAseq studies, along with expression of *CYP24A1*, indicative of active vitamin D signaling (Supplemental Figures 2B,C)[13, 14]. We detected *Vdr* and *Cyp27b1* mRNA in whole mouse thymi and in sorted total TECs (Supplemental Figure 1C). IF of thymic sections revealed abundant Vdr protein in the thymic cortex and medulla (Supplemental Figure 1D). Vdr expression was also confirmed in multiple cell types, including Aire^{+} TECs, using cell specific markers (Figure 1A; see also Supplemental Figure 1E for images of Vdr channels only).

Vdr expression was also validated in hematopoietic and stromal cells by flow cytometry (Figures 1B,C, gating strategy in Supplemental Figure 3). Its expression in both cortical TECs (cTECs) and mTECs suggests We analyzed the 1,25D-dependent induction of the Vdr target gene *Cyp24a1* in sorted TECs and in cultured thymic slices, which maintain tissue integrity and important cell-cell interactions [9]. 1,25D induced *Cyp24a1* 5- to 8-fold in thymic slices (Figure 1G). Given that TECs represent only ~1% of thymic cellularity, we treated sorted TECs and found that *Cyp24a1* was induced 50- to 100-fold by 1,25D (Figure 1G). This observation is also consistent with the levels of mTEC *Cyp24a1* mRNA observed by expression profiling

(Supplemental Figure 1F). Finally, the Vdr was mostly cytoplasmic in thymic slices cultured in vehicle, whereas it was more nuclear in the presence of 1,25D (Figure 1H). This suggests that the largely nuclear Vdr staining seen in multiple cell types in freshly isolated thymus (Supplemental Figure 1D) is consistent with active 1,25D signaling.

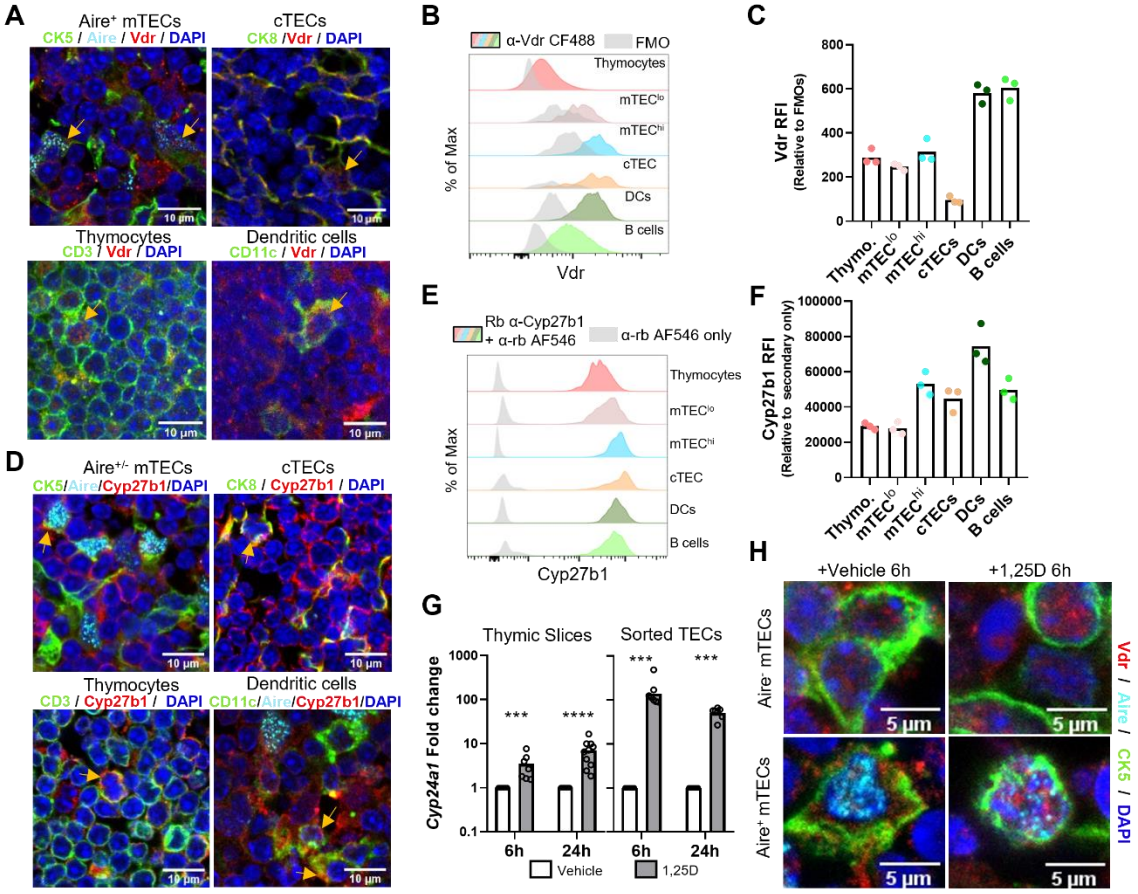

Figure 1. Active 1,25D signaling in the thymus. ***A.*** *IF microscopy of thymic sections showing Vdr staining in Aire^{+} mTECs, cTECs, thymocytes, and dendritic cells.* ***B,C.*** *Flow cytometric analysis of Vdr expression in multiple thymic cell types (fluorescence minus one, FMO, were gated on respective populations) (RFI, relative fluorescence intensity).* ***D.*** *Cytoplasmic Cyp27b1 staining in Aire$^{+/-}$ mTECs, cTECs, thymocytes, and dendritic cells.* ***E,F.*** *Flow cytometric analysis of Cyp27b1 expression in multiple thymic cell types.* ***G.*** *Induction of Cyp24a1 mRNA (log scale) by 1,25D in mouse thymic slices and in sorted TECs (CD45^{-} EpCAM^{+}).* ***H.*** *Vdr staining in Aire^{-} and Aire^{+} mTECs in vehicle or 1,25D-treated thymic slices. Data are individual mice (N ≥ 3, ≥ 2 independent experiments).*

Due to the enrichment of 1,25D signaling in TECs and the coexpression of the Vdr and Aire, we investigated the potential functional relationship of the two proteins. Expression of *Aire* and Aire-dependent TRA mRNAs was induced in thymic slices treated with 1,25D (Figures 2A,B).

Moreover, 1,25D treatment of thymic slices increased the number of Aire^{+} cells (Figures 2C,D). 1,25D also enhanced the colocalization of the Vdr with Aire in mTECs (Figures 2E,F). While the Vdr regulates transcription by pleiotropic mechanisms [15], its partial overlap with Aire suggests the two proteins may interact functionally. This notion is supported by the presence of 4 LXXLL motifs in mouse and human AIRE (Figure 3A)[16], which are found in nuclear receptor coactivators [17]. We observed a 1,25D-dependent co-IP of the human VDR with human AIRE expressed in HEK293 cells (Figure 3B). In addition, AIRE expressed in HEK293 cells was recruited in a 1,25D-dependent manner to a VDRE in the human *CYP24A1* gene in chromatin immunoprecipitation (ChIP) assays (Figure 3C). Re-ChIP experiments at the same VDRE confirmed the formation of a VDR-AIRE complex (Figure 3D).

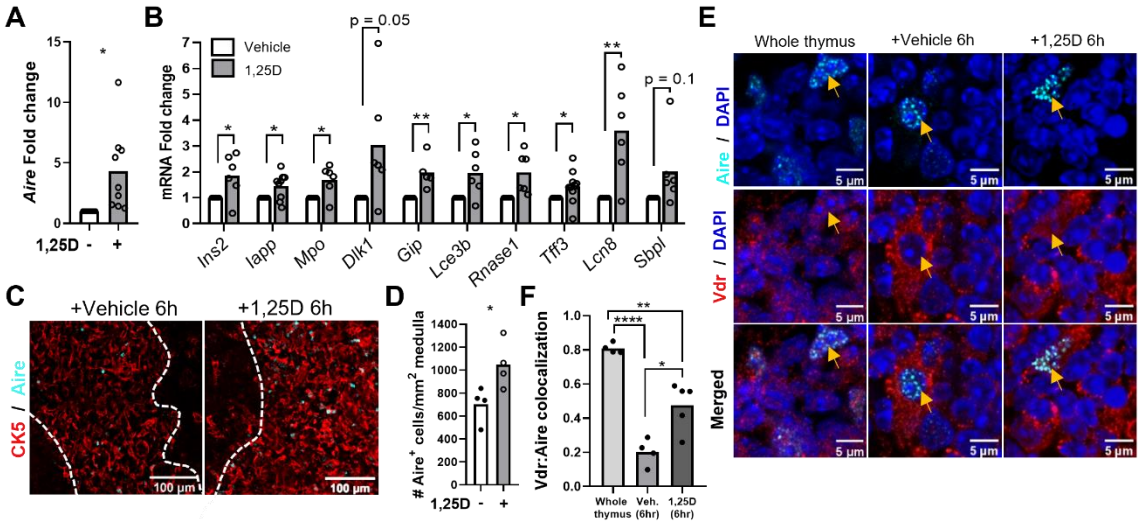

Figure 2. **1,25D signaling regulates *Aire* and Aire-dependent gene expression.** ***A.*** *Induction of Aire mRNA by 1,25D in mouse thymic slices (24h).* ***B.*** *Aire-dependent gene expression in 6h vehicle versus 1,25D-treated thymic slices.* ***C-D.*** *Representative images (C) of Aire^{+} mTECs in vehicle versus 1,25D treated thymic slices and quantification (D).* ***E.*** *Representative images of Vdr localization with Aire in whole thymus and vehicle- or 1,25D-treated thymic slices.* ***F.*** *Quantification of Vdr colocalization with Aire (Manders M1 coefficient). Data are individual mice (N ≥ 2, ≥ 2 experiments).*

Next, we examined the 1,25D-dependent recruitment of Aire to VDREs in mouse mTECs. We observed 1,25D-dependent binding of endogenous Vdr and Aire to a *Cyp24a1* VDRE in sorted mTECs (Figure 3E). A screen of mouse Vdr ChIP-seq datasets identified a peak of 1,25D-dependent Vdr binding adjacent to the *Rnase1* gene in an intestinal epithelial dataset (Supplemental Figure 1G)[18]. As shown above, *Rnase1* expression was induced in thymic slices by 1,25D (Figure 2B). We detected 1,25D-dependent recruitment of the Vdr and Aire to the same site in the *Rnase1* gene in sorted mTECs (Figure 3F). The potential function of AIRE as a VDR cofactor was further addressed using a minimal promoter composed of tandem VDREs inserted adjacent to a binding site for RNA polymerase II (TATA box). This arrangement was used to minimize the potential intervention of other classes of transcription factors on more complex

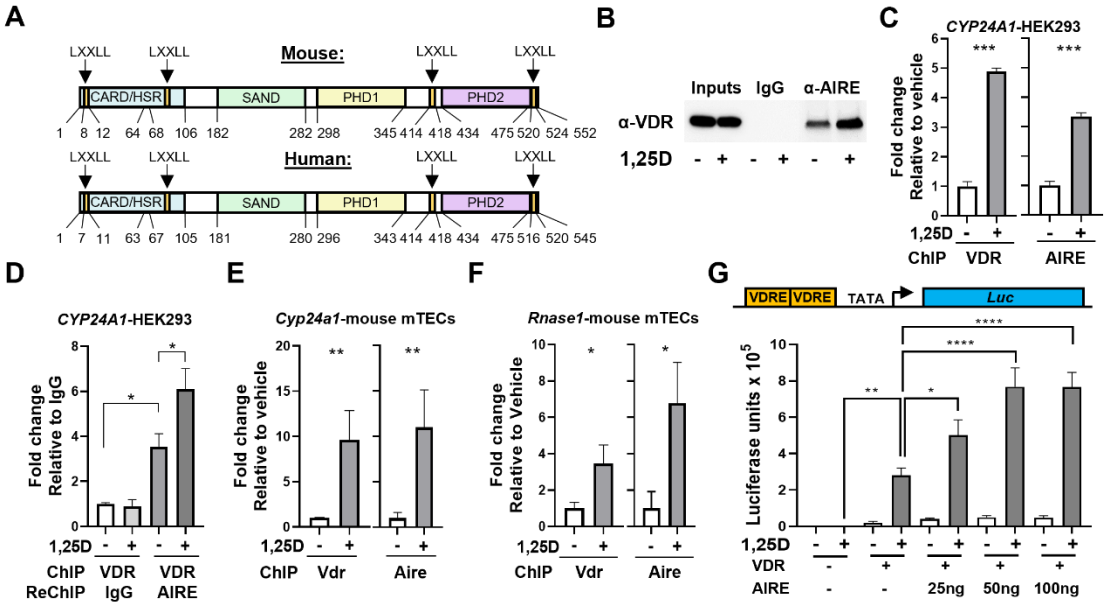

Figure 3. **The Vdr and Aire interact in a 1,25D-dependent manner.** ***A.*** *Domain structures of mouse and human Aire with LXXLL motifs indicated.* ***B.*** *1,25D enhanced co-IP of the human VDR with AIRE in HEK293 transfected cells.* ***C.*** *1,25D dependent ChIP of the human VDR (left) or AIRE (right) on CYP24A1 VDRE's in transfected HEK293 cells.* ***D.*** *Re-ChIP of VDR ChIP on CYP24A1 VDRE's with IgG or α-AIRE showing that the VDR and AIRE are present on CYP24A1 VDRE's together.* ***E.*** *ChIP of the mouse Vdr (left) or mouse Aire (right) on Cyp24a1 VDRE's from sorted primary mouse mTECs.* ***F.*** *ChIP of the mouse Vdr (left) or mouse Aire (right) on Rnase1 VDRE's from sorted primary mouse mTECs.* ***G.*** *Coactivation of 1,25D-dependent luminescence by AIRE in transfected HEK293 cells. Schematic showing minimal promoter construct (top) and summary data from two experiments (bottom). Data are mean± SD (N ≥ 3, 2 experiments).*

promoters. Co-expression of increasing amounts of AIRE enhanced 1,25D-dependent induction of a *luciferase* reporter gene (Figure 3G) in HEK293 cells. Collectively, these data reveal the 1,25D-dependent recruitment of AIRE to VDREs, and that AIRE functions as a VDR coactivator.

In conclusion, we find that 1,25D signaling, which has been implicated in autoimmunity [19], is active in thymic hematopoietic and stromal compartments, and induces the expression of Aire mRNA and protein in mTECs as well as the expression of a number of TRA genes. Moreover, AIRE is an interaction partner of the VDR and acts as a VDR coactivator. As Aire does not appear to be a site-specific binding protein [7], our data suggest a novel mechanism by which Aire can be recruited to chromatin. Induction of TRA gene expression by 1,25D could occur by direct binding of the Vdr to some genes or indirectly via induced Aire expression. This provides evidence that 1,25D signaling increases the amount or diversity of rare self-peptides presented to thymocytes during induction of central tolerance.

Mouse and human Aire contain 4 LXXLL motifs found in nuclear receptor coregulators [17]. The presence of 4 such motifs suggest they may act at least partially redundantly in VDR-AIRE interactions. It also raises the possibility that Aire can be recruited to chromatin by other nuclear receptors expressed in mTECs. Available sequence data reveal expression of several nuclear receptors in sorted MHC-II^{hi} mTECs (Supplemental Figure 2A). Notably, these include the gene encoding the androgen receptor (Ar). Androgens enhance *Aire* transcription in mTECs by inducing Ar binding to *Aire* promoter regions [20, 21], raising the possibility that Aire may also be a cofactor of the Ar. Collectively, these findings suggest that Aire may be recruited to chromatin by multiple agonist-bound nuclear receptors.

Acknowledgements

We acknowledge the Advanced Bioimaging Facility (ABIF) at McGill University for help with imaging experiments.

References

1. Bouillon, R., C. Marcocci, G. Carmeliet, D. Bikle, J.H. White, B. Dawson-Hughes, P. Lips, C.F. Munns, M. Lazaretti-Castro, A. Giustina, and J. Bilezikian. 2018. *Skeletal and Extraskeletal Actions of Vitamin D: Current Evidence and Outstanding Questions.* Endocrine Reviews. **40**(4): p. 1109-1151.
2. Arabi, A., R. El Rassi, and G. El-Hajj Fuleihan. 2010. *Hypovitaminosis D in developing countries-prevalence, risk factors and outcomes.* Nat Rev Endocrinol. **6**(10): p. 550-561.
3. Pettifor, J.M., K. Thandrayen, and T.D. Thacher, *Chapter 67 - Vitamin D Deficiency and Nutritional Rickets in Children*, in *Vitamin D (Fourth Edition)*, D. Feldman, Editor. 2018, Academic Press. p. 179-201.
4. Cantorna, M.T. and B.D. Mahon. 2004. *Mounting Evidence for Vitamin D as an Environmental Factor Affecting Autoimmune Disease Prevalence.* Exp. Biol. Med. **229**(11): p. 1136-1142.
5. Bhalla, A., E. Amento, B. Serog, and L. Glimcher. 1984. *1,25-Dihydroxyvitamin D3 inhibits antigen-induced T cell activation.* J Immunol. **133**(4): p. 1748-1754.
6. Klein, L., E.A. Robey, and C.-S. Hsieh. 2019. *Central CD4+ T cell tolerance: deletion versus regulatory T cell differentiation.* Nature Reviews Immunology. **19**(1): p. 7-18.
7. Mathis, D. and C. Benoist. 2009. *Aire.* Annu Rev Immunol. **27**: p. 287-312.
8. Yu, S. and M.T. Cantorna. 2008. *The vitamin D receptor is required for iNKT cell development.* Proc Natl Acad Sci U S A. **105**(13): p. 5207-12.
9. Sood, A., M. Dong, and H.J. Melichar. 2016. *Preparation and Applications of Organotypic Thymic Slice Cultures.* J Vis Exp(114).
10. Memari, B., M. Bouttier, V. Dimitrov, M. Ouellette, M.A. Behr, J.H. Fritz, and J.H. White. 2015. *Engagement of the Aryl Hydrocarbon Receptor in Mycobacterium tuberculosis-Infected Macrophages Has Pleiotropic Effects on Innate Immune Signaling.* J Immunol. **195**(9): p. 4479-91.
11. Arora, J., J. Wang, V. Weaver, Y. Zhang, and M.T. Cantorna. 2022. *Novel insight into the role of the vitamin D receptor in the development and function of the immune system.* J Steroid Biochem Mol Biol. **219**: p. 106084.
12. Heng, T.S., M.W. Painter, and C. Immunological Genome Project. 2008. *The Immunological Genome Project: networks of gene expression in immune cells.* Nat Immunol. **9**(10): p. 1091-4.
13. Tabula Sapiens, C., R.C. Jones, J. Karkanias, M.A. Krasnow, A.O. Pisco, S.R. Quake, J. Salzman, N. Yosef, B. Bulthaup, P. Brown, W. Harper, et al. 2022. *The Tabula Sapiens: A multiple-organ, single-cell transcriptomic atlas of humans.* Science. **376**(6594): p. eabl4896.
14. Bautista, J.L., N.T. Cramer, C.N. Miller, J. Chavez, D.I. Berrios, L.E. Byrnes, J. Germino, V. Ntranos, J.B. Sneddon, T.D. Burt, et al. 2021. *Single-cell transcriptional profiling of human thymic stroma uncovers novel cellular heterogeneity in the thymic medulla.* Nat Commun. **12**(1): p. 1096.

15. White, J.H., R. Salehi-Tabar, V. Dimitrov, and M. Bouttier, *Chapter 10 - Diverse Mechanisms of Transcriptional Regulation by the Vitamin D Receptor*, in *Vitamin D (Fourth Edition)*, D. Feldman, Editor. 2018, Academic Press. p. 175-187.
16. Nagamine, K., P. Peterson, H.S. Scott, J. Kudoh, S. Minoshima, M. Heino, K.J. Krohn, M.D. Lalioti, P.E. Mullis, S.E. Antonarakis, K. Kawasaki, et al. 1997. *Positional cloning of the APECED gene.* Nat Genet. **17**(4): p. 393-8.
17. Savkur, R.S. and T.P. Burris. 2004. *The coactivator LXXLL nuclear receptor recognition motif.* J Pept Res. **63**(3): p. 207-12.
18. Lee, S.M., E.M. Riley, M.B. Meyer, N.A. Benkusky, L.A. Plum, H.F. DeLuca, and J.W. Pike. 2015. *1,25-Dihydroxyvitamin D3 Controls a Cohort of Vitamin D Receptor Target Genes in the Proximal Intestine That Is Enriched for Calcium-regulating Components.* J Biol Chem. **290**(29): p. 18199-18215.
19. Dankers, W., E.M. Colin, J.P. van Hamburg, and E. Lubberts. 2017. *Vitamin D in Autoimmunity: Molecular Mechanisms and Therapeutic Potential.* Frontiers in Immunology. **7**.
20. Wilhelmson, A.S., M. Lantero Rodriguez, I. Johansson, E. Svedlund Eriksson, A. Stubelius, S. Lindgren, J.B. Fagman, P.J. Fink, H. Carlsten, O. Ekwall, et al. 2020. *Androgen Receptors in Epithelial Cells Regulate Thymopoiesis and Recent Thymic Emigrants in Male Mice.* Front Immunol. **11**: p. 1342.
21. Zhu, M.L., P. Bakhru, B. Conley, J.S. Nelson, M. Free, A. Martin, J. Starmer, E.M. Wilson, and M.A. Su. 2016. *Sex bias in CNS autoimmune disease mediated by androgen control of autoimmune regulator.* Nat Commun. **7**: p. 11350.

Chapter 2 Supplemental Figures

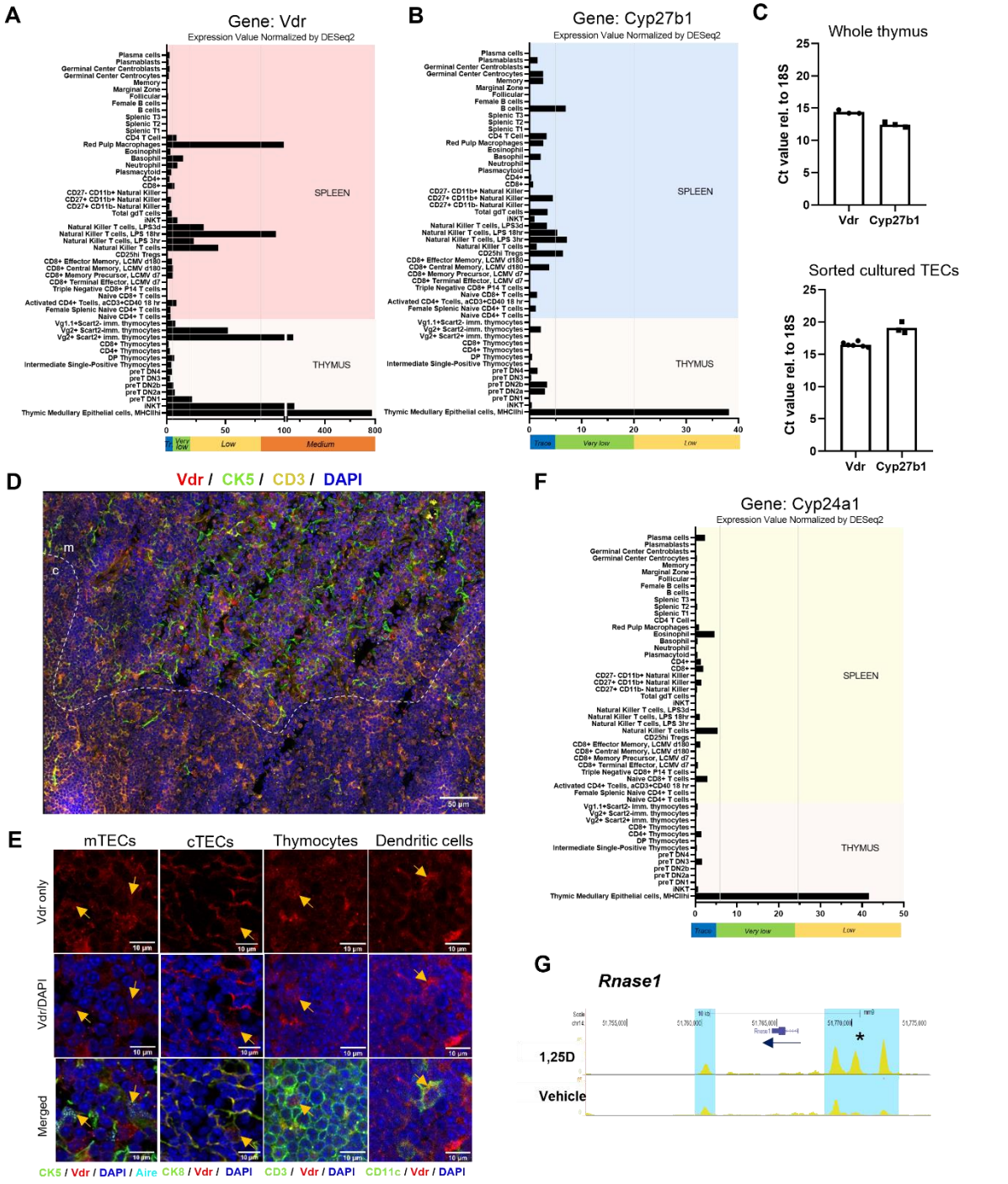

Supplemental Fig 1 : Active 1,25D signaling in the thymus. ***A.*** *RNA sequencing data showing Vdr mRNA expression in different mouse thymic and splenic cell types [13].* ***B.*** *RNA sequencing data showing Cyp27b1 mRNA expression in different mouse thymic and splenic cell types [13].* ***C.*** *Detection of Vdr and Cyp27b1 mRNA in mouse thymi (top) or sorted TECs cultured for 6h (bottom), gene expression normalized to 18S and shown as ΔCt values.* ***D.*** *Immunohistochemical staining of mouse thymus showing cortical (c) and medullary (m) Vdr staining in thymocytes (CD3+) and mTECs (CK5+).* ***E.*** *IF microscopy showing Vdr staining in Aire⁺ mTECs, cTECs, thymocytes, and dendritic cells.* ***F.*** *RNA sequencing data showing Cyp24a1 mRNA expression in different mouse thymic and splenic cell types [13].* ***G.*** *UCSC browser image showing mouse intestine VDR ChIP-seq tracks (GEO accession: GSE69179) at the Rnase1 locus. The areas surrounding the VDR binding sites up- and downstream (regions highlighted in blue) of the genes are shown. The binding site chosen for ChIP analysis is indicated with the asterisk. RNA sequencing data shown in Figs A,B and F was derived from data assembled by the ImmGen consortium [13]. Data are individual mice (N ≥ 3, ≥ 1 experiment).*

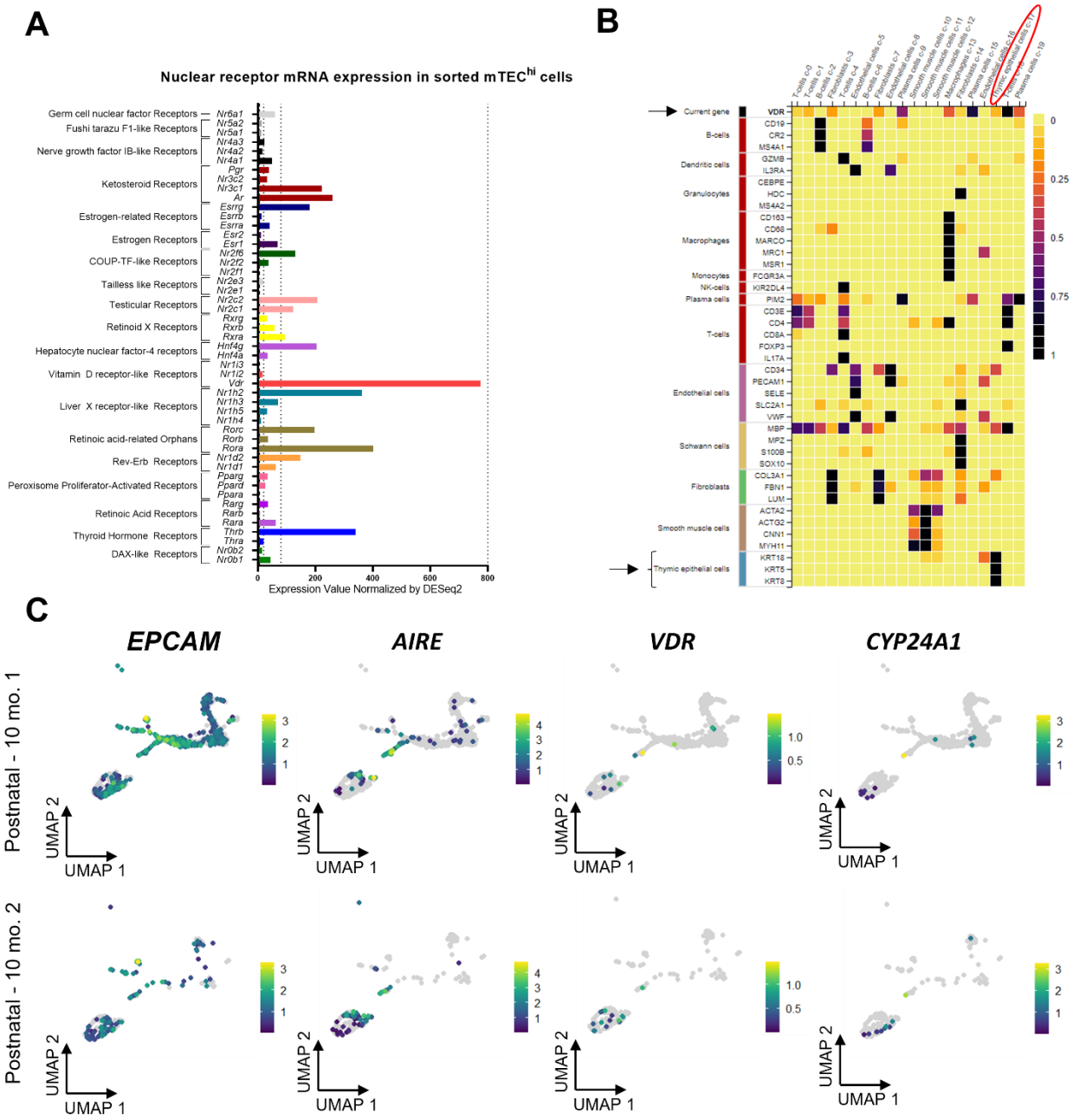

Supplemental Figure 2

Nuclear receptor mRNA expression in sorted mTEChi cells.
A. *RNA sequencing data showing mRNA expression of various nuclear receptors in sorted mouse MHC-II^{hi} mTECs (This data was derived from data assembled by the ImmGen consortium) [13].* ***B.*** *RNA sequencing data of human thymic cells indicating VDR mRNA expression (arrow) in human TECs. TEC markers KRT5, 8 and 18 are used a positive controls for TECs (double arrow) (Human Protein Atlas proteinatlas.org, image credit: Human Protein Atlas, https://www.proteinatlas.org/ENSG00000111424-VDR/single+cell+type/thymus, Tabula Sapiens, C., R.C. Jones, et al. 2022. The Tabula Sapiens: A multiple-organ, single-cell transcriptomic atlas of humans.* Science. **376**(6594): p. eabl4896*).* ***C.*** *scRNAseq analysis of TEC samples from duplicate 10-month-old human post-natal thymi* (GSM4466784/5) *[14].*

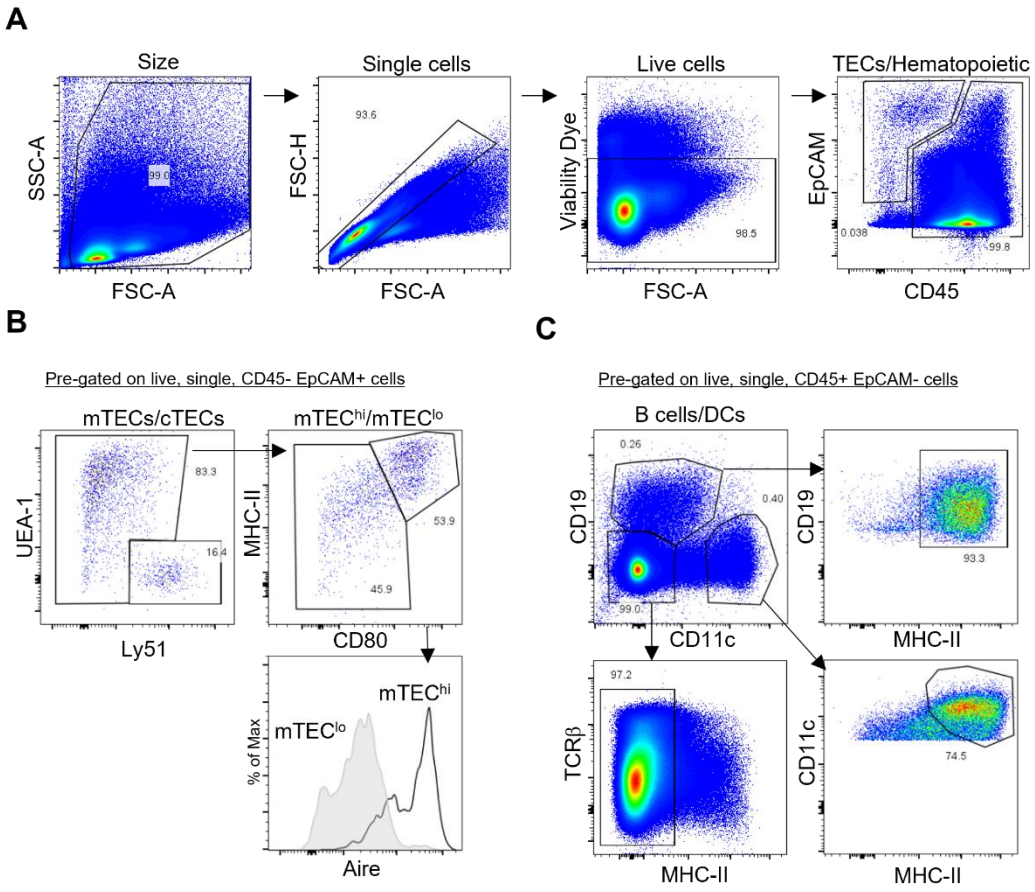

Supplemental Figure 3

Flow cytometry gating strategy for TEC subtypes and various hematopoietic cells

A-C. *Representative flow cytometry gating strategy including pre-gating on live, single, and stromal or hematopoietic cells (A); stromal cells (B) including mTEChi cells (UEA-1$^{+/-}$, Ly51^{-}, MHC-II^{hi}, CD80^{+}), mTEClo cells (UEA-1$^{+/-}$, Ly51^{-}, MHC-II$^{+/-}$, CD80^{-}), cTECs (Ly51^{+}, UEA-1^{-}); hematopoietic cells (C) including B cells (CD19^{+}, MHC-II^{+}, CD11c^{-}), DCs (CD11c^{+}, MHC-II^{+}, CD19^{-}), and thymocytes (TCRb$^{+/-}$, MHC-II^{-}, CD19^{-}, CD11c^{-}).*

	Target	Conjugate	Host	Clone	Company	Application	Reference
Primary antibodies	CD11c	Unconjugated	Armenian Hamster	N418	ThermoFisher	IF	14-0114-81
	Cyp27b1	Unconjugated	Rabbit	Polyclonal	ThermoFisher	IF/FC	PA5-79128
	Cytokeratin 5	Unconjugated	Rabbit	Poly19055	Biolegend	IF	905503
	TROMA-1 (Cytokeratin 8)	Unconjugated	Rat	N/A	DSHB	IF	DSHB
	Mouse/Human Vdr	Unconjugated	mouse	D-6	Santa Cruz	WB/ChIP	sc-13133
	Mouse/Human Aire	Unconjugated	Rat	5H12	ThermoFisher	ChIP/CoIP	14-5934-82
	CD16/32 (Fc block)	Unconjugated	Rat	S17011E	Biolegend	FC	156603
	EpCAM	PeCy7		G8.8	ThermoFisher	FC	25-5791-80
	CD45	eFluor 450		30-F11	ThermoFisher	FC	48-0451-82
	Aire	eFluor660		5H12	ThermoFisher	IF/FC	50-5934-80
	MHC Class II	APC-eFluor780		M5/114.15.2	ThermoFisher	FC	47-5321-80
	CD19	AF700		1D3	ThermoFisher	FC	56-0193-82
	CD3	eFluor660		17A2	ThermoFisher	IF/FC	50-0032-80
	Ly51	eFluor 710		6C3	ThermoFisher	FC	46-5891-80
	NK1.1	PE		PK136	Biolegend	FC	108707
	CD80	BV650		16-10A1	Biolegend	FC	104732
	CD11c	BV785		N418	Biolegend	FC	117335
	TCRβ	BV711		H57-597	Biolegend	FC	109243
	UEA-1	Dylight 594		N/A	Vector laboratories	FC	DL-1067
Secondary antibodies	horse anti mouse IgG	HRP		N/A	Cell Signaling	WB	#7076
	goat anti armenian hamster IgG	AF594		N/A	Biolegend	IF	405512
	goat anti rabbit IgG	AF488		N/A	ThermoFisher	IF/FC	A11034
	goat anti rat IgG	AF546		N/A	ThermoFisher	IF	A11081
Other reagents	DAPI	N/A		N/A	ThermoFisher	IF	D1306

Supplemental Table 1 – List of antibodies and reagents used.

Linking Chapter 2 to Chapter 3

Vitamin D deficiency is a risk factor for autoimmune diseases, and early work provided evidence that the vitamin D receptor was expressed in the thymus. In Chapter 2, we investigated the potential for vitamin D signaling in the thymus and its possible effects on central tolerance. We demonstrated that the Vdr and Cyp27b1 are widely expressed in the thymus, in both stromal and hematopoietic cell types, and that vitamin D signaling was active. Surprisingly, incubation of thymic slices with 1,25D for 6 hours induced Aire mRNA and protein, in addition to Aire-dependent TRA gene expression, highlighting a potential function for vitamin D signaling in central tolerance. The observation that human and mouse Aire contain 4 LXXLL motifs, found in cofactors that bind to agonist-bound nuclear receptors such as the Vdr, raised the possibility that they may interact *in vivo*. We demonstrated that the Vdr and Aire are interaction partners and are recruited to VDRE's in a 1,25D-dependent manner. Furthermore, we found that the Aire functioned as a coactivator of vitamin D-dependent transcription. These data suggest that interactions of Aire with nuclear receptors such as the Vdr may be a targeting mechanism by which Aire is recruited to its target genes. In chapter 3, we expanded on our initial study by investigating how the absence of 1,25D in *Cyp27b1* KO mice, which lacks the enzyme needed to generate 1,25D from 25D, affects thymic development, and in particular, TEC maturation.

Chapter 3: Altered epithelial cell differentiation and premature aging in the thymus in the absence of vitamin D signaling

Patricio Artusa[1], Loan Nguyen Yamamoto[2,3], Camille Barbier[1], Haig Djambazian[4], Yashar Aghazadeh Habashi[1], Aiten Ismailova[1], Marie-Ève Lebel[5], Ioannis Ragoussis[4], David Goltzman[2,3], Heather Melichar[5], and John H. White[1,2*]

Departments of Physiology[1] and Medicine[2], McGill University, Montreal Qc, Canada. Calcium Research Laboratory[3], McGill University Health Centre, Montreal QC, Canada. McGill University Genome Centre[4], McGill University, Montreal QC, Canada. Département de Médecine[5], Université de Montréal and Maisonneuve-Rosemont Hospital Research Center, Montreal QC, Canada.

*To whom correspondence should be addressed: john.white@mcgill.ca

Abstract

Interactions between thymocytes and medullary thymic epithelial cells (mTECs), which are critical for establishment of central tolerance, depend on the mTEC transcription factor autoimmune regulator (Aire) and Aire-driven expression of tissue restricted antigen (TRA) genes. Importantly, vitamin D signaling regulates Aire and TRA expression in mTECs, providing a basis for links between vitamin D deficiency and increased autoimmunity. Here, we show that mice lacking *Cyp27b1*, the enzyme catalyzing synthesis of hormonally active vitamin D, display a profound reduction in thymic cellularity. Moreover, Aire$^+$ mTECs are reduced 50%, TRA mRNA expression is attenuated, and medullary-cortical boundaries are largely absent in *Cyp27b1* KO mice. Correspondingly, T cell negative selection is impaired in null thymi. Single cell RNAseq revealed that *Cyp27b1* loss skews mTEC differentiation toward CCL21$^+$ cells at the expense of Aire$^+$ mTECs. Moreover, *Cyp27b1* KO TEC gene expression profiles displayed hallmarks of premature aging, with reduced expression of longevity factors *Igf1* and *Fgf21*, as well as genes implicated in maintenance of thymic cellularity. Thus, thymic vitamin D signaling regulates mTEC differentiation and function, and retards thymic aging.

Introduction

The thymus is a critical primary lymphoid organ whose microenvironment supports the multi-step process of T-lymphopoiesis. This gives rise to T cell populations that can recognize and eliminate foreign antigens but are tolerant of self - the body's own components [1]. Two-way communication of thymocytes with the thymic stroma, particularly thymic epithelial cells (TECs), is critical for normal lymphopoiesis. This interplay controls developing T cell migration, proliferation, differentiation and survival. TECs are organized spatially and functionally into cortical (cTEC) and medullary (mTEC) compartments [2]. Early T cell developmental checkpoints such as lineage commitment and positive selection are orchestrated by cTECs, whereas subsequent steps, including negative selection of self-reactive cells or differentiation into $FoxP3^{+}CD25^{+}$ regulatory (T_{reg}) cells, are largely controlled by mTECs. It is important to note that these processes occur optimally early in life, as the thymus is the most rapidly aging organ in the body. The aging thymus undergoes a process of regression, which is accompanied by a loss of cellularity and morphological disorganization [3]. In mice, this process starts within 4 weeks of life, with the degeneration of the TEC compartment playing a major role [4].

TEC populations are not uniform, and mTECs undergo a differentiation process to produce multiple specialized compartments [2]. mTEC subsets differ in major histocompatibility complex (MHC) and co-stimulatory molecule expression [5-9], which is required for negative selection and Treg development [10, 11]. $mTEC^{lo}$ ($CD80/CD86^{lo}$ MHC class II^{lo}) cells include "immature" progenitors, functionally mature cells and terminally differentiated TECs [5, 6, 12]. Immature $mTEC^{lo}$ differentiate into an $mTEC^{hi}$ population that expresses higher levels of co-stimulatory molecules and MHC class II ($CD80/CD86^{hi}$ MHC class II^{hi}) [13, 14]. Promiscuous gene expression by mTEC populations is critical for tolerance to tissue restricted antigens (TRA) [15-17]. The

frequency of thymic MHC class II^+ cells expressing a given TRA correlates with the mechanism of T cell tolerance [18]. A subset of $mTEC^{hi}$ cells express autoimmune regulator (Aire), which drives the transcription of numerous TRA genes and is critical for establishment of T cell tolerance [19]. Loss of human AIRE causes APECED (autoimmune polyendocrinopathy-candidiasis-ectodermal dystrophy), a rare, complex disease leading to tissue-specific autoimmune issues that differ widely between individuals.

We have been interested in how vitamin D signaling contributes to critical thymic events controlling establishment of T cell tolerance. Hormonally active 1,25-dihydroxyvitamin D (1,25D) is produced by consecutive hydroxylations; largely hepatic 25-hydroxylation, followed by 1a-hydroxylation catalyzed by the enzyme Cyp27b1 [20]. 1,25D activates the vitamin D receptor (Vdr), a member of the nuclear receptor family and ligand-regulated transcription factor. We found that the Vdr and Cyp27b1 are expressed in both hematopoietic and stromal compartments of the thymus, including mTECs, and that, moreover, Aire functions as a transcriptional cofactor of the Vdr [21]. These findings link vitamin D signaling to transcriptional events required for central tolerance. They also provide a molecular basis for clinical studies linking vitamin D deficiency to increased risk of development of autoimmune disorders [22-29].

Here, we investigated the effects of loss of vitamin D signaling on thymic morphogenesis, and differentiation and function of TECs using a *Cyp27b1* knockout (KO) mouse model. Thymi of null animals displayed a combination of markedly reduced cellularity, which accelerated with age, and impaired mTEC differentiation, favoring $CCL21^+/Aire^-$ over $Aire^+$ cells. This coincided with reduced Aire expression, impaired TRA gene transcription in *Cyp27b1* KO thymi, and a reduction in T cell negative selection. Moreover, single cell gene expression profiling of TEC populations revealed gene expression patterns in null animals consistent with premature thymic

aging, characterized by impaired expression of key thymic longevity factors. Based on these findings, we conclude that vitamin D signaling is necessary for normal thymic development and longevity, and for mTEC differentiation and function necessary for establishment of central tolerance.

Materials and Methods

Mice

Cyp27b1 KO mice were previously generated as described [30] on a mixed C56BL/6 and Balb/c background and housed in the McGill University Health Center Research Institute. KO mice were backcrossed with C57BL/6 mice for 2–5 generations. Wildtype C57BL/6J mice were used for controls. No difference in any measurements were observed when comparing the original KO to wildtype verses backcrossed littermates. KO or heterozygous breeders and experimental KO mice were kept on a rescue diet [30] to normalize Ca^{2+} levels.

Flow Cytometry

Up to $5x10^6$ cells were incubated with fixable viability dye (Thermo Fisher 65-0866-18) diluted in PBS at 4 °C for 20 min in 96-well U or V bottom plates. Cells were washed and resuspended with FACS buffer (PBS $^+$ 1% FBS, 2 mM EDTA) containing fluorophore conjugated antibodies (Abs) and FC block (Supplemental Table 1), and incubated for 30 min at 4 °C. For intracellular proteins, cells were fixed and permeabilized using the FoxP3 Fix/Perm Kit (Thermo Fisher) for 30 min at room temperature (RT), protected from light. Afterwards, cells were resuspended in 1X Perm/Wash buffer containing fluorophore-conjugated Abs and incubated for 30 min at 4 °C. Cells and UltraComp ebeads (Thermo Fisher) were used for compensation controls. Samples were acquired on a LSR Fortessa (BD Biosciences) and analyzed with FlowJo (BD Biosciences).

Cell sorting

TECs were enriched prior to sorting by positively selecting for $EpCAM^+$ cells by MACS (Miltenyi Biotec 130-105-958). Flow cytometric staining was performed as described above. Total TECs (Live, $EpCAM^+$, $CD45^-$) were sorted with a BD FACSAria Fusion into cold FACS buffer.

Immunofluorescence microscopy

Samples were fixed with 4% PFA and incubated with sucrose (Bioshop) solutions (10–30%) for ~8 hr each. Samples were embedded using base molds (Fisherscientific) containing O.C.T. compound (Fisherscientific), frozen on dry ice, and stored at -80 °C. 5–20 µm sections were obtained with a Leica CM3050 S Cryostat and Superfrost Plus slides (Fisherscientific). A hydrophobic barrier was applied (Millipore Sigma) and slides were blocked with PBS containing 2% BSA (w/v), 0.3% Triton X-100, 1% FBS, and 10% goat serum (Blocking buffer) for 1 hr at RT. Slides were incubated in a humidified chamber with primary Abs diluted in blocking buffer (Supplemental Table 1) overnight at 4 °C, secondary Abs conjugated to fluorophores diluted in blocking buffer for 1 hour at RT, fluorophore conjugated primary Abs for 1 hour at RT, and DAPI diluted in PBS for 5 minutes at RT. Slides were washed 3 times with 100 µM Tris buffer between each step, mounted with Fluoromount 4G (Thermo Fisher) and cover slips (No. 1.5;Fisher scientific), and imaged with a Zeiss LSM710 confocal microscope with 20–100X objectives. Images were analyzed with FIJI (ImageJ).

Gene expression

$5x10^6$ cells were lysed and RNA was extracted using FavorPrep Total RNA Mini Kit (Favorgen) and quantified with a NanoDrop 2000c (Thermo Fisher). 500ng of RNA was converted to cDNA

using AdvanTech 5X master mix. Oligo sequences (available upon request) were designed with Primer3 and primer specificity was verified by BLAST. 10 ng of cDNA was used per qPCR reaction and BlasTaq 2X qPCR MasterMix (abm). qPCR reactions and melting curves were done with a LightCycler 96 (Roche). Gene expression was normalized to 18S values. Fold changes for thymic slices were calculated by comparing gene expression between treatment conditions from individual mice.

Preparation of single cell suspensions

Thymi were cut into 1 mm pieces and digested in RPMI 1640 (Wisent) containing 10% FBS (Millipore Sigma) (R10) and Collagenase D (250 µg/mL), Papain (250 µg/mL), and DNase I (200 µg/mL) for 30 min at 37 °C with shaking. Cells were further released by pipetting up and down. Digestion buffer was freshly prepared the day of each experiment. Spleens were crushed through 70um filters with the back of a syringe and washed with 10mL of RPMI + 1% FCS. After centrifugation, red blood cells were lysed with ACK lysing buffer (Gibco) for 3 min at RT, washed, and counted. Bone marrow was flushed from isolated bones with 10 mL of RPMI using a 22G needle, centrifuged and resuspending in ACK lysing buffer for 3 min at RT, washed, and counted.

Single cell RNA sequencing

Two 8-week-old male wildtype and KO littermates were euthanized and TECs were enriched for and sorted as described above. A 10X Genomics Single-Cell 3′ transcriptome library was prepared (Génome Québec). Libraries were generated using the Chromium Next GEM Single Cell 3' GEM, Library & Gel Bead Kit v3.1, Chromium Next GEM Chip G Single Cell Kit and Single Index Kit T Set A (10X Genomics) as per the manufacturer's recommendations. The

targeted cell recovery was set to 3000. Libraries were quantified using the KAPA Library Quantification Kits - Complete kit (Universal) (Kapa Biosystems). Average fragment size was determined using a LabChip GXII (PerkinElmer) instrument. The libraries were normalized and pooled and then denatured in 0.02N NaOH and neutralized using HT1 buffer. The pool was loaded at 375pM on an Illumina NovaSeq SP lane using Xp protocol as per the manufacturer's recommendations. The run was performed for PE 28x91. A phiX library was used as a control and mixed with libraries at 1% level. Base calling was performed with RTA v3. bcl2fastq2 v2.20 was then used to demultiplex samples and generate Fastq reads. Cells were analyzed using the Seurat package. First, cells were QC'd by filtering for number of genes, number of unique UMIs, and mitochondrial content. Second, all four samples were integrated. The new integrated object was scaled and normalized, and dimensionality reduction was conducted with PCA using the first 20 principal components. Lastly, UMAPs were constructed, and clusters were identified using the shared nearest neighbor algorithm based on the first 20 principal components. For RNA velocity analysis, loom files were generated for individual samples. RNA velocity was performed with jupyter notebook using scvelo and scanpy libraries. Velocity plots were generated using the dynamical model. A list of 300 differentially expressed genes prepared from KO1 and WT1 samples were used for ingenuity pathway analysis.

Statistical analyses

Statistics were calculated using GraphPad Prism version 8 with parametric unpaired t tests, and non-parametric tests or parametric paired t tests for thymic slice data. Statistical significance is indicated by p-values * $p < 0.05$, ** $p < 0.01$, *** $p < 0.001$.

Results

Reduced cellularity and impaired negative selection in *Cyp27b1* KO thymi.

While thymi from 4-week-old wild-type and KO animals were similar in size, those of 6–10-week-old *Cyp27b1* KO mice were significantly smaller than their control counterparts (Figure 1A, Supplemental Figures 1A-B), corresponding to an approximately 50% reduction in total cellularity (Figure 1B). The reduced thymic size was accompanied by decreased splenic total $CD4^+$ and $CD8^+$ T cell numbers in KO animals (Figure 1C), consistent with systemic lymphopenia at 6-10 weeks. We then asked whether loss of *Cyp27b1* led to defects in specific hematopoietic components of the thymus. Thymocyte development in KO thymi was characterized by increased frequencies of $CD4^+$ single positive (4SP) thymocytes, and similar frequencies of double negative (DN), double positive (DP) and $CD8^+$ single positive (8SP) thymocytes (Figures 1D-E). The frequency of $FoxP3^+$ $CD25^+$ T_{regs} within total 4SP thymocytes was unaltered (Supplemental Figures 1C-D). The increase in 4SP thymocytes could not be explained by improved positive selection, as determined by CD5, CD69, or TCRβ expression (Supplemental Figure 1E). We further investigated the expression of the transcription factor Helios, which is upregulated in negatively selected thymocytes and serves as a marker of autoreactive $FoxP3^-$ thymocytes [31, 32]. There was a 40% reduction in the frequency of $Helios^+$ $FoxP3^-$ 4SP thymocytes (Figures 1F-G) in KO thymi, suggestive of impaired negative selection. Moreover, the number of cleaved caspase-3^+ thymocytes was reduced in the thymic medulla of KO mice (Figures 1H-I, Supplemental Figure 1G), further supporting this hypothesis.

γδ T cells also undergo lineage commitment and development in the thymus, but were largely unaffected by the loss of vitamin D signaling (Supplemental Figures 1H-I). Thymocyte development is supported by numerous antigen presenting cells (APCs) including resident DCs

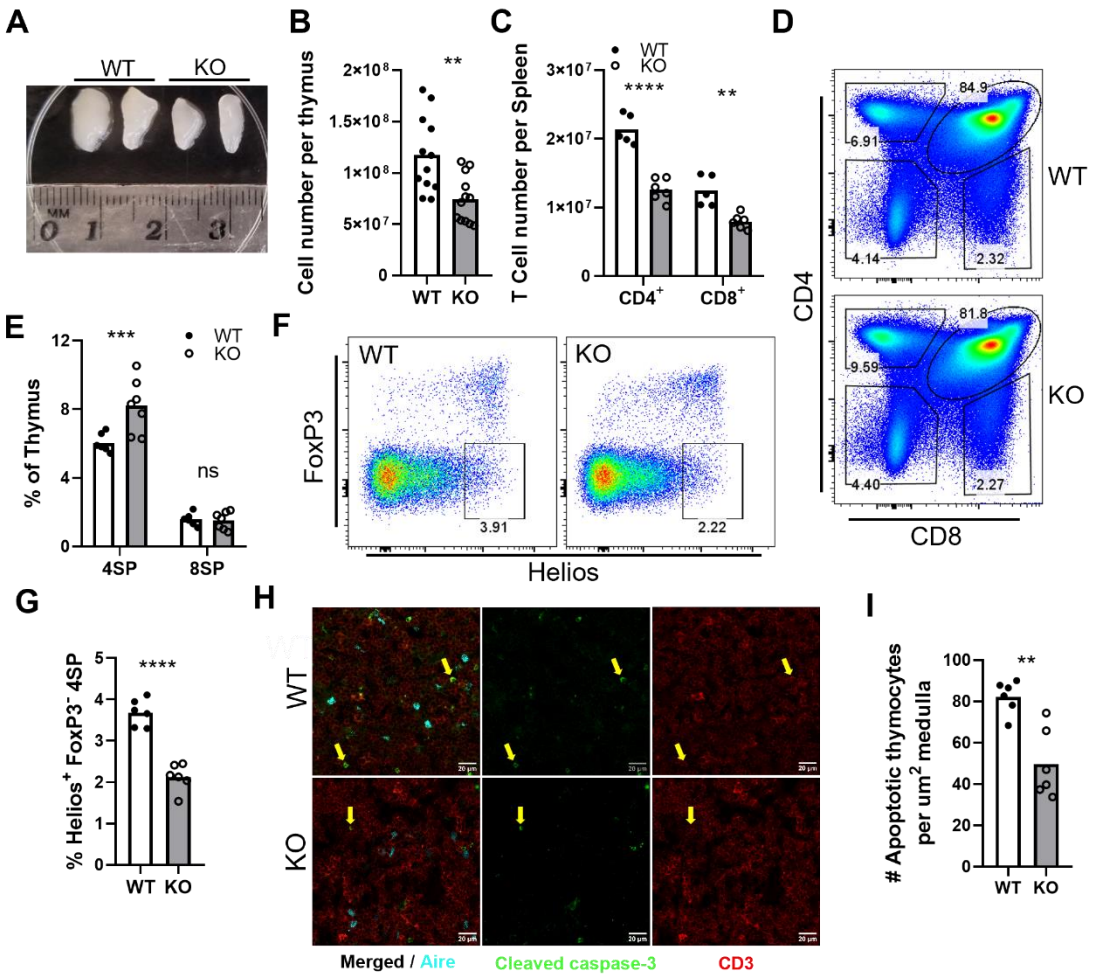

Figure 1. Reduced thymic cellularity and altered thymocyte selection in Cyp27b1 KO mice
__A.__ Representative pictures of 2 wildtype and 2 KO thymic lobes. __B.__ Total thymic cell number in 6–10-week-old mice.__C.__ Total CD4+ and CD8+ splenic T cell numbers in 6-10-week old mice.__D,E.__ Representative flow cytometry plots of thymocyte development (pre-gated on live, single cells) (D) and quantification of single positive (SP) populations (E). __F,G.__ Representative flow cytometry plots showing the frequency of highly autoreactive Helios+ FoxP3- 4SP thymocytes in WT vs KO thymi (F) and summary data (G).__H,I.__ Immunofluorescence microscopy images of cleaved-caspase 3 staining in the thymic medulla in non-epithelial cells (H) and quantification of positive cell density (I). All experiments were repeated at least twice with at least n=3 mice per group.

and B cells. Notably, thymic B cells express Aire and play a non-redundant role in the negative selection of autoreactive thymocytes [33]. In KO mice, DC frequencies were unaltered (Supplemental Figures 1J-K), but B cell frequencies were halved (Supplemental Figures 2A-B). However, Aire expression was unaffected in KO B cells (Supplemental Figures 2C-D). Moreover,

there was no evidence of a failure to commit to tissue residency as measured by frequencies of committed thymic IgM^{+} IgD^{-} and IgM^{-} IgD^{-} subpopulations (Supplemental Figures 2E-F), which would be indicative of a potentially systemic defect. Indeed, B cell numbers were also halved in KO spleens (Supplemental Figure 2G), and analysis of bone marrow showed an accumulation of pro B cell precursors and reduction in pre-B cell progeny (Supplemental Figures 2H-I). Collectively, these data demonstrate that lymphocyte homeostasis is perturbed in the absence of 1,25D with profound defects in thymic size and impaired negative selection of thymocytes.

Altered mTEC differentiation in *Cyp27b1* KO thymi.

mTECs are critically important for the negative selection of overly self-reactive thymocytes. We previously found that 1,25D signaling induced Aire expression in mouse thymic slices [21]. Consistent with these findings, there was a 40% reduction in *Aire* mRNA (Figure 2A), and 50% reduction in Aire^{+} cells as judged by immunofluorescence microscopy in null thymi

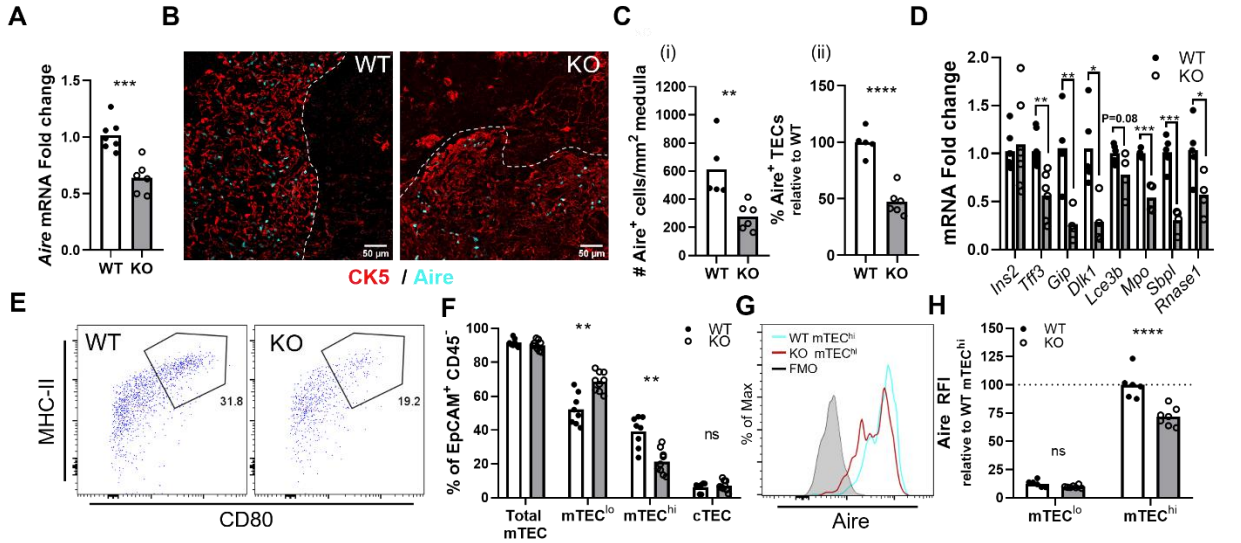

Figure 2. Impaired mTEC differentiation and Aire expression in Cyp27b1 KO mice ***A.*** *qPCR detection Aire mRNA expression in WT vs. KO mice.* ***B,C.*** *Immunofluorescent microscopy images showing Aire^{+} cells in WT versus KO thymi (B) and quantification (C). White line denotes regions containing Aire^{+} cells.* ***D.*** *Reduced TRA gene expression in KO mice. All experiments were repeated at least twice with at least n−3 mice per group.* ***E.*** *Representative flow cytometry plots of mTEC^{hi} cells (MHC-II^{hi} CD80^{+}) in WT versus KO thymi.* ***F.*** *Quantification of cTEC and mTEC frequencies in WT versus KO samples.* ***G.*** *Representative flow cytometry plot of Aire expression in WT versus KO mTEC^{hi} cells.* ***H.*** *Quantification of Aire expression in mTEC^{lo} and mTEC^{hi} cells, relative to WT mTEC^{hi} cells.*

(Figures 2 B,C). Furthermore, the expression of multiple Aire-dependent TRA mRNAs was reduced in the absence of *Cyp27b1* (Figure 2D). These observations were corroborated by flow cytometry (Figures 2E-F), which showed a depletion of mature Aire^{+} mTECs (mTEC^{hi}) at the expense of less mature mTECs (mTEC^{lo}), whereas cTEC frequencies were unaffected. Notably, Aire mean fluorescence intensity (MFI) was reduced by 30% in KO versus control mTEC^{hi} cells (Figures 2G-H). Taken together, this indicates that Aire expression is diminished by two factors: impaired mTEC^{hi} differentiation and reduced gene expression within differentiated cells. Closer analysis by IF revealed that the thymic medulla, which is defined by cytokeratin 5 expression (CK5) and Aire expression, was disorganized in KO mice (Figures 3A-B). Co-staining with CK5 and cytokeratin 8 (CK8), a pan-TEC marker, revealed a greatly increased number of CK5/8 double-positive cells in the KO cortex, extending well beyond the domains containing Aire^{+} cells

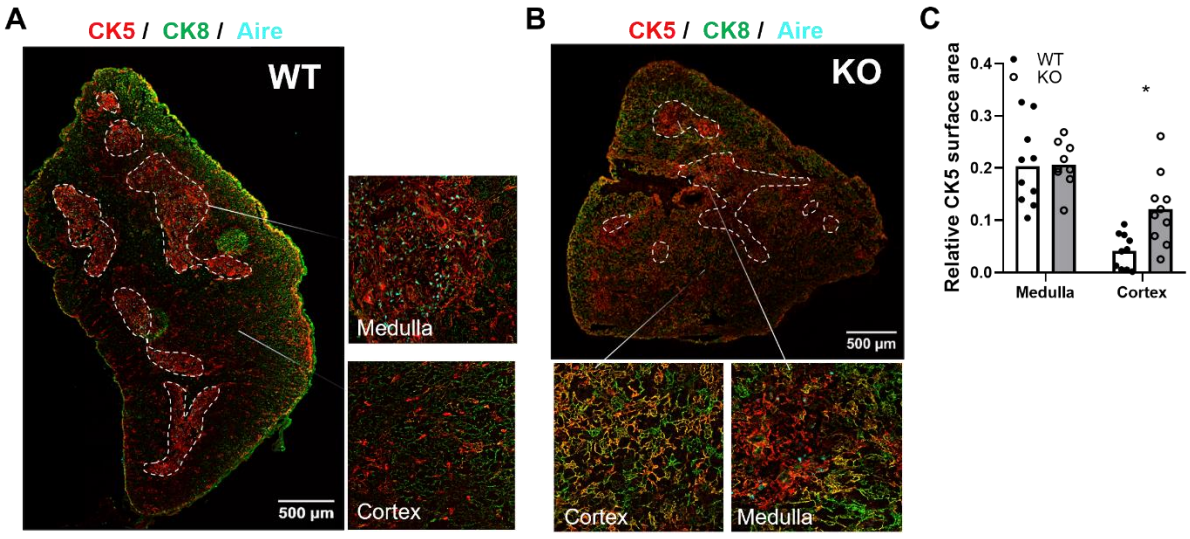

Figure 3. Disorganized thymic architecture in Cyp27b1 KO mice ***A.*** *Representative image of a wildtype thymus showing Aire staining restricted to areas of concentrated CK5 staining (medulla).* ***B.*** *Representative image of a Cyp27b1 KO thymus showing disseminated CK5 staining throughout the tissue without corresponding Aire+ cells.* ***C.*** *Quantification of CK5 staining in the medulla (defined as Aire^{+} regions) and cortex (defined as Aire- regions). All experiments were repeated at least twice with at least n=3 mice per group.*

(Figures 3A-B). Thus, mTEC differentiation and normal thymic morphology are disrupted in knockout animals.

Single-cell RNA sequencing of TEC populations reveals disrupted mTEC differentiation in *Cyp27b1* KO mice

To investigate further the defects in TEC development in KO animals further, we sorted total TECs (CD45- EpCAM^{+}) from two control and two KO mice and performed single cell RNA sequencing (Figure 4A). After pre-processing and integration of our samples using Seurat, we annotated 18 clusters (Figure 4B) based on differentially expressed genes (DEGS; see supplemental Table 1 for top 25 DEGs in each cluster, and Supplemental Figure 3A for heatmap). mTEClo, mTEChi and post-Aire cells predominated, along with smaller populations of cTECs and Tuft cells [34-36]. In addition, a cluster enriched for markers of S phase and G2M was consistent with previously described transient amplifying cells (TAC-TECs) [35]. A number of minor clusters were also identified, including those with markers for ciliated cells [37], Hassall's corpuscles, as well as populations with markers expressed in mTEC neuro and mTEC myo cells previously identified in human thymic samples (Figure 4B; Supplemental Table 1) [36].

As expected, the number of mTEC^{hi} cells were reduced in KO samples, whereas KO populations were enriched for *Ccl21a*$^{+}$ cells (Figures 4B-C, Supplemental Figures 3B-D). Overexpression of *Ccl21a* transcripts in KO thymic samples was validated by RT/qPCR (Supplemental Figure 3E) and flow cytometry (Figures 4D-E). Consistent with previous studies [34, 37], these cells were also enriched for expression of *Krt5*, *Il7*, *Lifr*, and podoplanin (*Pdpn*; Supplemental Figures 4A-F). CCL21^{+} mTECs have been identified as precursors of mature Aire^{+}

mTECs [39], suggesting that loss of 1,25D signaling partially blocks mTEC differentiation at this stage. However, a recent study using RNA velocity analysis proposed that *Ccl21a*$^{+}$ mTECs represent a distinct differentiation path from Aire^{+} mTECs, with TAC-TECs as the initiation point

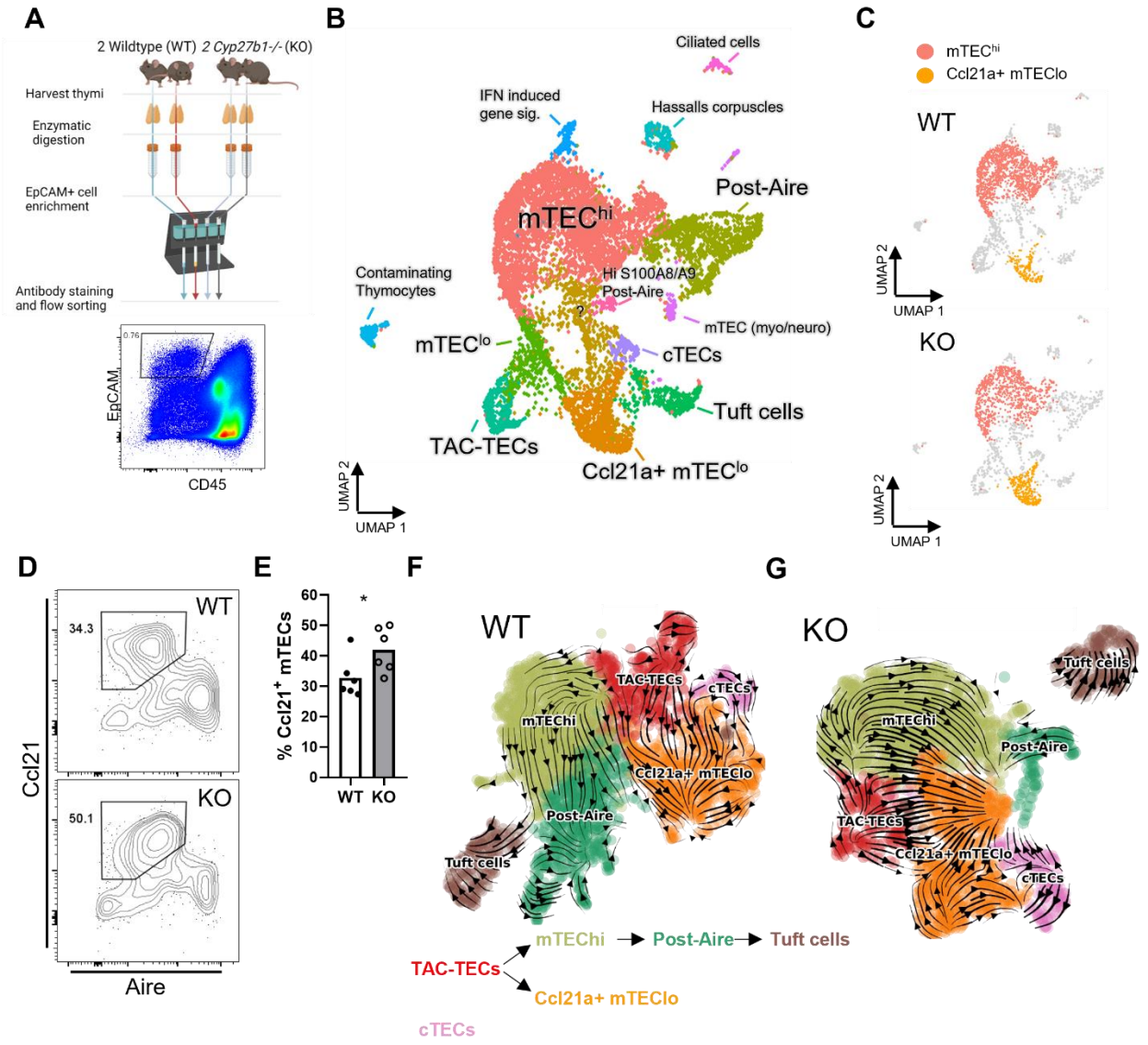

Figure 4 Divergent mTEC differentiation in Cyp27b1 KO mice ***A.*** *Schematic of single cell RNA sequencing sample preparation.* ***B.*** *Cluster annotation of integrated Seurat object containing all four samples, based on differential gene expression.* ***C.*** *Comparison of WT and KO clusters densities, mTEChi and Ccl21a+ mTEClo are highlighted.* ***D,E.*** *Validation of increased Ccl21+ mTECs in KO thymi by flow cytometry (pre-gated on live, single, CD45-, EpCAM+, UEA-1+, Ly51- cells)(D) and summary data (E).* ***F.*** *Representative RNA velocity plot of a WT sample, arrows point towards direction of predicted differentiation based on RNA splicing dynamics.* ***G.*** *RNA velocity plot of a KO sample. Flow cytometry experiments were done twice with n=3 mice per group.*

for both subsets. RNA velocity incorporates information about spliced versus unspliced RNAs in single cells to predict transitions in cell state and estimate differentiation trajectories [40]. We utilized scVelo, a toolkit developed for RNA velocity analysis [41], to estimate RNA velocity in individual sequenced samples. After pre-processing raw data with scanpy, clusters for the new UMAPs were annotated based on DEGs, and minor clusters and those unrelated to TECs (e.g., thymocytes) were removed prior to analysis. Velocity analysis of wild-type (Figure 4F, Supplemental Figure 5A) samples yielded a result consistent with the bifurcation model, where *Ccl21a*$^{+}$ mTECs do not appear to differentiate into mTEChi cells. The trajectory of RNA velocity analysis of KO samples was similar to wild-type, but with an increased density of arrows leading from TAC-TECs towards *Ccl21a*$^{+}$ mTECs (Figure 4E, Supplemental Figure 5B). The presence of a bifurcation was additionally corroborated by pseudotime analysis using monocle3 (Supplemental Figures 5C-D). These results would suggest that instead of impaired mTEClo-mTEChi differentiation in the absence of 1,25D, differentiation is skewed towards CCL21^{+} Aire^{-} cells at the expense of Aire^{+} cells.

Cyp27b1 KO TEC populations display hallmarks of premature aging.

TEC differentiation is regulated by multiple layers of inputs including intracellular signaling and crosstalk with thymocytes and other stromal cells [42]. To better understand the dysregulated signals in KO TECs we utilized Ingenuity Pathway Analysis (IPA). Notably, VDR/RXR activation was among the top 5 altered canonical pathways in KO vs control TECs (Supplemental Figure 6A). One of the advantages of IPA is the functionality to directly compare similar datasets. After filtering for thymic datasets and ranking by activation Z-score, the most similar datasets to ours included LCMV infected versus control thymi (Z-score = 32.67%); LCMV

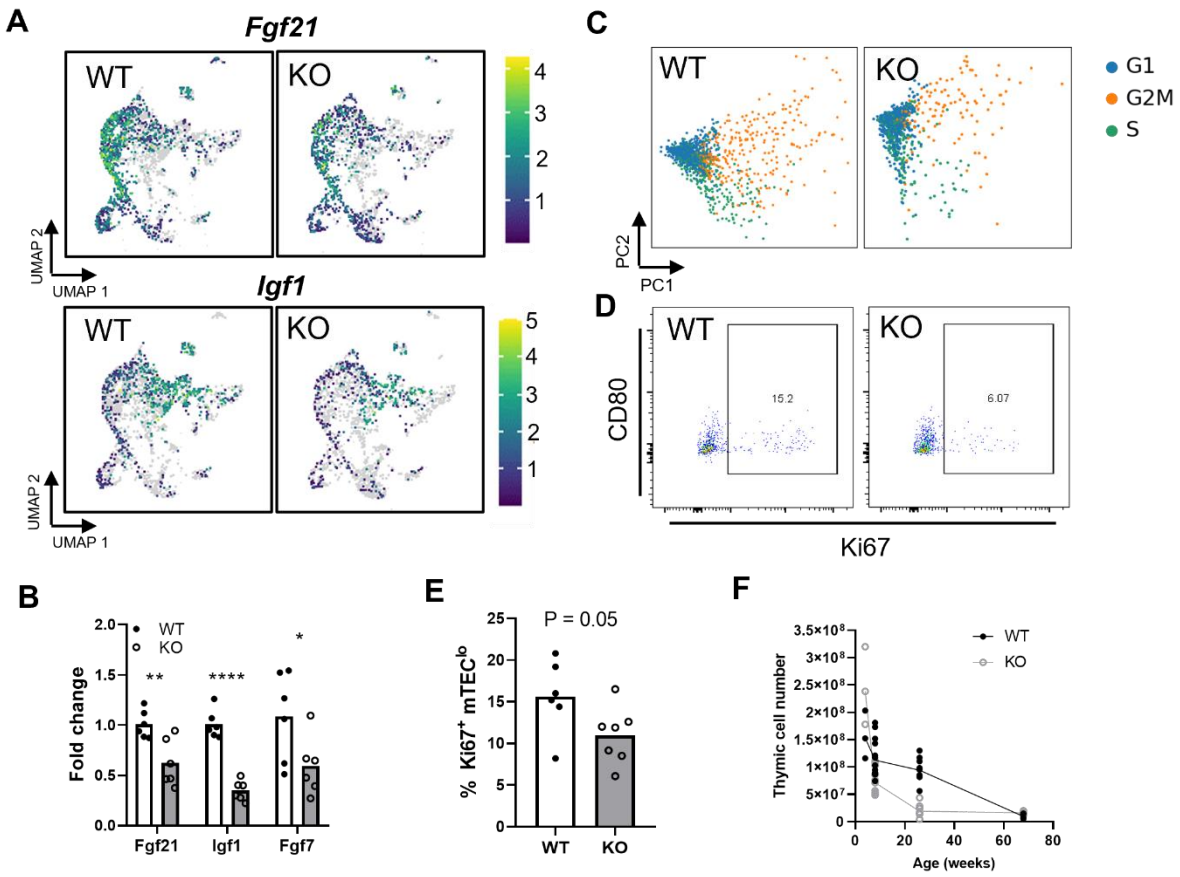

Figure 5 Accelerated thymic involution in Cyp27b1 KO mice ***A.*** *UMAPs indicating decreased expression of pro-longevity factors in KO TECs.* ***B.*** *Validation of thymic involution related gene expression.* ***C.*** *Cell cycle phase scoring for representative WT and KO TECs.* ***D,E.*** *Flow cytometric analysis of Ki67+ in mTEC^{lo} cells.* ***F.*** *Total thymic cell counts from young to old mice showing accelerated involution in KO samples. All experiments were repeated at least twice with at least n=3 mice per group.*

infection is characterized by severe thymic atrophy and impaired negative selection [43]. The second-most similar dataset was a comparison between middle-aged mice and young mice (Z-score = 24.28%) (Supplemental Figures 6B-C). Aging is associated with decreased thymic cellularity and impaired production of naïve T cells, primarily due to defects in the thymic stroma of aged individuals [3]. We looked in more depth at the aging dataset and found that upstream regulators induced during thymic involution were predicted to be activated in KO TECs. Further analysis revealed decreased expression in knockout thymi of several loci encoding proteins with

protective roles in thymic atrophy (Figure 5A), namely fibroblast growth factor 21 (*Fgf21*), fibroblast growth factor 7 (*Fgf7*), and insulin like growth factor 1 (*Igf1*). qPCR validation of these genes corroborated the reduction in gene expression by RNA sequencing (Figure 5B). Furthermore, expression of *Crip3*, whose ablation is associated with decreased thymic cellularity [44], was reduced in KO sequencing samples (Supplemental Figure 6D).

One of the hallmarks of thymic involution is impaired TEC proliferation. *Mki67*-expressing cells were reduced KO samples (Supplemental Figure 6E), and investigation of G1/S and G2M phase-specific genes (Figure 5C) was consistent with decreased cell cycling in KO TECs. Validation by flow cytometry revealed decreased $Ki67^{+}$ $mTEC^{lo}$ cells in KO samples. (Figures 5D-E). Thus, the gene expression profile in *Cyp27b1* KO mice is consistent with that of aging thymi. As thymic atrophy in wildtype mice begins at 3–4 weeks and continues for the first year of life, we compared control and KO animals (male and female) at different timepoints and found that cellularity of KO thymi steeply declined by 26 weeks of age, compared to an 18% decline in age- and sex-matched wild-type animals (Figure 5F). Collectively, these data show that in the absence of vitamin D signaling, TEC differentiation is defective, resulting in impaired negative selection of thymocytes. Furthermore, the data show that loss of *Cyp27b1* accelerates age associated thymic involution.

Discussion

Previous studies have identified a role for vitamin D signaling in the suppression of peripheral pro-inflammatory T cell responses [45], which is consistent with links between vitamin D deficiency and autoimmune conditions such as type 1 diabetes and multiple sclerosis [22, 28]. The potential prophylactic and therapeutic benefit of vitamin D supplementation in adults for prevention of autoimmune diseases remains unclear due to conflicting findings [46]. In contrast,

studies with children revealed clear associations between vitamin D status and type 1 diabetes risk. For example, a cohort study of 10,366 children born in northern Finland and followed for 30 years found that the frequency of type 1 diabetes was 0.12 (95% CI 0.03–0.51) for regular versus no supplementation and 0.22 (0.05–0.89) for those who received the recommended amount (2,000 IU daily) versus those who didn't [47]. This study is notable because there is no cutaneous synthesis of vitamin D year-round in northern Finland. A subsequent meta-analysis of two cohort studies and six case-control studies from diverse geographical locations revealed a pooled odds ratio of 0.71 (95% CI, 0.51-0.98) for vitamin D supplementation versus no supplementation in early life [47]. Since the naïve T cell pool is sustained by thymic output in the first 20 years of life [48], these studies suggest that vitamin D status may be especially relevant in early life during the period where thymic output is at its highest.

Here, we showed that vitamin D signaling is essential for normal $Aire^{+}$ TEC maturation, TRA gene expression, and thymic tissue development. Our findings link clinical observations to an *in vivo* thymic phenotype and provide a molecular basis for the potential role of vitamin D signaling in thymic homeostasis during childhood and infancy. In addition to TECs, the frequency of numerous hematopoietic populations was altered in KO thymi including B cells and 4SP thymocytes. We further found that B cell numbers were systemically reduced in KO mice. Thymic B cells participate in the negative selection of thymocytes and have non-overlapping roles with mTECs [49]. Therefore, reduction of thymic B cell numbers in *Cyp27b1* KO mice suggests their role in negative selection is impaired. Interestingly, 4SP but not 8SP thymocytes were elevated in *Cyp27b1* KO mice. A similar phenotype has also been observed in mouse models with defective thymic antigen presentation due to diminished mTEC, B cell or DC numbers [48-50].

Negative selection occurs in two waves, first in the cortex through interactions of developing thymocytes with DCs, followed by a second wave in the medulla [32, 52]. Thymocytes at these stages can be tracked by flow cytometry by gating on $CD4^+$ $CD8^{low}$ (cortical, $CCR7^{-/low}$) and 4SP (medullary, $CCR7^+$) cells. The transcription factor Helios serves as a readout of highly autoreactive T cells in the thymus [32]. It is upregulated on negatively selected cells and downregulated on positively selected cells [32]. In addition to impaired $Aire^+$ mTEC development, we observed decreased levels $Helios^+$ $FoxP3^-$ 4SP thymocytes (Figure 1 G). Interestingly, medullary, but not cortical, $Helios^+$ $FoxP3^-$ thymocytes were reduced in *Aire* KO mice, similar to our phenotype [31]. The same authors also examined T cell-specific transforming growth factor beta receptor KO mice, which displayed impaired medullary formation, and reduced $Aire^+$ cells and TRA expression. They found that medulla-associated $Helios^+$ FoxP3- 4SP thymocytes were reduced, but cortex associated $CD4^+$ CD8 low $Helios^+$ FoxP3- thymocytes were markedly increased [31]. Collectively, this suggests that impaired medullary negative selection, as in *Aire* KO and *Cyp27b1* KO models, does not impact cortical negative selection. Furthermore, as the phenotype in *Cyp27b1* KO mice parallels that of *Aire* KO mice, cortical negative selection is not likely to be regulated by 1,25D signaling. This is supported by our observations that the number of cleaved caspase 3^+ thymocytes was reduced in the medulla, but not cortex (Supplemental Figure 1F), of *Cyp27b1* KO mice. In addition, since the proportion of $FoxP3^+$ cells of 4SP was unaltered in *Cyp27b1* KO thymi, the reduction of apoptotic thymocytes was not due to disproportionate production of nTregs. While complete abrogation of AIRE results in a dramatic autoimmune phenotype, the effects of vitamin D deficiency in humans on autoimmune phenotypes are more subtle. This may be because Aire function is attenuated but not eliminated in *Cyp27b1* KO animals, as well as there being some level of compensation by cortical negative selection.

In addition to the impairment of negative selection in KO thymi, we observed striking changes in tissue organization characterized by an outgrowth of CK5 and CK8 expressing TECs. Previous reports indicate that these double positive cells are TEC progenitors [53]. Our single cell RNA sequencing results corroborated the increased presence of a CK5 (*Krt5*) expressing population (Supplemental Figure 4H), that also expressed *Ccl21a* and markers of junctional TECs (jTECs) such as Pdpn [38]. However, due to differences in tissue localization of CCL21^{+}, Pdpn^{+}, and CK5^{+} CK8^{+} populations it is likely that this *Ccl21a*$^{+}$ cluster represents multiple populations with similar gene expression. This is consistent with findings that Ccl21a^{+} Krt5^{+} intertypical TECs have characteristics of heterogenous TEC populations, including jTECs, TPA^{lo}, and Sca-1^{+} TECs, and have mature mTEC precursor potential [54]. However, whether CCL21^{+} TECs are precursors of mature Aire^{+} mTECs, representing a block in development at this stage in *Cyp27b1* KO mice, or represent a distinct terminally differentiated population, is disputed [35, 37, 38].

Prior RNA velocity experiments produced discordant results where one study found that CCL21^{+} Pdpn^{+} cells were precursors to TAC-TECs and another found that *Ccl21a*$^{+}$ TECs were products of TAC-TECs and not Aire^{+} TEC precursors [35, 37]. A portion of TAC-TECs are positive for Aire and/or *Ccl21a*, raising the possibility that these cells are derived from a common progenitor that co-express these markers, or that this represents a transition in cell state (e.g., *Ccl21a*$^{+}$ Aire^{-} to Aire^{+} *Ccl21a*$^{-}$). Experiments using a constitutively expressed Aire reporter revealed significant reporter expression in *Ccl21a*$^{+}$ cells but little in TAC-TECs, making it unlikely that *Ccl21a*$^{+}$ upregulate proliferative markers, becoming TAC-TECs, prior to becoming mature Aire^{+} CCL21^{-} TECs. Our findings in *Cyp27b1* KO mice are consistent with the branching differentiation model, suggesting that 1,25D promotes Aire^{+} TEC differentiation, whereas in its absence *Ccl21a*$^{+}$ TEC differentiation is favored. This is consistent with findings that ablation of

Aire$^+$ TEC differentiation with a-RANKL antibodies resulted in a significant increase in the proportion of CCL21$^+$ TECs [35]. While not statistically significant, there was a strong trend for increased CCL21$^+$ TEC counts. Increased CCL21$^+$ TEC numbers in the absence of Aire have also been noted in other studies [55]. Together, these results suggest that the signals that drive CCL21$^+$ TEC differentiation are at least partially distinct from those that drive Aire$^+$ TEC differentiation and CCL21$^+$ TEC development may be increased in the absence of Aire$^+$ TECS, possibly as compensatory mechanism to attract more RANKL bearing thymocytes to induce more Aire$^+$ TEC differentiation.

Finally, we found premature thymic involution and a gene expression profile consistent with accelerated thymic aging in *Cyp27b1* KO mice. Thymic involution is characterized by progressive atrophy, structural changes, and reduced output of naïve T cells [56]. This contributes to a peripheral phenotype of immunosenescence where the host loses the ability to fight new infections and clear tumors, due to reductions in T cell repertoire diversity [56]. Thymic involution arises largely from defects in the thymic stromal niche causing changes in the thymic microenvironment [56]. In *Cyp27b1* KO mice, thymic cellularity was dramatically diminished by 26 weeks, whereas reductions in control thymi were modest (~18%).

We also found that KO thymi displayed other hallmarks of aging such as reduced TEC proliferation and distorted cortical-medullary boundaries [57]. Furthermore, the expression of *Fgf21*, *Fgf7*, and *Igf1* were downregulated in *Cyp27b1* KO TECs. These genes encode proteins that protect from thymic involution and are downregulated in aging thymi [3]. *Fgf21* and *Fgf7* are part of the fibroblast growth factor family, which regulates a variety of developmental processes systemically including epithelial cell differentiation and proliferation [58]. In the thymus, *Fgf21* is expressed in TECs, and its overexpression promotes thymocyte production in aged mice, whereas

loss of *Fgf21* in middle-aged mice accelerates thymic involution and delays T cell reconstitution following irradiation and hematopoietic stem cell transplant [59]. Notably, we observed that *Fgf21* appears to be predominantly expressed by mTEC^{hi} cells (Figure 3B) and mTEC^{lo} on the trajectory towards mTEC^{hi} cells. Since Aire mRNA expression was unperturbed in *Fgf21* KO mice [59], this suggests that the reduction of Aire^{+} mTECs in *Cyp27b1* KO mice precedes the reduction in *Fgf21* gene expression and other potential downstream effects on thymic size. This is consistent with another study using *Fgf21* KO mice that did not reveal defects in TEC proliferation or differentiation [60]. *Fgf7* has been shown to be important for thymic size [61] and naïve T cell output [62]. Loss of *Fgf7* signaling through receptor (FgfR2-lllb) knockout mice results in impaired TEC proliferation and a failure of immature CK5^{+} cells to progress to mature CK5^{-} cells in embryonic thymi [63]. *Fgf7* mRNA was induced by 1,25D treatment in human breast cancer MCF-7 cells [64], raising the possibility that *Fgf7* expression may be directly regulated by vitamin D signaling in the thymus.

Igf1 belongs to a family of neuroendocrine factors that regulate cell proliferation, differentiation, apoptosis during organ growth, and recovery from injury [65]. In the thymus, Igf1 signaling induces proliferation of human TECs *in vitro*, and exogenous Igf1 treatment in mouse models enhanced cTEC and mTEC numbers, overall thymic cellularity, and thymic output [66]. Various clinical studies have been conducted examining the potential association between 1,25D supplementation and circulating Igf1 levels, some finding that supplementation enhances Igf1 expression [67], whereas others finding no effect of 1,25D [68]. In *Vdr* KO mice, the receptor for Igf1 (Igfr1) but not Igf1 itself was found to be downregulated in the liver, indicating a role for vitamin D in regulating Igf1 signaling. Our data establishes a link between vitamin D and Igf1 signaling in the thymus. We found that *Igf1* is expressed by post-Aire TECs and Hassall's

corpuscles. Validation studies revealed that *Igf1* mRNA expression is sharply downregulated in the absence of 1,25D. Collectively, the phenotype in *Cyp27b1* KO mice is associated accelerated thymic aging, characterized by decreased proliferating TECs and expression of genes encoding of multiple pro-thymic cytokines that control TEC proliferation and homeostasis. We additionally found that Aire$^+$ TEC differentiation was impaired in *Cyp27b1* KO mice, whereas that of CCL21$^+$ TECs was enhanced and was associated with a phenotype consistent with defective negative selection.

References

1. Klein, L., B. Kyewski, P.M. Allen, and K.A. Hogquist. 2014. *Positive and negative selection of the T cell repertoire: what thymocytes see (and don't see).* Nat Rev Immunol. **14**(6): p. 377-91.
2. Kadouri, N., S. Nevo, Y. Goldfarb, and J. Abramson. 2020. *Thymic epithelial cell heterogeneity: TEC by TEC.* Nat Rev Immunol. **20**(4): p. 239-253.
3. Liang, Z., X. Dong, Z. Zhang, Q. Zhang, and Y. Zhao. 2022. *Age-related thymic involution: Mechanisms and functional impact.* Aging Cell. **21**(8): p. e13671.
4. Wu, H., X. Qin, H. Dai, and Y. Zhang. 2018. *Time-course transcriptome analysis of medullary thymic epithelial cells in the early phase of thymic involution.* Mol Immunol. **99**: p. 87-94.
5. Bornstein, C., S. Nevo, A. Giladi, N. Kadouri, M. Pouzolles, F. Gerbe, E. David, A. Machado, A. Chuprin, B. Tóth, O. Goldberg, S. Itzkovitz, N. Taylor, P. Jay, V.S. Zimmermann, J. Abramson, and I. Amit. 2018. *Single-cell mapping of the thymic stroma identifies IL-25-producing tuft epithelial cells.* Nature. **559**(7715): p. 622-626.
6. Miller, C.N., I. Proekt, J. von Moltke, K.L. Wells, A.R. Rajpurkar, H. Wang, K. Rattay, I.S. Khan, T.C. Metzger, J.L. Pollack, A.C. Fries, W.W. Lwin, E.J. Wigton, A.V. Parent, B. Kyewski, D.J. Erle, K.A. Hogquist, L.M. Steinmetz, R.M. Locksley, and M.S. Anderson. 2018. *Thymic tuft cells promote an IL-4-enriched medulla and shape thymocyte development.* Nature. **559**(7715): p. 627-631.
7. Michel, C., C.N. Miller, R. Küchler, B. Brors, M.S. Anderson, B. Kyewski, and S. Pinto. 2017. *Revisiting the Road Map of Medullary Thymic Epithelial Cell Differentiation.* J Immunol. **199**(10): p. 3488-3503.
8. Ribeiro, C., N.L. Alves, and P. Ferreirinha. 2019. *Medullary thymic epithelial cells: Deciphering the functional diversity beyond promiscuous gene expression.* Immunol Lett. **215**: p. 24-27.
9. St-Pierre, C., A. Trofimov, S. Brochu, S. Lemieux, and C. Perreault. 2015. *Differential Features of AIRE-Induced and AIRE-Independent Promiscuous Gene Expression in Thymic Epithelial Cells.* The Journal of Immunology. **195**(2): p. 498.
10. Tai, X., M. Cowan, L. Feigenbaum, and A. Singer. 2005. *CD28 costimulation of developing thymocytes induces Foxp3 expression and regulatory T cell differentiation independently of interleukin 2.* Nature immunology. **6**(2): p. 152-162.
11. Salomon, B., D.J. Lenschow, L. Rhee, N. Ashourian, B. Singh, A. Sharpe, and J.A. Bluestone. 2000. *B7/CD28 costimulation is essential for the homeostasis of the CD4$^+$ CD25$^+$ immunoregulatory T cells that control autoimmune diabetes.* Immunity. **12**(4): p. 431-440.
12. Metzger, T.C., I.S. Khan, J.M. Gardner, M.L. Mouchess, K.P. Johannes, A.K. Krawisz, K.M. Skrzypczynska, and M.S. Anderson. 2013. *Lineage tracing and cell ablation identify a post-Aire-expressing thymic epithelial cell population.* Cell reports. **5**(1): p. 166-179.

13. Gäbler, J., J. Arnold, and B. Kyewski. 2007. *Promiscuous gene expression and the developmental dynamics of medullary thymic epithelial cells.* European journal of immunology. **37**(12): p. 3363-3372.
14. Gray, D., J. Abramson, C. Benoist, and D. Mathis. 2007. *Proliferative arrest and rapid turnover of thymic epithelial cells expressing Aire.* The Journal of experimental medicine. **204**(11): p. 2521-2528.
15. McCaughtry, T.M., T.A. Baldwin, M.S. Wilken, and K.A. Hogquist. 2008. *Clonal deletion of thymocytes can occur in the cortex with no involvement of the medulla.* The Journal of experimental medicine. **205**(11): p. 2575-2584.
16. Stritesky, G.L., Y. Xing, J.R. Erickson, L.A. Kalekar, X. Wang, D.L. Mueller, S.C. Jameson, and K.A. Hogquist. 2013. *Murine thymic selection quantified using a unique method to capture deleted T cells.* Proceedings of the National Academy of Sciences. **110**(12): p. 4679-4684.
17. Klein, L., B. Kyewski, P.M. Allen, and K.A. Hogquist. 2014. *Positive and negative selection of the T cell repertoire: what thymocytes see (and don't see).* Nature Reviews Immunology. **14**(6): p. 377-391.
18. Malhotra, D., J.L. Linehan, T. Dileepan, Y.J. Lee, W.E. Purtha, J.V. Lu, R.W. Nelson, B.T. Fife, H.T. Orr, and M.S. Anderson. 2016. *Tolerance is established in polyclonal CD4$^+$ T cells by distinct mechanisms, according to self-peptide expression patterns.* Nature immunology. **17**(2): p. 187-195.
19. Mathis, D. and C. Benoist. 2009. *Aire.* Annual Review of Immunology. **27**(1): p. 287-312.
20. Bouillon, R. and D. Bikle. 2019. *Vitamin D Metabolism Revised: Fall of Dogmas.* J Bone Miner Res. **34**(11): p. 1985-1992.
21. Patricio Artusa, M.-È.L., Camille Barbier, Babak Memari, Reyhaneh Salehi-Tabar, Sophia Karabatsos, Aiten Ismailova, Heather J. Melichar, John H. White. 2023. *Aire is a coactivator of the vitamin D receptor.* J. Immunol. In press.
22. Bouillon, R., C. Marcocci, G. Carmeliet, D. Bikle, J.H. White, B. Dawson-Hughes, P. Lips, C.F. Munns, M. Lazaretti-Castro, A. Giustina, and J. Bilezikian. 2018. *Skeletal and Extraskeletal Actions of Vitamin D: Current Evidence and Outstanding Questions.* Endocrine Reviews. **40**(4): p. 1109-1151.
23. Thacher, T.D. and B.L. Clarke. 2011. *Vitamin D Insufficiency.* Mayo Clinic Proceedings. **86**(1): p. 50-60.
24. Martineau, A.R., D.A. Jolliffe, R.L. Hooper, L. Greenberg, J.F. Aloia, P. Bergman, G. Dubnov-Raz, S. Esposito, D. Ganmaa, A.A. Ginde, E.C. Goodall, C.C. Grant, C.J. Griffiths, W. Janssens, I. Laaksi, S. Manaseki-Holland, D. Mauger, D.R. Murdoch, R. Neale, J.R. Rees, S. Simpson, I. Stelmach, G.T. Kumar, M. Urashima, and C.A. Camargo. 2017. *Vitamin D supplementation to prevent acute respiratory tract infections: systematic review and meta-analysis of individual participant data.* Bmj-British Medical Journal. **356**.
25. Urashima, M., T. Segawa, M. Okazaki, M. Kurihara, Y. Wada, and H. Ida. 2010. *Randomized trial of vitamin D supplementation to prevent seasonal influenza A in schoolchildren.* The American Journal of Clinical Nutrition. **91**(5): p. 1255-1260.
26. Çamurdan, O.M., E. Döğer, A. Bideci, N. Çelik, and P. Cinaz. 2012. *Vitamin D status in children with Hashimoto thyroiditis.* Journal of Pediatric Endocrinology and Metabolism. **25**(5-6): p. 467-470.
27. Metwalley, K.A., H.S. Farghaly, T. Sherief, and A. Hussein. 2016. *Vitamin D status in children and adolescents with autoimmune thyroiditis.* Journal of Endocrinological Investigation. **39**(7): p. 793-797.
28. Cantorna, M.T. and B.D. Mahon. 2004. *Mounting Evidence for Vitamin D as an Environmental Factor Affecting Autoimmune Disease Prevalence.* Exp. Biol. Med. **229**(11): p. 1136-1142.
29. Mailhot, G. and J.H. White. 2020. *Vitamin D and Immunity in Infants and Children.* Nutrients. **12**(5).

30. Panda, D.K., D. Miao, M.L. Tremblay, J. Sirois, R. Farookhi, G.N. Hendy, and D. Goltzman. 2001. *Targeted ablation of the 25-hydroxyvitamin D 1alpha -hydroxylase enzyme: evidence for skeletal, reproductive, and immune dysfunction.* Proc Natl Acad Sci U S A. **98**(13): p. 7498-503.
31. McCarron, M.J., M. Irla, A. Serge, S.M. Soudja, and J.C. Marie. 2019. *Transforming Growth Factor-beta signaling in alphabeta thymocytes promotes negative selection.* Nat Commun. **10**(1): p. 5690.
32. Daley, S.R., D.Y. Hu, and C.C. Goodnow. 2013. *Helios marks strongly autoreactive CD4$^+$ T cells in two major waves of thymic deletion distinguished by induction of PD-1 or NF-kappaB.* J Exp Med. **210**(2): p. 269-85.
33. Castaneda, J., Y. Hidalgo, D. Sauma, M. Rosemblatt, M.R. Bono, and S. Nunez. 2021. *The Multifaceted Roles of B Cells in the Thymus: From Immune Tolerance to Autoimmunity.* Front Immunol. **12**: p. 766698.
34. Bornstein, C., S. Nevo, A. Giladi, N. Kadouri, M. Pouzolles, F. Gerbe, E. David, A. Machado, A. Chuprin, B. Toth, O. Goldberg, S. Itzkovitz, N. Taylor, P. Jay, V.S. Zimmermann, J. Abramson, and I. Amit. 2018. *Single-cell mapping of the thymic stroma identifies IL-25-producing tuft epithelial cells.* Nature. **559**(7715): p. 622-626.
35. Wells, K.L., C.N. Miller, A.R. Gschwind, W. Wei, J.D. Phipps, M.S. Anderson, and L.M. Steinmetz. 2020. *Combined transient ablation and single-cell RNA-sequencing reveals the development of medullary thymic epithelial cells.* Elife. **9**.
36. Ki, S., D. Park, H.J. Selden, J. Seita, H. Chung, J. Kim, V.R. Iyer, and L.I.R. Ehrlich. 2014. *Global transcriptional profiling reveals distinct functions of thymic stromal subsets and age-related changes during thymic involution.* Cell Rep. **9**(1): p. 402-415.
37. Dhalla, F., J. Baran-Gale, S. Maio, L. Chappell, G.A. Hollander, and C.P. Ponting. 2020. *Biologically indeterminate yet ordered promiscuous gene expression in single medullary thymic epithelial cells.* EMBO J. **39**(1): p. e101828.
38. Onder, L., V. Nindl, E. Scandella, Q. Chai, H.W. Cheng, S. Caviezel-Firner, M. Novkovic, D. Bomze, R. Maier, F. Mair, B. Ledermann, B. Becher, A. Waisman, and B. Ludewig. 2015. *Alternative NF-kappaB signaling regulates mTEC differentiation from podoplanin-expressing precursors in the cortico-medullary junction.* Eur J Immunol. **45**(8): p. 2218-31.
39. Hyeon, J.W., S.Y. Kim, J. Lee, J.S. Park, K.J. Hwang, S.M. Lee, S.A. An, M.K. Lee, and Y.R. Ju. 2015. *Alternative application of Tau protein in Creutzfeldt-Jakob disease diagnosis: Improvement for weakly positive 14-3-3 protein in the laboratory.* Sci Rep. **5**: p. 15283.
40. La Manno, G., R. Soldatov, A. Zeisel, E. Braun, H. Hochgerner, V. Petukhov, K. Lidschreiber, M.E. Kastriti, P. Lonnerberg, A. Furlan, J. Fan, L.E. Borm, Z. Liu, D. van Bruggen, J. Guo, X. He, R. Barker, E. Sundstrom, G. Castelo-Branco, P. Cramer, I. Adameyko, S. Linnarsson, and P.V. Kharchenko. 2018. *RNA velocity of single cells.* Nature. **560**(7719): p. 494-498.
41. Bergen, V., M. Lange, S. Peidli, F.A. Wolf, and F.J. Theis. 2020. *Generalizing RNA velocity to transient cell states through dynamical modeling.* Nat Biotechnol. **38**(12): p. 1408-1414.
42. Lopes, N., A. Serge, P. Ferrier, and M. Irla. 2015. *Thymic Crosstalk Coordinates Medulla Organization and T cell Tolerance Induction.* Front Immunol. **6**: p. 365.
43. Elsaesser, H.J., M. Mohtashami, I. Osokine, L.M. Snell, C.R. Cunningham, G.M. Boukhaled, D.B. McGavern, J.C. Zuniga-Pflucker, and D.G. Brooks. 2020. *Chronic virus infection drives CD8 T cell-mediated thymic destruction and impaired negative selection.* Proc Natl Acad Sci U S A. **117**(10): p. 5420-5429.
44. Kirchner, J., K.A. Forbush, and M.J. Bevan. 2001. *Identification and characterization of thymus LIM protein: targeted disruption reduces thymus cellularity.* Mol Cell Biol. **21**(24): p. 8592-604.
45. Bhalla, A., E. Amento, B. Serog, and L. Glimcher. 1984. *1,25-Dihydroxyvitamin D3 inhibits antigen-induced T cell activation.* J Immunol. **133**(4): p. 1748-1754.
46. Bouillon, R., C. Marcocci, G. Carmeliet, D. Bikle, J.H. White, B. Dawson-Hughes, P. Lips, C.F. Munns, M. Lazaretti-Castro, A. Giustina, and J. Bilezikian. 2019. *Skeletal and Extraskeletal*

Actions of Vitamin D: Current Evidence and Outstanding Questions. Endocr Rev. **40**(4): p. 1109-1151.
47. Hyppönen, E., E. Läärä, A. Reunanen, M.-R. Järvelin, and S.M. Virtanen. 2001. *Intake of vitamin D and risk of type 1 diabetes: a birth-cohort study.* The Lancet. **358**(9292): p. 1500-1503.
48. Murray, J.M., G.R. Kaufmann, P.D. Hodgkin, S.R. Lewin, A.D. Kelleher, M.P. Davenport, and J.J. Zaunders. 2003. *Naive T cells are maintained by thymic output in early ages but by proliferation without phenotypic change after age twenty.* Immunol Cell Biol. **81**(6): p. 487-95.
49. Yamano, T., J. Nedjic, M. Hinterberger, M. Steinert, S. Koser, S. Pinto, N. Gerdes, E. Lutgens, N. Ishimaru, M. Busslinger, B. Brors, B. Kyewski, and L. Klein. 2015. *Thymic B Cells Are Licensed to Present Self Antigens for Central T Cell Tolerance Induction.* Immunity. **42**(6): p. 1048-61.
50. Ohnmacht, C., A. Pullner, S.B. King, I. Drexler, S. Meier, T. Brocker, and D. Voehringer. 2009. *Constitutive ablation of dendritic cells breaks self-tolerance of CD4 T cells and results in spontaneous fatal autoimmunity.* J Exp Med. **206**(3): p. 549-59.
51. Hinterberger, M., M. Aichinger, O. Prazeres da Costa, D. Voehringer, R. Hoffmann, and L. Klein. 2010. *Autonomous role of medullary thymic epithelial cells in central CD4($^{+}$) T cell tolerance.* Nat Immunol. **11**(6): p. 512-9.
52. McCaughtry, T.M., T.A. Baldwin, M.S. Wilken, and K.A. Hogquist. 2008. *Clonal deletion of thymocytes can occur in the cortex with no involvement of the medulla.* J Exp Med. **205**(11): p. 2575-84.
53. Lee, E.N., J.K. Park, J.R. Lee, S.O. Oh, S.Y. Baek, B.S. Kim, and S. Yoon. 2011. *Characterization of the expression of cytokeratins 5, 8, and 14 in mouse thymic epithelial cells during thymus regeneration following acute thymic involution.* Anat Cell Biol. **44**(1): p. 14-24.
54. Baran-Gale, J., M.D. Morgan, S. Maio, F. Dhalla, I. Calvo-Asensio, M.E. Deadman, A.E. Handel, A. Maynard, S. Chen, F. Green, R.V. Sit, N.F. Neff, S. Darmanis, W. Tan, A.P. May, J.C. Marioni, C.P. Ponting, and G.A. Hollander. 2020. *Ageing compromises mouse thymus function and remodels epithelial cell differentiation.* Elife. **9**.
55. Lkhagvasuren, E., M. Sakata, I. Ohigashi, and Y. Takahama. 2013. *Lymphotoxin beta receptor regulates the development of CCL21-expressing subset of postnatal medullary thymic epithelial cells.* J Immunol. **190**(10): p. 5110-7.
56. Thomas, R., W. Wang, and D.M. Su. 2020. *Contributions of Age-Related Thymic Involution to Immunosenescence and Inflammaging.* Immun Ageing. **17**: p. 2.
57. Aw, D., A.B. Silva, M. Maddick, T. von Zglinicki, and D.B. Palmer. 2008. *Architectural changes in the thymus of aging mice.* Aging Cell. **7**(2): p. 158-67.
58. Beenken, A. and M. Mohammadi. 2009. *The FGF family: biology, pathophysiology and therapy.* Nat Rev Drug Discov. **8**(3): p. 235-53.
59. Youm, Y.H., T.L. Horvath, D.J. Mangelsdorf, S.A. Kliewer, and V.D. Dixit. 2016. *Prolongevity hormone FGF21 protects against immune senescence by delaying age-related thymic involution.* Proc Natl Acad Sci U S A. **113**(4): p. 1026-31.
60. Nakayama, Y., Y. Masuda, H. Ohta, T. Tanaka, M. Washida, Y.I. Nabeshima, A. Miyake, N. Itoh, and M. Konishi. 2017. *Fgf21 regulates T cell development in the neonatal and juvenile thymus.* Sci Rep. **7**(1): p. 330.
61. Dooley, J., M. Erickson, W.J. Larochelle, G.O. Gillard, and A.G. Farr. 2007. *FGFR2IIIb signaling regulates thymic epithelial differentiation.* Dev Dyn. **236**(12): p. 3459-71.
62. Alpdogan, O., V.M. Hubbard, O.M. Smith, N. Patel, S. Lu, G.L. Goldberg, D.H. Gray, J. Feinman, A.A. Kochman, J.M. Eng, D. Suh, S.J. Muriglan, R.L. Boyd, and M.R. van den Brink. 2006. *Keratinocyte growth factor (KGF) is required for postnatal thymic regeneration.* Blood. **107**(6): p. 2453-60.
63. Revest, J.M., R.K. Suniara, K. Kerr, J.J. Owen, and C. Dickson. 2001. *Development of the thymus requires signaling through the fibroblast growth factor receptor R2-IIIb.* J Immunol. **167**(4): p. 1954-61.

64. Lyakhovich, A., N. Aksenov, P. Pennanen, S. Miettinen, M.H. Ahonen, H. Syvala, T. Ylikomi, and P. Tuohimaa. 2000. *Vitamin D induced up-regulation of keratinocyte growth factor (FGF-7/KGF) in MCF-7 human breast cancer cells.* Biochem Biophys Res Commun. **273(**2): p. 675-80.
65. LeRoith, D. and S. Yakar. 2007. *Mechanisms of disease: metabolic effects of growth hormone and insulin-like growth factor 1.* Nat Clin Pract Endocrinol Metab. **3**(3): p. 302-10.
66. Chu, Y.W., S. Schmitz, B. Choudhury, W. Telford, V. Kapoor, S. Garfield, D. Howe, and R.E. Gress. 2008. *Exogenous insulin-like growth factor 1 enhances thymopoiesis predominantly through thymic epithelial cell expansion.* Blood. **112**(7): p. 2836-46.
67 Ameri, P., A. Giusti, M. Boschetti, M. Bovio, C. Teti, G. Leoncini, D. Ferone, G. Murialdo, and F. Minuto. 2013. *Vitamin D increases circulating IGF1 in adults: potential implication for the treatment of GH deficiency.* Eur J Endocrinol. **169**(6): p. 767-72.
68. Trummer, C., V. Schwetz, M. Pandis, M.R. Grubler, N. Verheyen, M. Gaksch, A. Zittermann, W. Marz, F. Aberer, A. Lang, C. Friedl, A. Tomaschitz, B. Obermayer-Pietsch, T.R. Pieber, S. Pilz, and G. Treiber. 2017. *Effects of Vitamin D Supplementation on IGF-1 and Calcitriol: A Randomized-Controlled Trial.* Nutrients. **9**(6).

Chapter 3 Supplemental Figures

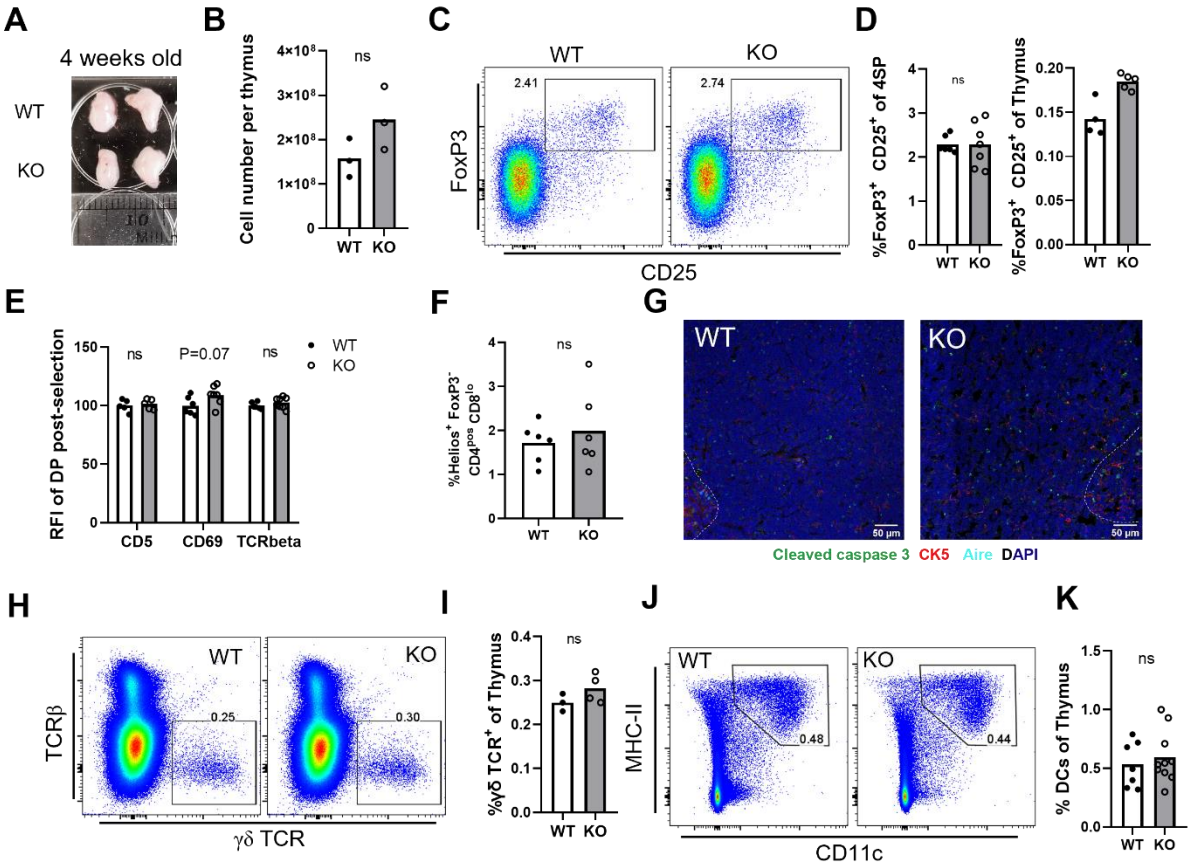

Supplemental Figure 1. Characterization of thymic hematopoietic cell frequencies in Cyp27b1 KO mice ***A.*** *Duplicate thymic lobes from WT (top) and KO (bottom) 4-week-old mice.* ***B.*** *Total thymic cell number in 4-week-old WT versus KO mice.* ***C.*** *Representative flow cytometry plots of regulatory T cells (pre-gated on live, CD4$^+$, TCRβ$^+$, CD8$^-$ cells) in WT vs KO thymi.* ***D.*** *Summary data showing the frequency of regulatory T-cells of 4SP (i) or total thymic (ii) compartments.* ***E.*** *Relative fluorescence intensity of markers in post selection (CD69$^{+/-}$, TCRβ^{hi}) DP thymocytes, relative to average of WT expression.* ***F.*** *Frequency of Helios$^+$ CD4$^+$ CD8^{lo} DP thymocytes.* ***G.*** *Representative IF images of cleaved caspase 3 staining in WT and KO thymic cortex. All experiments were repeated at least twice with at least n=3 mice per group.* ***H,I.*** *Representative flow cytometry plots of γδ T-cells (pre-gated on live cells) in WT vs KO mice (H) and summary data (I).* ***J,K.*** *Representative flow cytometry plots of dendritic cells (DCs) (pre-gated on live, CD45$^+$, EpCAM$^-$, CD19$^-$ cells) in WT vs KO mice (J) and summary data (K).*

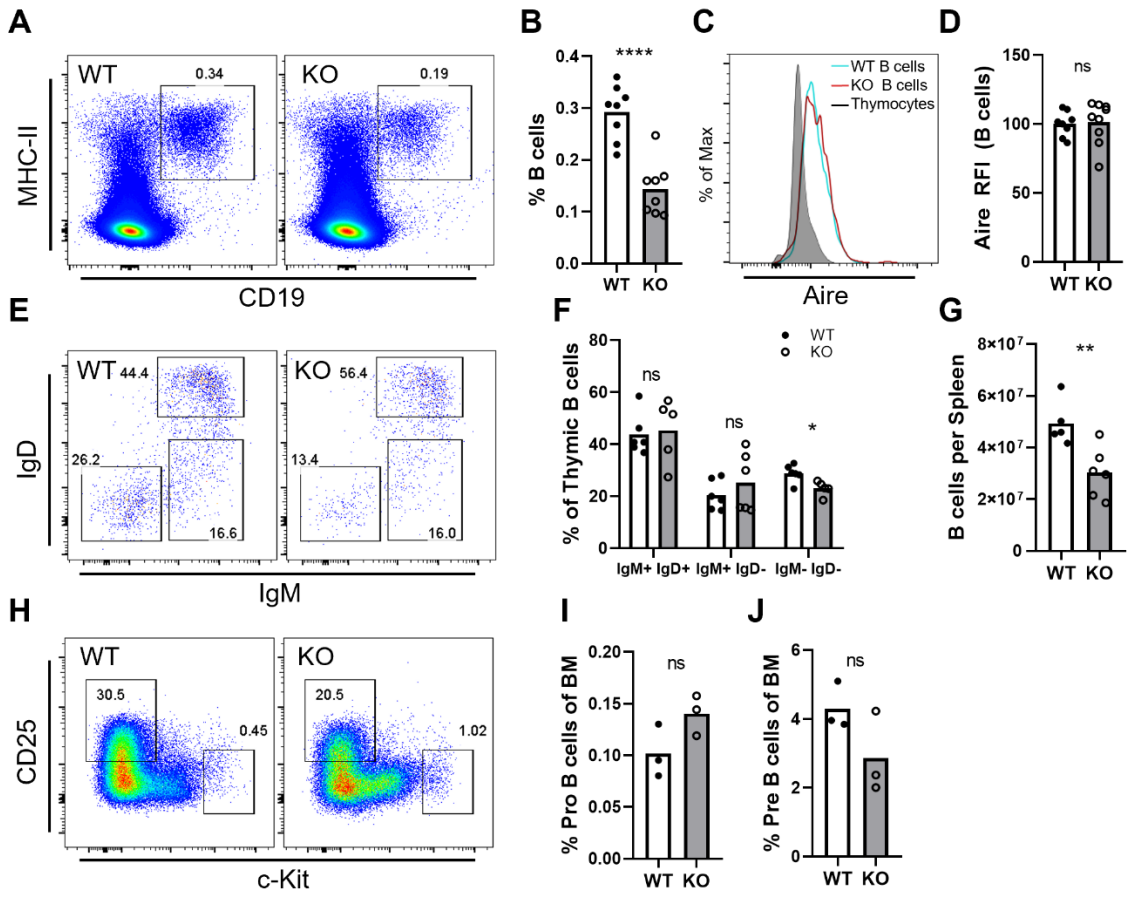

Supplemental Figure 2. Systemic B cell lymphopenia in Cyp27b1 KO mice ***A.*** *Representative flow cytometry plots of B cells in WT and KO thymi (pre-gated on CD45$^+$, EpCAM$^-$, CD11c$^-$, live, single cells).* ***B.*** *Summary of thymic B cell frequencies.* ***C,D.*** *Representative flow cytometry plot of Aire expression in B cells (C) and quantification (D) of the relative fluorescence intensity (relative to average of WT expression).* ***E.*** *Representative flow cytometry plots of thymic B cell subsets (IgD$^+$ IgM$^+$; "recirculating", IgM$^+$ IgD$^-$/IgM$^-$ IgD$^-$; "resident").* ***F.*** *Quantification of committed and "circulating" B cell subtypes in WT versus KO thymi.* ***G.*** *Splenic B cell frequencies in 6-10-week old mice.* ***H-J.*** *Representative flow cytometry plots of pre- (CD25$^+$ c-Kit$^-$) and pro-B cells (CD25$^-$ c-Kit$^+$)(H) in WT and KO bone marrow and quantification of their frequencies (I-J). All experiments were repeated at least twice with at least n=3 mice per group.*

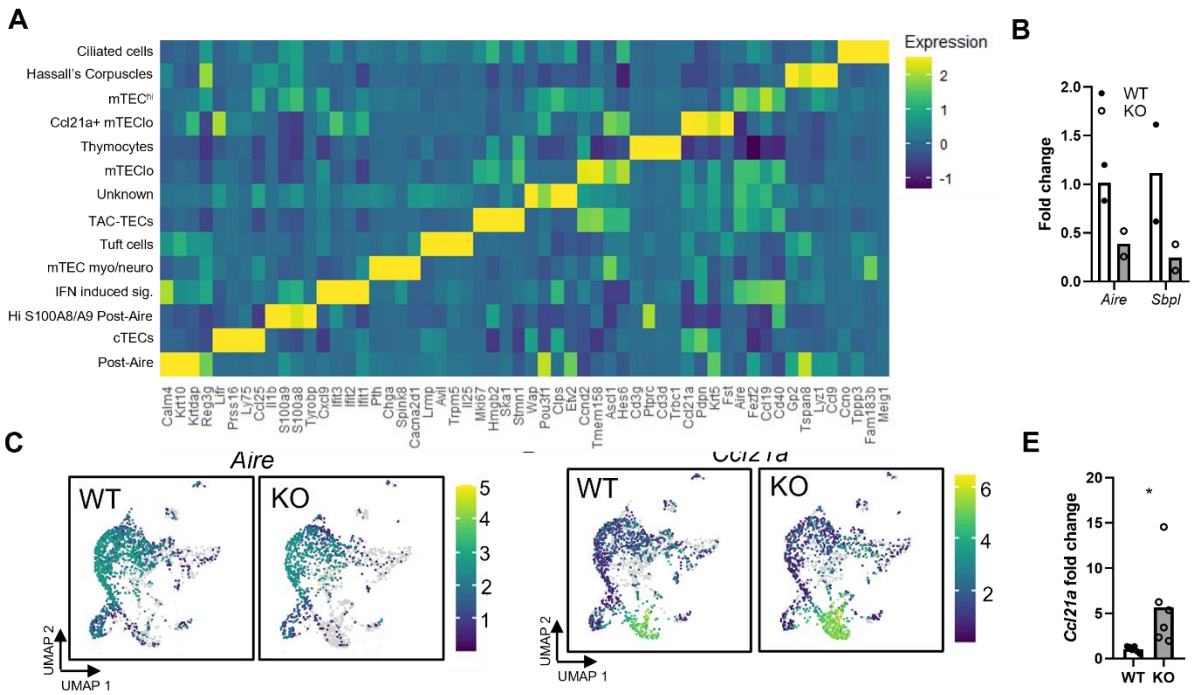

Supplemental Figure 3. Divergent mTEC differentiation in Cyp27b1 KO mice ***A.*** *qPCR data from sequenced samples.* ***B.*** *UMAPs of TAC-TEC enriched genes..* ***C.*** *UMAPs showing Aire expression in WT and KO samples.* ***D.*** *UMAPs showing Ccl21a expression in representative WT versus KO samples.* ***D.*** *qPCR validation of Ccl21a expression* ***E.*** *Heatmap of 4 top 20 DEGs per cluster.*

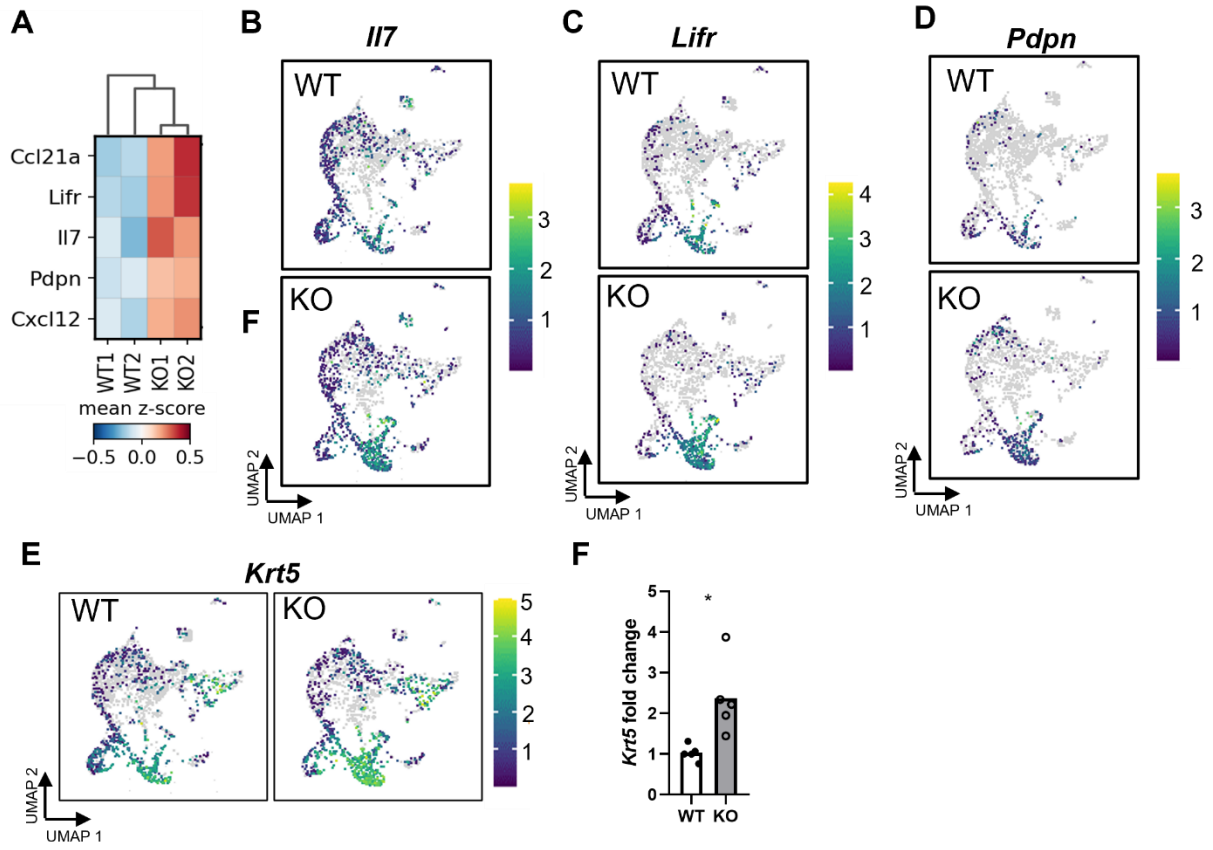

Supplemental Figure 4. Increased jTEC marker expression in Cyp27b1 KO mice ***A.*** *Matrixplot of jTEC genes in all sequenced samples.* ***B-D*** *UMAPs showing decreased expression of jTEC markers, Il7, Lifr, Pdpn, in the Ccl21a+ positive cluster.* ***E,F.*** *UMAP showing increased Krt5 transcripts in KO Ccl21a*$^{+}$ *TECs (E), and qPCR validation (F).*

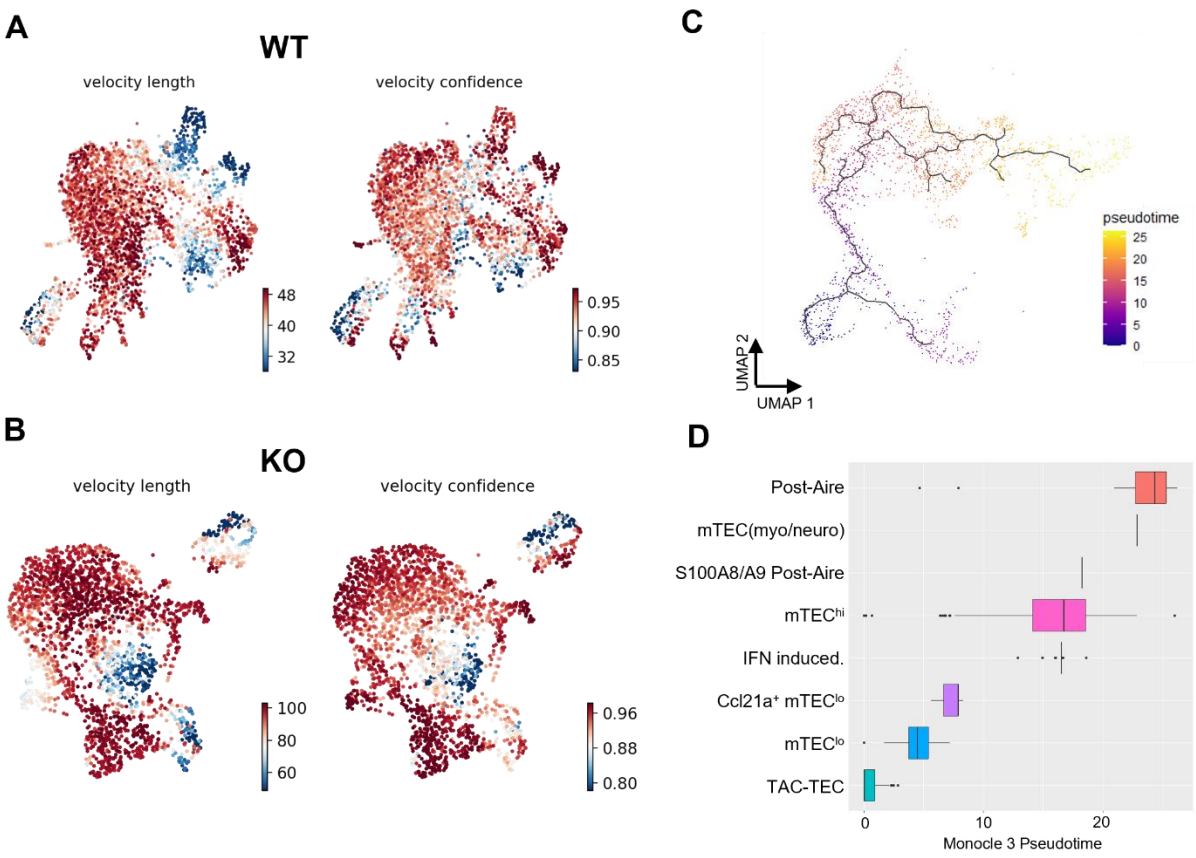

Supplemental Figure 5. Trajectory analysis ***A****. Velocity length (left) and velocity confidence (right) of WT.* ***B.*** *Velocity length (left) and velocity confidence (right) of KO.* ***C.*** *Pseudotime projection of representative WT TEC sample.* ***D.*** *Pseudotemporal ordering of TEC clusters in a WT sample.*

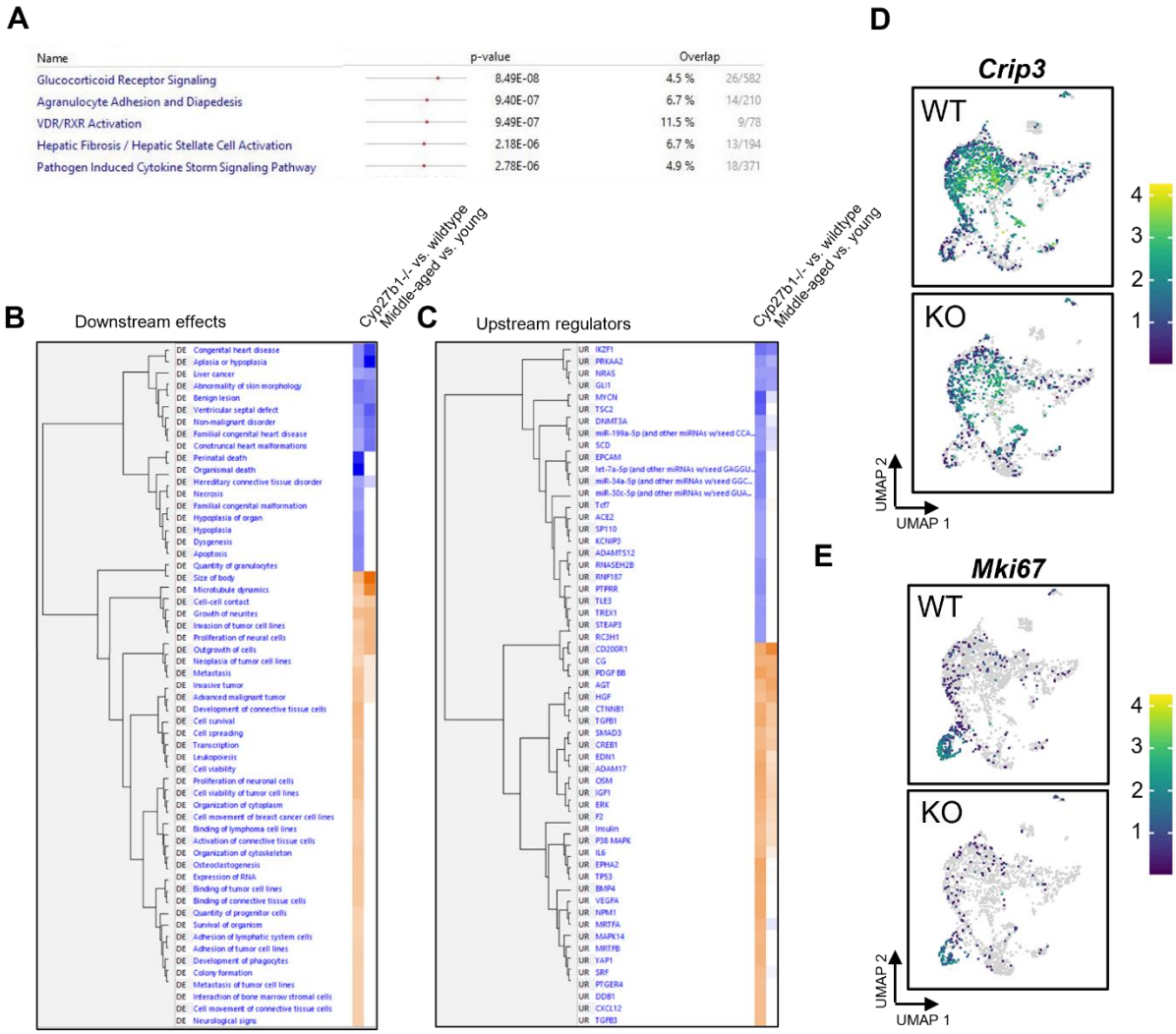

Supplemental Figure 6. Enrichment of aging pathways in Cyp27b1 KO ***A.*** *Top canonical pathways in Cyp27b1 KO vs WT TECs.* ***B.*** *Comparison of downstream effects (Z-score 45.83%) between our dataset and a middle-aged mice versus young mice dataset.* ***C.*** *Comparison of upstream regulators (Z-score 51.30%) between our dataset and a middle-aged mice versus young mice dataset.* ***C.*** *Predicted BMP4 pathway activation in Cyp27b1 KO TECs by IPA.* ***D.*** *Representative UMAPs of Crip3 expression in wildtype and KO TECs.* ***E.*** *Representative UMAPs of Mki67 expression in wildtype and KO TECs.*

Supplemental Table 1 – List of Differentially expressed genes

mTEChi

Gene Name	avg_log2FC	p_val_adj
Mt4	2.248	4.94E-213
S100a8	2.080	8.96E-203
Crhbp	1.997	0
Fabp6	1.969	1.11E-79
Lypd8	1.942	2.81E-57
Pcp4	1.835	7.35E-61
Obp2a	1.661	1.11E-205
Sncg	1.648	4.52E-176
Pyy	1.635	1.03E-73
Defb19	1.631	2.60E-101
S100a9	1.559	1.49E-82
Crip1	1.557	2.46E-135
Tbc1d4	1.557	0
S100a6	1.556	2.73E-137
AW112010	1.552	3.30E-121
Ccl27a	1.547	3.96E-195
Calca	1.542	3.33E-97
Fgf21	1.528	3.07E-203
Pomc	1.437	5.98E-107
Nts	1.434	6.41E-15
Crabp1	1.404	3.62E-28
Csn2	1.397	2.41E-239
Lgals2	1.389	1.18E-67
Calca	1.369	7.16E-110
Gal	1.369	0.015902959

CCL21+, mTEClo

Gene Name	avg_log2FC	p_val_adj
Ccl21a	4.253	0
Apoe	2.998	0
Ifi27l2a	2.734	0
Krt5	2.688	0
Tagln	2.645	4.11E-250
Ccl11	2.629	6.02E-158
Mgp	2.473	0
Krt14	2.450	1.67E-303
Ctsl	2.325	0
Acta2	2.224	5.01E-105
Igfbp5	2.201	3.83E-230
Lifr	1.984	0
Socs3	1.978	1.09E-243
Id1	1.930	0
Gas1	1.898	0
Hpgd	1.864	1.96E-287
Rbp1	1.681	9.30E-303
Igfbp4	1.640	9.49E-235
Ascl1	1.639	4.29E-216
Ly6a	1.488	8.29E-159
Isg15	1.485	1.30E-182
Gpx3	1.477	4.27E-136
Atf3	1.471	2.38E-85
Fst	1.433	5.93E-254
Ifit3	1.407	1.99E-165

Post-Aire

Gene Name	avg_log2FC	p_val_adj
Calm4	4.487	1.22E-176
Krtdap	4.485	1.46E-201
Krt10	4.074	3.36E-209
Reg3g	3.955	1.68E-23
Sbsn	3.940	1.27E-222
Wfdc2	3.927	6.95E-70
Dapl1	3.914	9.90E-239
Lgals7	3.775	5.78E-160
Krt16	3.773	2.39E-157
Crct1	3.506	2.83E-200
Dmkn	3.452	1.79E-212
Calml3	3.342	1.01E-197
Spink5	3.233	5.46E-155
Defb6	3.198	4.21E-140

mTEClo

Gene Name	avg_log2FC	p_val_adj
Ccnd2	2.033	2.16E-173
Tmem158	1.648	4.32E-116
Ascl1	1.604	2.24E-144
Hes6	1.513	2.73E-142
Stmn1	1.237	1.71E-117
Tubb5	1.135	2.01E-122
Dut	1.074	1.81E-121
Nkx6-2	1.065	1.00E-99
Fgf21	0.955	8.44E-78
Vim	0.924	6.37E-95
H2afz	0.901	6.18E-67
Hmgb2	0.853	1.41E-29
Olfm4	0.771	3.90E-63
Hist1h1b	0.763	3.51E-31

Krt79	3.161	3.64E-173
Scgb1a1	3.147	6.02E-19
Anxa1	3.143	1.66E-64
Ifitm1	3.070	2.27E-44
Ltf	3.038	3.71E-59
Spink1	3.025	4.64E-10
Gsto1	2.971	1.45E-36
Ly6g6c	2.854	8.40E-157
Cnfn	2.841	5.24E-182
Gm94	2.805	2.29E-105
Spink5	2.796	7.91E-54

Unknown

Gene Name	**avg_log2FC**	**p_val_adj**
Gm26917	2.48199085	9.91E-16
Wap	0.69027834	0.154828355
Lifr	0.66283792	1.24E-57
Fgl2	0.50693686	1
Snhg11	0.48815608	0.282748307
Mt2	0.48398488	1
Clps	0.48309626	1
Ccl8	0.4821778	1.89E-13
Cbr2	0.4261964	1.44E-08
Krt5	0.42305376	3.32E-08
Gm8113	0.3991534	0.032790927
Tchh	0.36997676	4.50E-16
Etv2	0.34005012	5.85E-22
Pou3f1	0.33716992	1.45E-30
Ccl25	0.33624516	0.003640127
Rgs4	0.33450063	3.64E-10
Jchain	0.33320809	2.58E-34
Pds5b	0.32924118	0.111361917
Defb3	0.31870468	0.001815959
Igfbp5	0.31811168	1.29E-05
Ceacam10	0.31277888	3.63E-09
Cd44	0.29337331	1.33E-17
Fn1	0.29183855	8.00E-21
F830016B08Rik	0.2889918	1
Ccl21a	0.27555925	2.22E-16

Tuft cells

Gene Name	**avg_log2FC**	**p_val_adj**
Lrmp	3.668	4.93E-123
Gnat3	3.039	1.57E-56
Plac8	2.942	9.21E-71
Rgs13	2.937	6.22E-27
Gng13	2.891	5.78E-66

Pclaf	0.739	1.94E-72
Ttn	0.716	1.02E-58
Hells	0.677	2.25E-30
Hsp90aa1	0.665	1.93E-67
Ltb	0.652	2.48E-76
Cks1b	0.651	5.34E-99
Wfdc18	0.635	5.70E-60
Tuba1b	0.587	1.86E-43
Rgs5	0.564	5.33E-56
Tyms	0.528	1.01E-50
Uhrf1	0.510	1.28E-51

TAC-TECs (proliferative)

Gene Name	**avg_log2FC**	**p_val_adj**
Hmgb2	2.995	3.97E-200
Stmn1	2.586	3.65E-186
Hist1h1b	2.296	4.37E-134
Pclaf	2.252	5.95E-189
Tubb5	2.160	7.12E-173
Mki67	2.074	5.48E-189
Ube2c	2.031	1.54E-148
H2afz	1.981	1.57E-180
Cdk1	1.966	1.47E-192
Top2a	1.958	2.21E-152
Cks2	1.897	7.40E-171
Dut	1.837	1.07E-162
Birc5	1.758	4.36E-199
Tuba1b	1.744	1.22E-140
Cks1b	1.728	1.54E-185
Hist1h2ae	1.632	3.60E-133
Cenpf	1.579	1.39E-138
Hist1h2ap	1.523	7.11E-75
Tpx2	1.512	5.12E-148
Cdca8	1.490	2.18E-186
H2afx	1.474	4.71E-153
Tyms	1.447	1.33E-159
Hmmr	1.417	4.66E-109
Cdc20	1.412	3.63E-115
Nusap1	1.339	1.07E-164

IFN inducible signature

Gene Name	**avg_log2FC**	**p_val_adj**
Cxcl9	2.7022339	2.34E-24
Ifit2	2.5461959	2.16E-33
Ifit3	2.5234329	3.13E-31
Isg15	1.9867238	1.00E-26
Cxcl10	1.9717959	9.33E-28

Avil	2.735	1.54E-78
Plk2	2.538	8.37E-70
Rgs2	2.522	1.46E-62
Mctp1	2.498	2.20E-65
Alox5ap	2.488	4.27E-43
Gnb3	2.435	2.21E-21
Fyb	2.333	2.13E-37
Atp1a2	2.318	1.58E-70
Trpm5	2.248	2.90E-44
Atp2a3	2.239	2.04E-56
Aldh2	2.189	9.67E-41
Ptpn18	2.184	6.79E-40
Bmx	2.126	4.98E-20
Dclk1	2.123	9.47E-10
Ahnak2	2.119	5.12E-53
Ltc4s	2.097	6.54E-64
Plcb2	2.041	3.06E-39
Ly6g6f	1.981	6.86E-97
Cd24a	1.924	2.12E-41
Cited2	1.919	3.33E-39

Hassall's corpuscles

Gene Name	**avg_log2FC**	**p_val_adj**
Serpinb6a	5.02710385	1.28E-111
Ccl20	4.75331796	1.03E-81
Pglyrp1	4.59964719	2.99E-71
Lyz1	4.33156685	6.32E-54
Ccl9	4.24989338	2.18E-122
Ccl6	4.17627796	9.17E-89
Wfdc17	3.97477788	1.04E-70
Serpinb1a	3.87994416	2.26E-110
Wfdc18	3.79542267	7.01E-54
Hamp	3.64774375	1.69E-53
Gp2	3.26931929	4.05E-55
2200002D01Rik	3.19154547	2.55E-106
Iapp	3.10051284	3.57E-40
AW112010	3.01438871	3.94E-84
Cyp2a5	2.93438255	4.58E-66
Tnfaip2	2.90016146	4.60E-44
Clu	2.87634331	4.81E-56
Bcl2a1b	2.84108229	7.48E-94
Prg2	2.83153195	1.13E-11
H2-M2	2.79383311	1.02E-57
Mmp7	2.78557914	1.65E-64
Fxyd2	2.65743364	2.48E-45
Bcl2a1a	2.62382223	1.26E-76
Krt71	1.8886249	0.000161
Iapp	1.817474	7.41E-38
Ifit1	1.8090876	9.12E-35
Igtp	1.7250543	3.41E-51
Ppy	1.6086228	5.23E-48
Rsad2	1.5906117	2.39E-36
Pyy	1.5585921	8.62E-46
Serpinb12	1.4651385	2.43E-15
Ripply2	1.4371285	0.000581
Irgm1	1.4093312	1.69E-36
Gbp4	1.3780901	9.68E-42
Psca	1.3673161	2.66E-10
Krt9	1.3315156	0.536792
Ifit3b	1.3019715	6.70E-39
Iigp1	1.2816209	2.15E-31
F830016B08Rik	1.2693476	1.19E-45
Gbp2	1.2256418	0.395441
Oasl1	1.1594754	1.88E-48
Ido1	1.1179737	2.64E-38
Ccl5	1.1070957	8.38E-34

Thymocytes

Gene Name	**avg_log2FC**	**p_val_adj**
Trbc2	5.2899371	2.94E-111
Cd3g	4.0905162	1.28E-114
Trbc1	4.0809531	6.02E-69
Satb1	3.9399273	4.63E-92
Cd3d	3.8210763	1.01E-111
Itm2a	3.6176453	5.05E-73
Ptprc	3.5632122	1.20E-112
Lef1	3.1747985	4.47E-66
Rgs10	2.3996263	2.03E-51
Ptpn18	2.27641	7.53E-88
Dusp5	2.0120754	3.16E-69
Ccr7	1.9226482	3.69E-71
Ms4a4b	1.8710749	6.02E-64
Nr4a1	1.796812	6.81E-86
Hist1h1e	1.6823975	9.53E-29
Ltb	1.6376677	9.72E-27
Dusp2	1.6359427	1.41E-35
Nkg7	1.5801269	3.67E-74
Fyb	1.4836332	2.39E-49
Klk8	1.4497244	1.06E-46
Izumo1r	1.4464987	7.89E-39
Rgs2	1.3166726	6.16E-17
Rgs1	1.2218845	2.11E-72

Tnfrsf11b	2.57230655	2.43E-61
Reg3g	2.47290395	9.93E-11
cTECs		
Gene Name	**avg_log2FC**	**p_val_adj**
Prss16	5.05874876	1.00E-82
Ctsl	4.71435568	1.10E-76
Ccl25	4.20071415	1.02E-74
Cxcl12	4.12089046	6.84E-82
Tbata	3.81182192	4.05E-76
Fxyd2	3.5384194	7.38E-64
Psmb11	3.46046659	5.64E-57
Ly75	3.21797359	9.16E-68
Synm	2.9709793	5.12E-60
Isg20	2.63024087	4.86E-47
Snhg11	2.61226207	1.86E-28
Lifr	2.59673364	5.68E-47
Pltp	2.5236999	3.42E-58
Hpgd	2.24650519	1.92E-42
Cbr2	2.18529442	4.64E-40
Cd83	2.03148715	1.53E-42
S100a10	1.90918136	3.91E-34
Igfbp5	1.83542964	5.30E-25
Slc22a7	1.73323748	4.48E-39
Inmt	1.5679059	0.036765818
Mgll	1.53022495	2.02E-37
Oat	1.52311151	6.61E-31
Oma1	1.44516687	1.60E-13
Crip3	1.42945167	8.49E-24
Nefm	1.32408446	2.12E-42
Ciliated cells		
Gene Name	**avg_log2FC**	**p_val_adj**
Dynlrb2	3.15353779	1.32E-44
Tppp3	3.10329861	3.07E-23
Fam183b	3.0941365	9.04E-38
Hsp90aa1	3.03465939	6.89E-37
Meig1	2.94289299	2.93E-35
Mlf1	2.79229263	1.02E-41
4933434E20Rik	2.78243348	1.08E-32
Nudc	2.67064686	8.05E-40
Tubb4b	2.63993345	8.94E-35
Lrrc23	2.62171421	1.94E-37
Ccno	2.60909578	8.12E-37
Rsph1	2.57107922	1.71E-31
Tmem107	2.54486346	7.47E-31
Tekt1	2.49657038	1.39E-40

Il2rb	1.1355703	1.79E-75
Vim	1.0895285	6.73E-29
mTEC myo/neuro		
Gene Name	**avg_log2FC**	**p_val_adj**
Pth	8.9833934	6.40E-41
Chga	7.1028115	1.52E-40
Spink8	3.3673119	5.52E-40
Cacna2d1	3.1584495	9.37E-52
Rbp4	3.0737758	8.74E-27
Cryba2	2.9404446	1
Aqp5	2.906813	1.81E-38
Mt3	2.8832569	1
Igfbp5	2.6015512	4.51E-31
Clca3b	2.6012439	5.15E-10
Cd177	2.5801445	7.25E-19
Chga	2.4883212	1.01E-43
Ascl1	2.4717094	3.93E-33
Mafb	2.3257126	8.09E-10
Cited2	2.2312789	1.15E-28
Scg2	2.0994604	5.17E-29
Car8	1.9488165	1.07E-13
Bex1	1.9403222	7.18E-38
Fbxo2	1.9062631	1.17E-34
Tspan1	1.8523053	1.10E-37
Fam183b	1.8391988	2.04E-21
Ceacam10	1.8361628	1.69E-16
Cd34	1.8288353	0.238101
Timp2	1.783631	3.30E-20
Btg2	1.7478245	1.69E-33
Hi S100A8/A9 Post-Aire		
Gene Name	**avg_log2FC**	**p_val_adj**
Il1b	4.797871	1.92E-37
S100a9	4.5832992	7.82E-05
Tyrobp	4.1854179	5.12E-38
Retnlg	3.4918726	8.02E-26
S100a8	3.2198531	0.009796
Cxcl2	3.0155677	2.32E-18
Fcer1g	3.0080299	1.28E-27
Ccl17	2.8950466	4.25E-20
Cst3	2.7196469	1.61E-17
Ccl22	2.7045249	3.46E-17
Rgs1	2.5171338	1.22E-26
G0s2	2.5065689	1.33E-21
Lgals3	2.4588622	1.10E-29
Lst1	2.4525352	1.03E-31

Cks2	2.42303807	1.45E-35	Samsn1	2.4463797	5.97E-13
Deup1	2.37102742	2.46E-31	Ptprc	2.4269203	7.40E-39
Vpreb3	2.33293491	2.49E-23	Gngt2	2.2184625	1.36E-28
Foxj1	2.32458798	5.30E-38	Spi1	2.1708897	6.77E-24
1110004E09Rik	2.31551112	5.42E-40	Ccr7	2.1454686	4.85E-14
Ly6c1	2.31405148	2.66E-11	Retnla	2.1158327	2.56E-09
1700016K19Rik	2.24601138	1.66E-33	Ccrl2	2.1120625	7.70E-28
4833427G06Rik	2.24286994	2.03E-16	Cd14	2.0414517	1.80E-14
Ccdc34	2.23376758	3.49E-30	Bcl2a1b	2.006279	4.98E-13
Nme5	2.20256918	3.86E-32	Cd44	1.9085836	1.31E-22
1110017D15Rik	2.05640716	9.52E-23	Nr4a1	1.8759796	3.92E-24

Linking Chapter 3 to Chapter 4

In Chapter 3, we investigated how the absence of 1,25D signaling in *Cyp27b1* KO mice regulates thymic development, TEC maturation, and indirectly, the process of negative selection. I found that Aire^{+} mTEC maturation, Aire protein expression in mTEC^{hi} cells, and TRA gene expression, were diminished in KO mice, consistent with our findings in Chapter 2 that 1,25D upregulated Aire expression in thymic slices. Analysis of thymocyte phenotypes provided evidence that negative selection may be impaired in the absence of 1,25D, consistent with the defects observed in Aire^{+} mTECs but requiring further investigation in order to draw any conclusions. Surprisingly, we observed that thymic size and cellularity were decreased in KO mice, in addition to peripheral T cell lymphopenia in the spleen. Investigation of thymic architecture by immunofluorescent microscopy revealed alterations in the composition and organization of the thymic medulla and cortex. scRNAseq and validation experiments revealed that a population of CCL21^{+} mTECs was expanded in KO thymi, indicating divergent differentiation of mTEC precursors populations in the absence of 1,25D. Ingenuity pathway analysis indicated that *Cyp27b1* KO TECs had a gene signature associated with thymic aging, which is characterized by thymic atrophy, decreased TEC proliferation, blurred cortico-medullary boundaries, decreased naïve T cell output, etc. Further analysis of *Cyp27b1* KO mice revealed decreased gene expression of factors controlling thymic size, including *Crip3*, *Fgf21*, *Fgf7*, and *Igf1*. Furthermore, TEC proliferation was decreased, and thymic involution was accelerated in KO thymi. These data show that 1,25D slows age-dependent thymic involution, in addition to its role in Aire^{+} TEC maturation.

Chapters 2 and 3 collectively demonstrate that 1,25D controls thymic processes that regulate the generation of a self-tolerant T cell repertoire. In Chapter 4, I investigated another

thymic mechanism that regulates the formation of an effective T cell repertoire. Specifically, how TdT, a non-templated DNA polymerase that generates ~90% of TCR diversity in developing thymocytes, regulates the diversity of $CD4^+$ T cell effector differentiation during infection.

Chapter 4: Increased germinal center follicular helper T cell differentiation in TdT deficient mice

Patricio Artusa[1,2], Caitlin Schneider[2,3], Dakota Rogers[1,2], Judith N. Mandl[1,2,3]

[1]Department of Physiology, McGill University, Montreal, Canada. [2]McGill Research Centre for Complex Traits, McGill University, Montreal, Canada. [3]Department of Microbiology and Immunology, McGill University, Montreal, Canada.

*To whom correspondence should be addressed:
judith.mandl@mcgill.ca

Abstract

The antigen recognition receptors of T cells (TCRs) of an individual determine the breadth of their T cell arsenal with which to fight any pathogen they may encounter yet not much is known about how TCR sequence relates to effector T cell function. Terminal deoxynucleotidyl transferase (TdT) accounts for 90-95% of T cell repertoire diversity, but an effect of the absence of TdT on immune responses has not been well described. Previous work suggested that the TdT-independent repertoire may be enriched for TCRs that bind peptide-MHC binding more efficiently and it is well-established that CD4 T cell avidity for antigen influences cell fate decisions during differentiation. Thus, we hypothesized that $CD4^+$ T cell effector differentiation will be altered in TdT-deficient mice. We investigated CD4 T cell responses to pathogens where CD4 T cells are critical to host protection. Here, we show that TdT KO mice had significantly increased follicular helper T (Tfh) cell differentiation upon infection with *Cryptococcus neoformans*, *Heligmosomoides polygyrus*, or lymphocytic choriomeningitis virus. We observed alterations in TCR Vβ usage in responding Tfh cells and evidence of increased TCR signaling in TdT KO mice. Surprisingly, increased Tfh differentiation was observed when TdT-deficiency was restricted to both B cells and T cells only. Overall, we found that the germline repertoire is enriched for TCRs that are biased towards Tfh differentiation providing a link between TCRs lacking N-region nucleotides and effector function.

Introduction

$CD4^+$ T cells are fundamental in coordinating protective adaptive immune responses. They carry out their critical functions of activating innate immune cells, B cells, and cytotoxic T cells after recognition of discrete pathogen derived peptides embedded in class II major histocompatibility molecules (pMHC-II) using their unique T cell receptor (TCR). The TCR repertoire of an individual is extremely diverse and has been experimentally estimated to be upwards of $1.3x10^6$ unique αβ-receptors in human blood [1-3]. TCR diversity is generated in thymocytes by both somatic recombination of αβ-TCR genes and by non-templated nucleotide additions into V(D)J TCR gene junctions, catalyzed by terminal deoxynucleotidyl transferase (TdT). It has been estimated by sequencing of T cells from TdT-deficient mice that 90–95% of TCR diversity is generated by TdT [4].

T cell repertoire diversity is a critical regulator of T cell responses to infection, cancer, and autoimmune disease [5-8]. Despite such associations, it is incompletely understood how the presence of specific TCR sequences in a repertoire collectively correlate with disease onset or protection. TdT knockout (KO) mice were not more susceptible to acute infection with distinct viral pathogens, despite having massively reduced T cell repertoire diversity [9]. TdT expression is highly conserved among vertebrates and its tissue-specific expression is tightly regulated [10], suggesting an evolutionary rationale for its activity. Thus, it has been posited that N-region diversity generated by TdT may have other, as of yet undefined functions [9].

It is well documented that TCR signal strength influences cell fate decisions during $CD4^+$ T cell differentiation, and strong TCR signals favor the differentiation of T helper (Th) 1, germinal center follicular helper T (GC-Tfh), and Th17 cells [11-16]. Due to the vast sequence diversity, the T cell repertoire is made up of TCR sequences with diverse TCR affinities which can vary up

to 1,000-fold even within individual antigen specific populations [17]. Furthermore, single naïve $CD4^+$ T cells were shown to preferentially differentiate into certain effector cells during infection in part due to their unique TCR [18]. TdT catalyzes nucleotide additions into the complementarity determining region 3 (CDR3) region of the TCR, which is the primary TCR motif responsible for contacting peptide, presented by MHC, thus conferring peptide specificity [19, 20]. Previous work suggested that the TdT independent repertoire may be enriched for TCRs that bind pMHC more efficiently [21]. This suggests that TdT may encode TCRs with lower pMHC reactivity.

Therefore, we hypothesized that TdT KO mice would have altered $CD4^+$ T cell effector differentiation during infection. Previous studies only investigated the phenotype in TdT KO mice in the context of acute infection, where highly reactive T cells dominate the response. Thus, we utilized pathogens that result in persistent infection in mice. We found that GC-Tfh cell differentiation was increased in TdT KO mice during chronic infection with diverse pathogens. The increased GC-Tfh differentiation in TdT KO mice was TCR-intrinsic and there was evidence for higher avidity TCRs in TdT KO mice. Finally, the increased GC-Tfh differentiation in TdT KO mice had both T cell and B cell intrinsic components. Together, these data show that TCRs generated without N-nucleotides favor GC-Tfh differentiation.

Methods and Materials

Mice

TdT KO mice were generated by Diane Mathis and kindly shared by A. Feeney, Scripps [22]. Wild type C57BL/6 and CD45.1 B6.SJL mice were purchased from Jackson Laboratories and bred in-house. SMARTA Tg Rag KO mice were obtained from Ethan Shevach, NIH [23]. $TCR\beta^{KO}$ mice were shared by Irah King (McGill) [24]. J_H KO mice were shared by Jörg Fritz (McGill) [25]. All

mice in this study were on a C57BL/6J background and used for experiments at 8-12 weeks of age. Animal housing, care and research were in accordance with the Guide for the Care and Use of Laboratory animals and all procedures performed were approved by the McGill University Facility Animal Care Committee.

Infection models

C. neoformans H99 was obtained from Kyung Kwon-Chung, NIH. Frozen stocks (-80°C) were prepared from fresh cultures on YPD agar plates into 15% glycerol. Three days before infection, *C. neoformans* was streaked onto a YPD agar plate and incubated for 2 days at 30°C. One day before infection, a single colony was inoculated in YPD broth and incubated for 16 hours at 30°C with shaking. *C. neoformans* infections were done as described [26]. Tissue was harvested 20 days post infection. Stage III Heligmosomoides polygyrus larvae were obtained from Irah King (McGill). Mice were infected by oral gavage of 200 larvae in 200uL. Tissue was harvested 14 days post infection. LCMV clone 13 stocks were initially obtained by Martin Richer (McGill). Frozen stocks (-80°C) were generated by expanding the virus on a BHK-21 cell monolayer and quantified by viral plaque forming assay using Vero cell monolayers [27]. LCMV cl13 infections were done as described [28]. Serum for viral kinetics was collected weekly by nicking the ventral tail artery and spinning down blood at 12,000rpm for 10 minutes. Mice were euthanized up to 50 days post infection by anesthetizing with isoflurane and terminal blood collection by retro-orbital bleed.

Tissue processing

Lymph nodes (inguinal or mediastinal), thymus, and spleen were harvested into ice cold RPMI containing 1% fetal calf serum, 1% penicillin/streptomycin, and 1% L-glutamine (1% RPMI). Tissue was crushed through a 70 um filter with the back of a syringe and washed with 1% RPMI.

Spleens were further treated with RBC lysis buffer for 3 minutes and re-filtered. *C. neoformans* Infected lungs were harvested into ice cold PBS and dissociated with scissors before being incubated in 10mL digestion buffer containing 1mg/mL collagenase D, 50U/mL DNase I, 1mg/mL hyaluronidase, 1% L-glutamine, and 1% pen/strep in RPMI at 37°C with agitation for 30 min. Tissue was crushed through a 100μM filter with 1% FCS in PBS. Aliquot were taken, serially diluted, and grown on YPD agar plates to calculate lung fungal burdens. Remaining cells were re-suspended in 10mL of 37% Percoll in RPMI and centrifuged at 2000rpm at 22°C for 20 minutes. Cell pellets were treated with RBC lysis buffer for 3 minutes and re-filtered. Counts were determined using a hemocytometer.

T cell re-stimulation and flow cytometry

Cytokine production by T cells was measured by stimulation of $1x10^6$ lung single cell suspension with α-CD3 and α-CD28 (Invitrogen; 2μg/mL) in 96-well round bottom plates with brefeldin A and monensin (Invitrogen; diluted 500x) for 5 hours at 37°C. For flow cytometric staining, all samples were incubated with Fixable Viability Dye (eBioscience), diluted 1:1,000 in PBS, for 20 minutes at 4°C. Extracellular antibodies were diluted in FACS buffer (2% fetal calf serum and 5mM EDTA in PBS) with Fc-receptor block (eBioscience) and incubated for 30 minutes at 4°C. For Tfh staining, cells were incubated with biotinylated CXCR5 (SPRCL5) simultaneously with other extracellular antibodies and were subsequently incubated fluorophore conjugated streptavidin (Biolegend) in FACS buffer for 30 minutes 4°C. Samples were either fixed with 1% paraformaldehyde or samples requiring intracellular staining were fixed and permeabilized using the FoxP3 Transcription Factor Fixation/Permeabilization kit (Life Technologies) for 30 minutes at 4°C. Intracellular antibodies were diluted in permeabilization wash buffer and incubated for 30-60 minutes at 4°C. All samples were acquired within 2 days of staining. MHC tetramer stains were

performed by incubating cells with diluted tetramers in FACS buffer containing sodium azide for 30 minutes at 37°C. Directly conjugated antibodies used were as follows: Bcl6 (K1112-91), TCRβ (H57-597), CD5 (53-7.3), TCR Vβ screening panel (557004) from BD Biosciences; RoRγt (B2D), IL-4 (11B11), IL-13 (eBio13A), CD44 (IM7), CD62L (MEL-14), CD25 (PC61), CD69 (H1.2F3), TdT (19-3), IL-2 (JES6-5H4), CD45.1 (A20), CD45.2 (104) from eBioscience; B220 (RA3-B62), CD4 (RM4.5), CD8 (53-6.7), FoxP3 (FJK-16s), GATA3 (16E10A23), T-bet (4B10), PD-1 (29F.1A12), IL-5 (TRFK5), IL-17 (TC11-18H10.1), IFNγ (XMG1.2), TNFα (MP6-XT22) from Biolegend. GP_{66-77}:I-A^b MHC tetramers for initial experiments were a gift from Heather Melichar (UdeM). I-A^b DIYKGVYQFKSV (GP66-77) biotinylated monomers were obtained from the NIH Tetramer Core Facility and were tetramerized by adding APC (S868) or PE (866) conjugated streptavidin at 4°C with agitation (Invitrogen). Monomers were incubated overnight, and unbound monomers were filtered out (Amicon-Millipore #UFC510024). Data were acquired on an LSRFortessa or FACS Canto (BD Bioscience) and analyzed using FlowJo (Tree Star).

Bone marrow chimeras

The femur and tibias of donor mice were collected. Bone marrow was obtained by flushing the bones with 1% RPMI. Cells were passed through a 70μM filter and treated with RBC lysis buffer for 3 minutes. Recipient mice were irradiated twice (550 rads) 3-4 hours apart and injected with 5-10x10^6 bone marrow cells I.V. within 4 hours of the last irradiation. Recipient mice were given bottles of neomycin water (2g/L) which were replaced every 3 days for 2 weeks. Chimeric mice were utilized for experiments 8-12 weeks post reconstitution.

SMARTA T cell transfers

T cells were collected from CD45.2$^+$ SMARTA Tg Rag KO wildtype or TdT KO lymph nodes as described above and 10^5 were injected I.V. into recipient CD45.1 wildtype mice in 200uL of PBS. One day later, recipient mice were infected by intravenous injection of $2x10^6$ PFU of LCMV clone 13 in 200uL of PBS.

Statistics

Data was analyzed by unpaired t-tests with Welch's correction or with non-parametric tests with Mann-Whitney correction (GraphPad Prism). The cutoff for significance was $P < 0.05$ for all analyses.

Results

The adult TdT-independent repertoire is biased towards GC-Tfh differentiation

TdT KO mice were infected with pathogens that result in chronic infection in mice, where CD4$^+$ T cells are critical for protection. To simultaneously evaluate the differentiation of multiple CD4$^+$ T cell lineages, we infected TdT KO mice with the fungal opportunistic pathogen *Cryptococcus neoformans (C. neoformans)*. We found that 20 days post infection, there were no significant differences in the proportion or number of activated CD4$^+$ or CD8$^+$ T cells in the lung or lung draining lymph node in TdT KO mice, indicating robust activation and recruitment of T cells despite the reduction in repertoire diversity (Supplemental Figures 1A-C). A significantly different cytokine response was elicited in the lungs of TdT KO mice, characterized by a two-fold increase of IL-17A producing (Th17) cells and a two-fold decrease in IL-4, IL-5, and IL-13 producing (Th2) cells (Supplemental Figures 1D-G). No difference was observed in the proportion of IFNγ-producing (Th1) cells. In agreement with these data, we observed significantly increased

RoRγt (Th17) expression, decreased GATA-3 (Th2) expression, and unchanged T-bet (Th1) expression in activated $CD4^+$ T cells of TdT KO mice (Supplemental Figures 1H,I). IL-5 is a critical cytokine for the recruitment of eosinophils to the lung during *C. neoformans* infection [29]. While the decrease in Th2 cells was subtle, we observed a two-fold reduction in the number of eosinophils recruited to the lung indicating that this subtle difference had important functional consequences (Supplemental Figures 1J,K). In the lung draining lymph node, Bcl-6-expressing $CXCR5^+$ $PD\text{-}1^{hi}$ (GC-Tfh) cells were significantly increased in TdT KO mice (Supplemental Figure lI, Figures 1A,B). Lung fungal burden was not significantly different in TdT KO mice 20 days post infection, indicating that the altered T helper cell differentiation was not driven by differences in the amount of antigen (Figure 1C).

We next investigated whether the altered T helper cell responses in TdT KO mice were specific to a subset of T cells responding to *C. neoformans* antigens or whether this phenotype could be observed in another infection model. We infected TdT KO mice with *Heligmosomoides polygyrus* (*H. polygyrus)*, a natural mouse pathogen that establishes persistent infection in the small intestine of mice [30]. Th1 and Th17 responses were not robustly induced by *H. polygyrus* infection 14 days post infection, and no differences were observed in the proportion of IFNγ or IL-17A producing cells in the mesenteric lymph nodes (Supplemental Figures A,B). Unlike during *C. neoformans* infection, there was no significant difference in Th2 differentiation in TdT KO animals, perhaps indicating that the decreased Th2 differentiation in TdT KO mice during *C. neoformans* infection was due to biases in particular *C.neoformans*-specific clones or counter-regulation by the increased Th17 differentiation (Supplemental Figures 2C,D). In agreement with our previous results, we observed significantly increased GC-Tfh differentiation in TdT KO mice during *H. polygyrus* infection (Figures 1D,E).

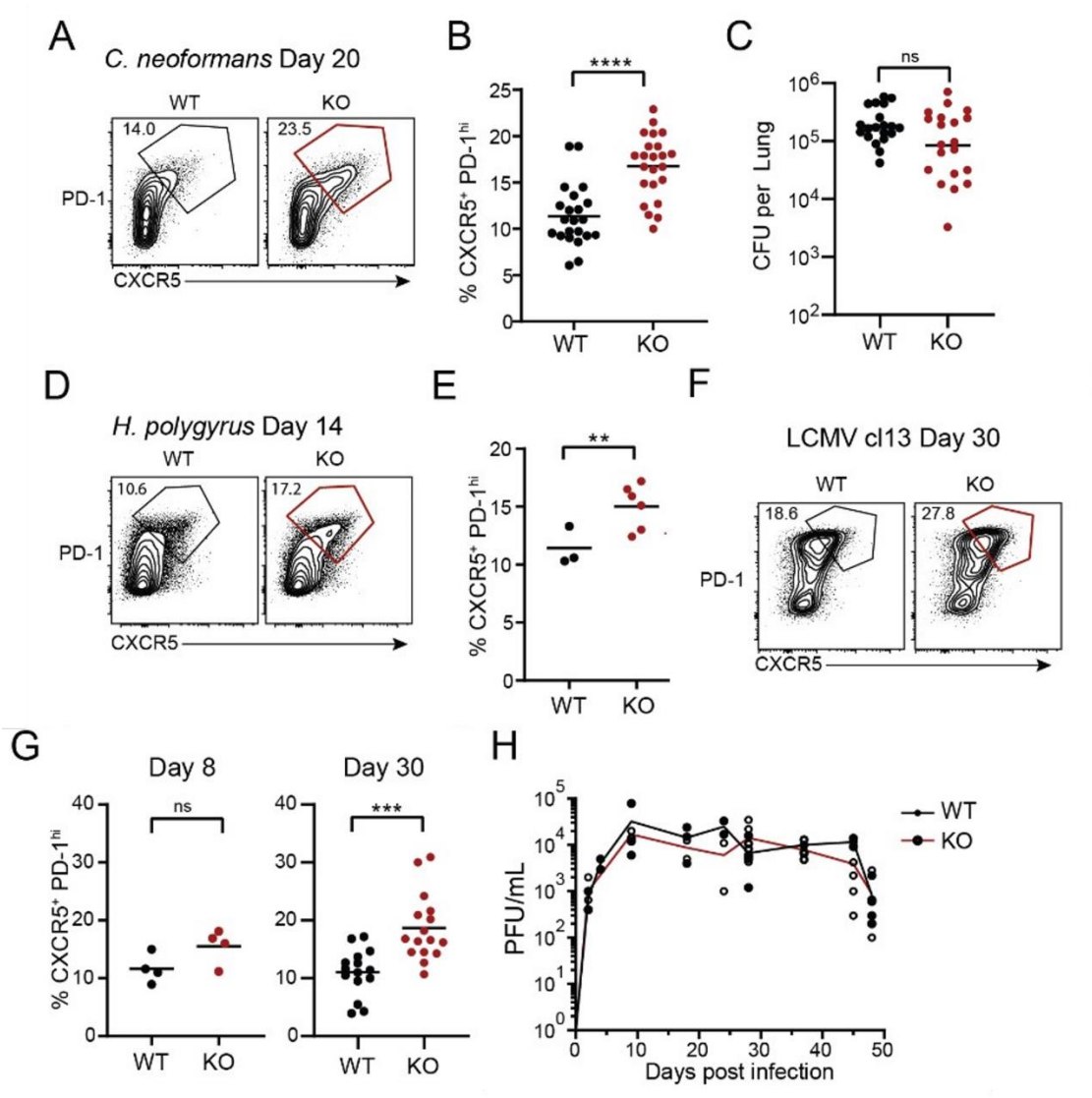

Figure 1. TdT deficiency leads to increased GC-Tfh differentiation. A,B. *GC-Tfh differentiation was assessed in WT versus KO mice at 20 days post infection with C.neoformans. Representative flow cytometry plots (gated on CD4$^+$ FoxP3$^-$ CD44^{hi}) of CXCR5$^+$ PD-1^{hi} Tfh cells* ***(A)****, and data summarized from 4 experiments* ***(B)****.* ***C.*** *C. neoformans pathogen burden in the lungs of WT versus KO mice 20 days post infection.* ***D,E.*** *GC-Tfh differentiation was assessed in WT or KO mice at 14 days post infection with H. polygyrus. Representative flow cytometry plots (gated on CD4$^+$ FoxP3$^-$ CD44^{hi}) of CXCR5$^+$ PD-1^{hi} Tfh cells* ***(D)****, and data summarized from 1 experiment* ***(e)****.Tfh differentiation was assessed in wild type (WT) or TdT-deficient (KO) mice at 8- and 30-days post infection with LCMV cl13 (cl13).* ***E,F,G.*** *Representative flow cytometry plots (gated on CD4$^+$ FoxP3$^-$ CD44^{hi}) of CXCR5$^+$ PD-1^{hi} GC-Tfh cells* ***(E)****, and data summarized from 3 experiments* ***(G)****.* ***H.*** *Serum viral load in WT or KO mice up to 48 days post infection with LCMV cl13.*

The signals driving Tfh differentiation have been well studied in the context of lymphocytic choriomeningitis virus (LCMV) infection. To better characterize the increased GC-Tfh differentiation in TdT KO mice, we infected them with LCMV clone 13 (cl13), which results in persistent infection in mice [31]. We observed significantly increased GC-Tfh differentiation in TdT KO mice at 30 days post infection (Figures 1F,G). Surprisingly, no difference in serum viral load was observed in TdT KO mice up to 50 days post infection (Figure 1H). Taken together, these data indicate that increased GC-Tfh differentiation is a general property of the adult TdT-independent repertoire. Furthermore, despite the vast reduction in repertoire diversity, TdT KO mice are equally capable of responding to and limiting viral replication and lung fungal burden.

Increased T follicular helper cell responses are associated with an altered repertoire of responding T cells in TdT KO mice

The established function of TdT is to catalyze the addition of non-templated nucleotides into TCR junctions to generate N-region diversity during V(D)J recombination in thymocytes and immature B cells. However, TdT has been reported to be able to catalyze templated nucleotide additions, raising the possibility that TdT may have an unknown function in lymphocytes [32-34]. To address this, we crossed SMARTA TCR transgenic mice to TdT KO mice and investigated whether the increased GC-Tfh differentiation observed in TdT KO mice was due to its role in generating N-region diversity. The SMARTA TCR is specific for the immunodominant LCMV GP_{61-80} epitope. 100,000 CD45.2$^+$ SMARTA$^+$ x TdT$^{+/+}$ or TdT KO CD4$^+$ T cells were transferred into CD45.1$^+$ wildtype mice, and recipient mice were infected 1 day later with LCMV cl13 (Supplemental Figure 3A). On day 30 post infection, no difference in Tfh differentiation was

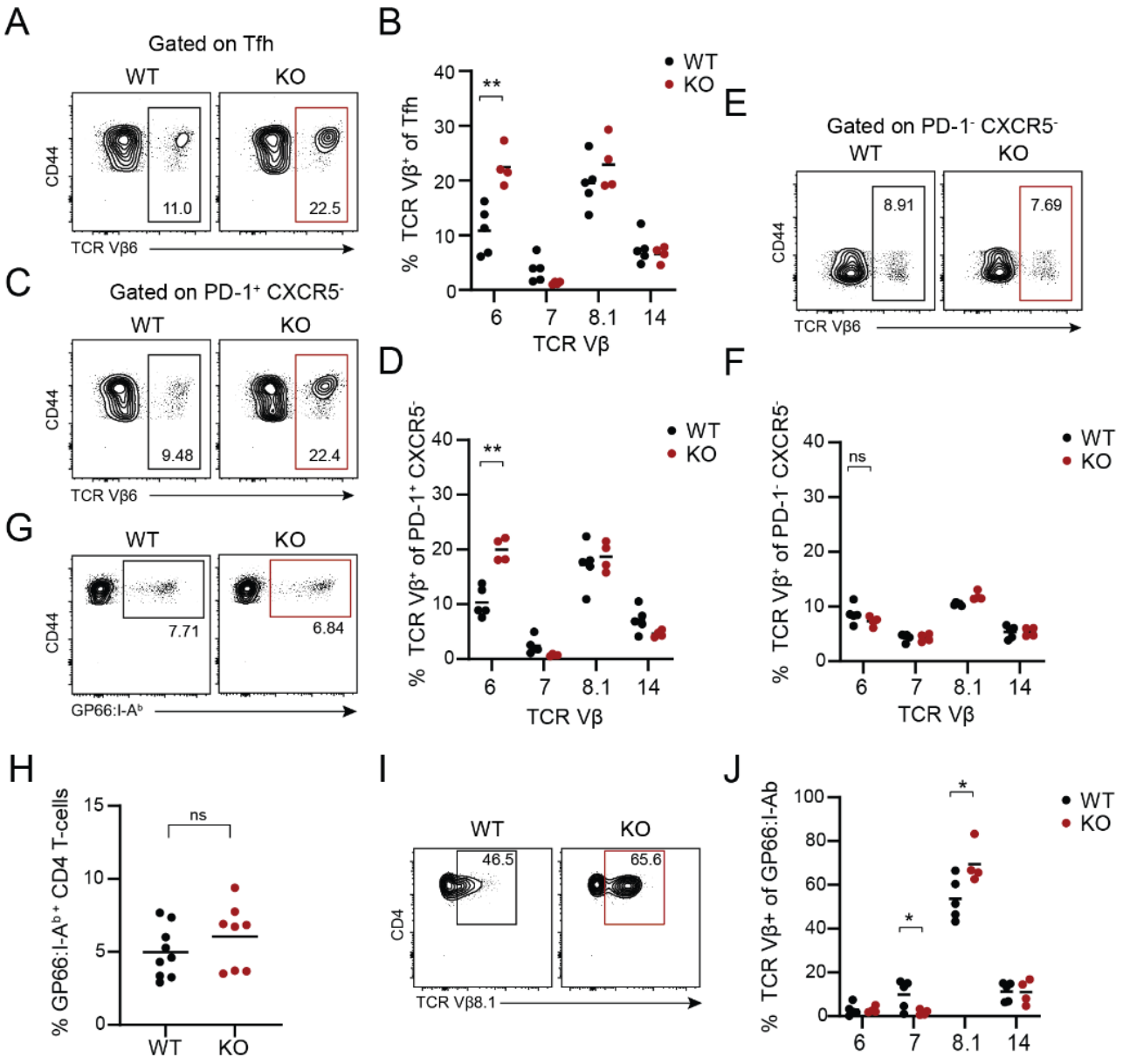

Figure 2. Altered TCRVβ repertoire diversity in responding GC-Tfh cells of TdT KO mice. **A-F.** *TCRVβ expression in different subsets of activated CD4$^+$ T cells were analyzed on Day 30 of LCMV cl13 infection.* ***A, B.*** *Representative flow cytometry plots (gated on CD4$^+$ FoxP3$^-$ CD44^{hi}) of TCR Vβ6 expression in PD-1^{hi} CXCR5$^+$ (GC-Tfh) cells* ***(A)****, and data summarized from 1 experiment* ***(B)****.* ***C,D.*** *Representative flow cytometry plots (gated on CD4$^+$ FoxP3$^-$ CD44^{hi}) of TCR Vβ6 expression in PD-1$^-$ CXCR5$^-$ cells* ***(C)****, and data summarized from 1 experiment* ***(D)****.* ***E,F.*** *Representative flow cytometry plots (gated on CD4$^+$ FoxP3$^-$ CD44^{hi}) of TCR Vβ6 expression in PD-1$^-$CXCR5$^-$ cells* ***(E)****, and data summarized from 1 experiment* ***(F)****.****G,H.*** *Representative flow cytometry plots (gated on CD4$^+$ FoxP3$^-$ CD44^{hi}) of GP66:I-Ab-specific cells on Day 30 LCMV cl13 infection* ***(G)****, and data summarized from 2 experiments* ***(H)****.* ***I,J.*** *Representative flow cytometry plot of TCR Vβ8.1 expression in GP66:I-Ab specific activated CD4$^+$ T cells* ***(I)****, and data summarized from 1 experiment* ***(J)****.*

observed in transferred SMARTA wildtype versus SMARTA TdT KO T cells (Supplemental Figure 3B,C).

Since the altered GC-Tfh differentiation in TdT KO mice was intrinsic to the TCR, we hypothesized that specific TCRs biased towards the GC-Tfh fate would be enriched in TdT KO mice. We compared TCR Vβ chain usage in TdT KO versus wildtype mice during LCMV cl13 infection. 15 TCR Vβ chains were tested in preliminary experiments (data not shown), and TCR Vβ6, Vβ7, Vβ8.1, and Vβ14 were further analyzed due to their high prevalence. On day 30 post LCMV cl13 infection, up to 50% of the GC-Tfh response was captured by the TCR Vβ chains analyzed (Supplemental Figure 3D). Two times more GC-Tfh cells in TdT KO mice expressed the TCR Vβ6 chain compared to wildtype cells. No significant differences in TCR Vβ7, Vβ8.1, or Vβ14 usage were observed (Figures 2A,B). TCR Vβ6 usage was not different in naïve CD4 T cells in TdT KO mice, indicating the increased TCR Vβ6 usage in TdT KO GC-Tfh cells was not due to a pre-existing bias in naïve cells (Supplemental Figure 2E,F). Furthermore, we observed significantly increased TCR Vβ6 usage in PD-1 expressing $CXCR5^-$ CD4 T cells in TdT KO mice but not in $PD\text{-}1^-$ cells, indicating that increased TCR Vβ6 usage in TdT KO mice was not uniformly increased in all antigen experienced CD4 T cells.

Earlier studies found that the immunodominance hierarchies for hen egg-white lysozyme (HEL) or *Mycobacterium tuberculosis* 65kDa heat shock protein (Hsp65) were unchanged in TdT KO mice [9]. Another study found that $CD8^+$ T cell immunodominance hierarchies in response to influenza A virus PR8 infection was shifted in TdT KO mice [35]. The altered TCR usage in TdT KO mice during LCMV cl13 infection led us to hypothesize that immunodominance may be shifted during LCMV infection. However, the overall proportion of GP66:I-A^b specific $CD4^+$ T cells was unchanged in TdT KO mice (Figure 2G,H). A significantly higher proportion of GP66:I-

Ab^+ specific cells expressed Vβ8.1 TCRs (Figure 2I,J). Therefore, while there was no significant change in TCR Vβ8.1 usage at the population level we could see differences in TCR Vβ usage in virus-specific cells. Taken together, these data support that the increased GC-Tfh differentiation in TdT KO mice is due to differences in the diversity of responding T cells.

Evidence of increased TCR signaling in TdT KO T cells

How the strength of TCR signaling instructs Tfh cell differentiation has been well documented. While Tfh cells can be generated at low, intermediate, or high affinity signaling [36], several studies reported that strong TCR signals biased T helper differentiation into the GC-Tfh lineage [16, 18, 37]. Therefore, we investigated if TCR avidity distribution was skewed upwards in TdT KO mice. CD5 is a cell surface glycoprotein expressed on T cells and a subset of B cells [38]. CD5 is a negative regulator of TCR signaling and its expression is set in the thymus in proportion to the TCR signal received [39]. CD5 expression is maintained on peripheral naïve T cells through homeostatic interactions with dendritic cells and correlates with self-pMHC and foreign-pMHC binding strength [40]. We found that CD5 expression was significantly increased in TdT KO CD4 and CD8 double negative (DN) thymocytes and pre-selection double positive (DP) thymocytes, indicating stronger TCR signals perceived during β-selection. (Figures 3A,B). CD5 expression was unchanged in CD4 single positive (4SP) thymocytes and in peripheral naïve $CD4^+$ T cells, potentially indicating increased negative selection of TdT KO thymocytes (Figures 3C,D). However, frequencies of 4SP and 8SP thymocytes were significantly increased TdT KO mice (Supplemental Figures 4A,B), suggesting that a significant proportion of cells were making the transition to mature thymocyte populations in TdT KO thymi.

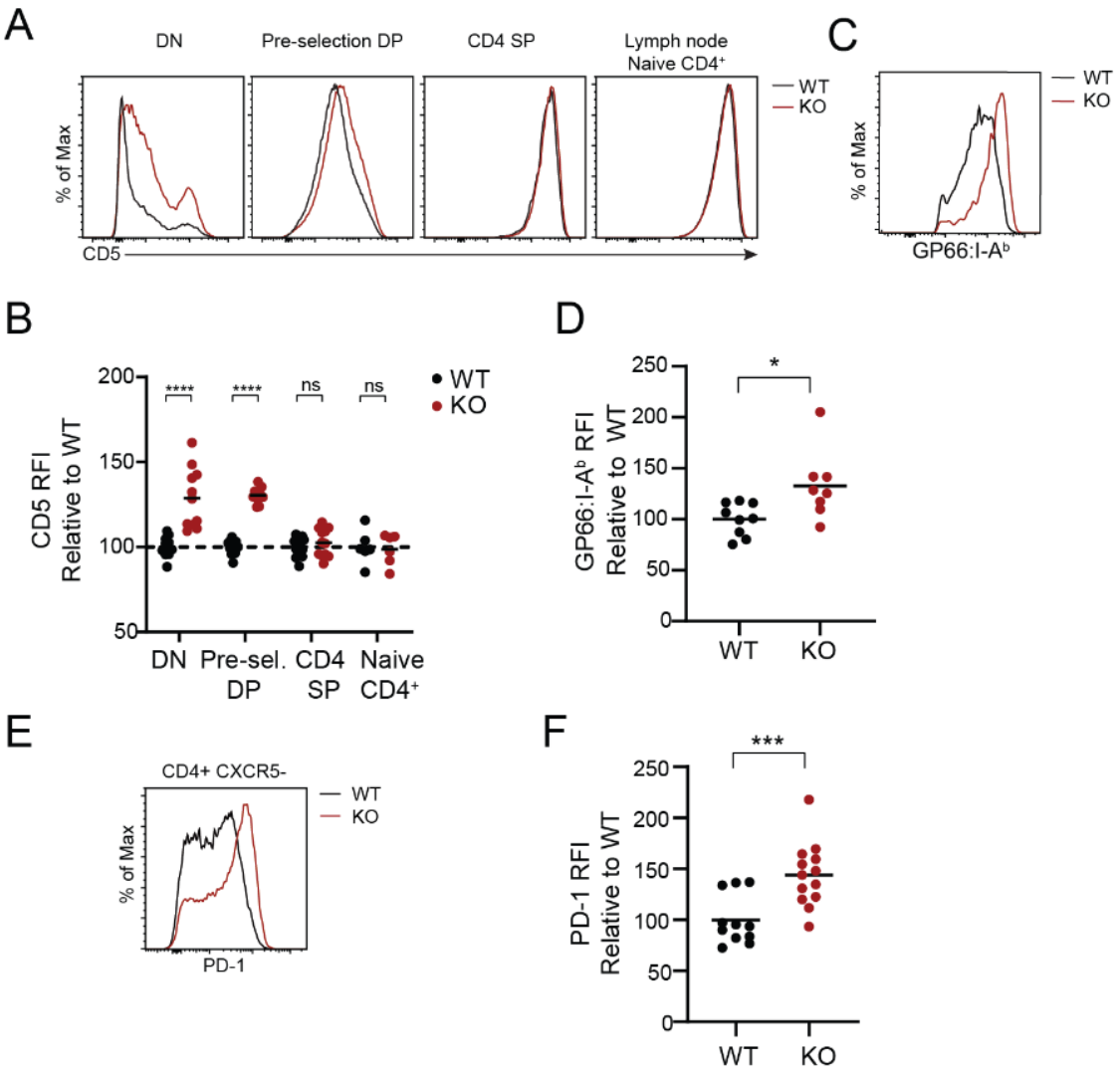

Figure 3. Evidence of stronger TCR signaling in TdT KO mice. ***A,B.*** *Representative flow cytometry plots of CD5 expression in CD4 and CD8 double negative (DN), CD4 and CD8 double positive CD69$^-$ pre-selection (DP) thymocytes, FoxP3$^-$ CD4$^+$ single positive thymocytes (4SP), and lymph node naïve CD4$^+$ T cells from uninfected mice* ***(A)****, data summarized from 4 experiments* ***(B)****.* ***C,D.*** *Representative flow cytometry plot of GP66:I-Ab expression on GP66-specific CD4$^+$ T cells from Day 30 LCMV cl13 infected mice* ***(C)****, data summarized from 2 experiments* ***(D)****.* ***E,F.*** *Representative flow cytometry plot of PD-1 expression on CXCR5$^-$ (Non-Tfh) CD4$^+$ T cells from Day 30 LCMV cl13 infected mice* ***(E)****, data summarized from 3 experiments* ***(F)****.*

We next investigated whether there was evidence for higher avidity clones in TdT KO mice during LCMV cl13 infection. We found that on average, GP66:I-A^b specific T cells in TdT KO mice had 25% increased tetramer binding strength (Figures 3C,D). Furthermore, PD-1 expression was significantly increased in $CXCR5^-$ CD4 T cells in LCMV cl13 infected TdT KO mice, indicating the presence of increased TCR signaling (Figures 3E,F). Taken together, TdT KO T cells have a phenotype that is associated with increased TCR signaling.

The increased GC-Tfh response in TdT KO mice has both T cell and B cell intrinsic components

TdT is expressed in immature B cells and also regulates B cell repertoire diversity [22]. Furthermore, B cells regulate the functional maturation of Tfh cells [41]. This raised the possibility that TdT-deficient B cells may be contributing to the GC-Tfh phenotype observed. To test this, we generated bone marrow chimeras where TdT deficiency was restricted to T cells only (KO T only), B cells only (KO B only), or both. (Figure 4A) GC-Tfh responses were significantly increased in KO T only and KO B only chimeras relative to WT T/B chimeras 30 days post LCMV cl13 infection. Interestingly, neither individually fully recapitulated the increased GC-Tfh response observed in KO T/B chimeras (Figures 4B,C). These data show that increased GC-Tfh differentiation in TdT KO mice has both T cell and B cell intrinsic components. In KO T only, but not KO T/B chimeras, there was significantly increased serum viral loads at day 30 post infection (Figure 4D). This data demonstrates that reduced T cell repertoire diversity in T cell specific TdT KO mice results in decreased pathogen control.

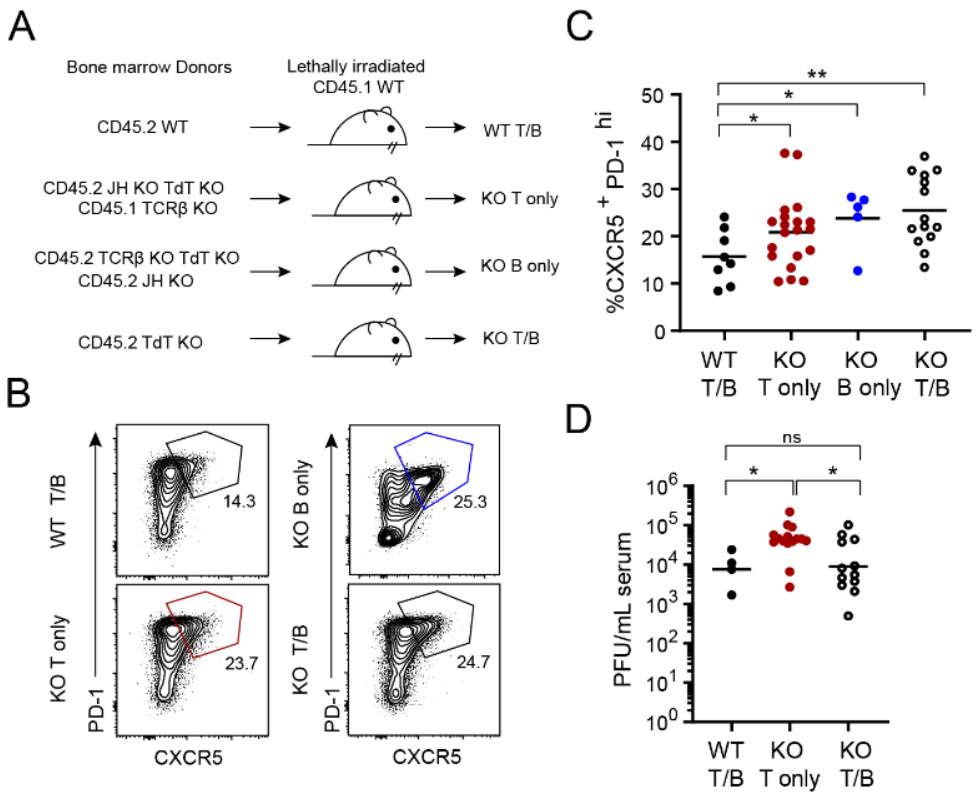

Figure 4. Increased Tfh differentiation in TdT KO mice has T cell and B cell intrinsic components. ***A.*** *Schematic indicating combinations of bone marrow to generate mice where TdT is deficient in T cells or in B cells only.* ***B,C.*** *Representative flow cytometry plots (gated on* $CD4^+$ $FoxP3^-$ $CD44^{hi}$*) of* $CXCR5^+$ $PD\text{-}1^{hi}$ *GC-Tfh cells 30 days post LCMV cl13 infection* ***(B)****, and data summarized from 3 experiments* ***(C)****.* ***D.*** *Serum viral load on Day 30 post LCMV cl13 infection.*

Discussion

TdT expression is highly conserved in vertebrates which indicates that it must have some benefit to the organism. However, an effect of the lack of TdT expression on $CD4^+$ T cell responses has not been reported. We found that GC-Tfh differentiation was increased in TdT KO mice in response to genetically diverse pathogens, indicating that increased GC-Tfh differentiation was a general property of the adult TdT-independent repertoire. This was associated with altered TCR Vβ diversity of responding $CD4^+$ T cells in TdT KO mice during LCMV cl13 infection. TdT KO SMARTA T cells did not have increased GC-Tfh differentiation compared to TdT-sufficient SMARTA T cells during LCMV cl13 infection, supporting that TdT expression in T cells regulates GC-Tfh differentiation in a mechanism intrinsic to the TCR. GC-Tfh differentiation has been shown to be favored by intermediate to strong TCR signals during an immune response. We found evidence that TdT KO T cells bear more highly reactive TCRs, notably having higher GP66:I-A^b tetramer binding strength and increased PD-1 expression during chronic LCMV cl13 infection. Future studies may aim to expand on this by tetramer pull down assay or surface plasmon resonance assays [42, 43]. However, it is unclear how many TCR:pMHC-II combinations must be tested to convincingly make generalizations about the entire repertoire.

TdT catalyzes between 2 and 5 non-templated nucleotides into TCR junctions on average [4]. TCR sequencing of TdT KO mice showed that average CDR3α/β lengths were reduced by 1-2 amino acids [35]. Therefore, while in wildtype mice CDR3 lengths are normally distributed with an average of 9-10 amino acids, this is shifted to 7-9 normally distributed amino acids in TdT KO mice [4]. Associations between CDR3 length and T-helper cell lineages have been described in antigen specific $CD4^+$ T cell populations. Two previous studies found that PLP_{56-70} specific Th2 cells had significantly longer CDR3α sequences (13-14 amino acids) than Th1 cells (~12 amino

acids) [44, 45]. Th17 cells had even shorter CDR3α sequences (~11 amino acids) [45]. In *in vivo* polarized PCC-specific Tfh cells, CDR3α and CDR3β lengths were 8 and 9 amino acids long, respectively [16]. Together, these studies showed that in certain antigen specific populations, Tfh and Th17 cells have the shortest average CDR3 lengths and Th2 cells have the longest CDR3 lengths while Th1 cells are intermediate to these populations. In TdT KO mice, where average CDR3 lengths are between 8-9 amino acids, we observed increased GC-Tfh differentiation. This extends the finding that PCC-specific Tfh cells were biased for T cells bearing shorter CDR3 regions to a polyclonal T cell repertoire. Furthermore, TdT may be necessary to generate lower avidity TCRs biased towards increased Th2 differentiation.

GC-Tfh cells are protective during chronic LCMV infection [46] [47]. In global TdT KO mice, the increased GC-Tfh response was not associated with improved control of LCMV cl13 or *C. neoformans* infections. In bone marrow chimera experiments, we observed higher viral loads at day 30 post LCMV cl13 infection when TdT deficiency was restricted to T cells only, despite elevated GC-Tfh cells compared to wildtype chimeras. However, it is not surprising that reduced T cell repertoire diversity would result in impaired control of a rapidly mutating virus, despite the subtle increase in GC-Tfh cells. Despite these expectations, experimental evidence supporting that pathogen control is impaired in TdT deficient mice has not been provided until now. Interestingly, these data also show that that increased B cell repertoire diversity, relative to KO B only chimeras, is not protective during persistent LCMV infection.

There are multiple potential explanations for the role B cell repertoire diversity may have in this model. Firstly, autoimmune regulator (Aire) expressing thymic resident B cells have recently been shown to positively regulate the negative selection of thymocytes [48]. Thymic B cells express tissue restricted antigen due to the action of Aire and through the presentation of

antigens derived from extracellular proteins captured with the BCR [48, 49]. The additional ability to capture antigen and present it to T cells for negative selection has been demonstrated to not have a redundant role with Aire-generated antigen [50]. This implies that the B cell repertoire to some degree regulates the antigens expressed during negative selection. B cell intrinsic TdT expression may play a role in the antigens presented since human thymic B cells were found to have highly diverse BCR repertoires with N-nucleotide containing CDR3 sequences. [51]. In agreement with the hypothesis that B cell repertoire diversity may regulate T cell repertoire diversity generated in the thymus, B cell knockout (μMT or J_H KO) mice had vastly reduced T cell repertoire diversity [52]. In global TdT KO mice, reduced B cell repertoire diversity may allow certain high avidity T cells to escape negative selection. Theoretically, these cells may be more prone to differentiating into GC-Tfh cells due to their increased TCR avidity. Tfh differentiation is a multistep process involving priming by DCs followed by maintenance by antigen-specific B cells via inducible T cell stimulator (ICOS)-ICOS ligand interactions [53, 54]. Reduced B cell repertoire diversity may result in increased B cell clone sizes, potentially increasing the probability of germinal center B cells encountering cognate Tfh cells, and thus resulting in increased maturation or survival signals provided to Tfh cells.

Collectively, we demonstrated an association between TCR sequence and $CD4^+$ T cell effector function. TdT KO $CD4^+$ T cells lacking N-region diversity were biased towards GC-Tfh differentiation. By restricting the TdT-deficiency to T cells, we found that the decreased T cell repertoire diversity in TdT KO mice lead to impaired control of LCMV during persistent infection.

References

1. Robins, H.S., et al., *Comprehensive assessment of T cell receptor beta-chain diversity in alphabeta T cells.* Blood, 2009. **114**(19): p. 4099-107.
2. Warren, R.L., et al., *Exhaustive T cell repertoire sequencing of human peripheral blood samples reveals signatures of antigen selection and a directly measured repertoire size of at least 1 million clonotypes.* Genome Res, 2011. **21**(5): p. 790-7.
3. Casrouge, A., et al., *Size estimate of the alpha beta TCR repertoire of naive mouse splenocytes.* J Immunol, 2000. **164**(11): p. 5782-7.
4. Cabaniols, J.P., et al., *Most alpha/beta T cell receptor diversity is due to terminal deoxynucleotidyl transferase.* J Exp Med, 2001. **194**(9): p. 1385-90.
5. Luo, W., et al., *Limited T cell receptor repertoire diversity in tuberculosis patients correlates with clinical severity.* PLoS One, 2012. **7**(10): p. e48117.
6. Cui, J.H., et al., *TCR Repertoire as a Novel Indicator for Immune Monitoring and Prognosis Assessment of Patients With Cervical Cancer.* Front Immunol, 2018. **9**: p. 2729.
7. Chang, C.M., et al., *Characterization of T cell Receptor Repertoire in Patients with Rheumatoid Arthritis Receiving Biologic Therapies.* Dis Markers, 2019. **2019**: p. 2364943.
8. Sheikh, N., et al., *Clonotypic Diversification of Intratumoral T Cells Following Sipuleucel-T Treatment in Prostate Cancer Subjects.* Cancer Res, 2016. **76**(13): p. 3711-8.
9. Gilfillan, S., et al., *Efficient immune responses in mice lacking N-region diversity.* Eur J Immunol, 1995. **25**(11): p. 3115-22.
10. Feeney, A.J., *Junctional sequences of fetal T cell receptor beta chains have few N regions.* J Exp Med, 1991. **174**(1): p. 115-24.
11. van Panhuys, N., F. Klauschen, and R.N. Germain, *T cell-receptor-dependent signal intensity dominantly controls CD4(+) T cell polarization In Vivo.* Immunity, 2014. **41**(1): p. 63-74.
12. Constant, S., et al., *Extent of T cell receptor ligation can determine the functional differentiation of naive CD4+ T cells.* J Exp Med, 1995. **182**(5): p. 1591-6.
13. Milner, J.D., et al., *Cutting edge: lack of high affinity competition for peptide in polyclonal CD4+ responses unmasks IL-4 production.* J Immunol, 2010. **184**(12): p. 6569-73.
14. Hosken, N.A., et al., *The effect of antigen dose on CD4+ T helper cell phenotype development in a T cell receptor-alpha beta-transgenic model.* J Exp Med, 1995. **182**(5): p. 1579-84.
15. Gomez-Rodriguez, J., et al., *Itk-mediated integration of T cell receptor and cytokine signaling regulates the balance between Th17 and regulatory T cells.* J Exp Med, 2014. **211**(3): p. 529-43.
16. Fazilleau, N., et al., *The function of follicular helper T cells is regulated by the strength of T cell antigen receptor binding.* Nat Immunol, 2009. **10**(4): p. 375-84.
17. Huang, J., et al., *The kinetics of two-dimensional TCR and pMHC interactions determine T cell responsiveness.* Nature, 2010. **464**(7290): p. 932-6.
18. Tubo, N.J., et al., *Single naive CD4+ T cells from a diverse repertoire produce different effector cell types during infection.* Cell, 2013. **153**(4): p. 785-96.
19. Garcia, K.C., et al., *An alphabeta T cell receptor structure at 2.5 A and its orientation in the TCR-MHC complex.* Science, 1996. **274**(5285): p. 209-19.
20. Chlewicki, L.K., et al., *High-affinity, peptide-specific T cell receptors can be generated by mutations in CDR1, CDR2 or CDR3.* J Mol Biol, 2005. **346**(1): p. 223-39.
21. Gilfillan, S., et al., *More efficient positive selection of thymocytes in mice lacking terminal deoxynucleotidyl transferase.* Int Immunol, 1994. **6**(11): p. 1681-6.
22. Gilfillan, S., et al., *Mice lacking TdT: mature animals with an immature lymphocyte repertoire.* Science, 1993. **261**(5125): p. 1175-8.
23. Oxenius, A., et al., *Virus-specific MHC-class II-restricted TCR-transgenic mice: effects on humoral and cellular immune responses after viral infection.* Eur J Immunol, 1998. **28**(1): p. 390-400.

24. Mombaerts, P., et al., *Mutations in T cell antigen receptor genes alpha and beta block thymocyte development at different stages.* Nature, 1992. **360**(6401): p. 225-31.
25. Gu, H., Y.R. Zou, and K. Rajewsky, *Independent control of immunoglobulin switch recombination at individual switch regions evidenced through Cre-loxP-mediated gene targeting.* Cell, 1993. **73**(6): p. 1155-64.
26. Sionov, E., et al., *Type I IFN Induction via Poly-ICLC Protects Mice against Cryptococcosis.* PLoS Pathog, 2015. **11**(8): p. e1005040.
27. Welsh, R.M. and M.O. Seedhom, *Lymphocytic choriomeningitis virus (LCMV): propagation, quantitation, and storage.* Curr Protoc Microbiol, 2008. **Chapter 15**: p. Unit 15A 1.
28. Smith, L.K., et al., *Interleukin-10 Directly Inhibits CD8(+) T Cell Function by Enhancing N-Glycan Branching to Decrease Antigen Sensitivity.* Immunity, 2018. **48**(2): p. 299-312 e5.
29. Huffnagle, G.B., et al., *IL-5 is required for eosinophil recruitment, crystal deposition, and mononuclear cell recruitment during a pulmonary Cryptococcus neoformans infection in genetically susceptible mice (C57BL/6).* J Immunol, 1998. **160**(5): p. 2393-400.
30. Reynolds, L.A., K.J. Filbey, and R.M. Maizels, *Immunity to the model intestinal helminth parasite Heligmosomoides polygyrus.* Semin Immunopathol, 2012. **34**(6): p. 829-46.
31. Stamm, A., et al., *An intermediate dose of LCMV clone 13 causes prolonged morbidity that is maintained by CD4+ T cells.* Virology, 2012. **425**(2): p. 122-32.
32. Boubakour-Azzouz, I., et al., *Terminal deoxynucleotidyl transferase requires KU80 and XRCC4 to promote N-addition at non-V(D)J chromosomal breaks in non-lymphoid cells.* Nucleic Acids Res, 2012. **40**(17): p. 8381-91.
33. Gouge, J., et al., *Structural basis for a novel mechanism of DNA bridging and alignment in eukaryotic DSB DNA repair.* EMBO J, 2015. **34**(8): p. 1126-42.
34. Loc'h, J., S. Rosario, and M. Delarue, *Structural Basis for a New Templated Activity by Terminal Deoxynucleotidyl Transferase: Implications for V(D)J Recombination.* Structure, 2016. **24**(9): p. 1452-63.
35. Haeryfar, S.M., et al., *Terminal deoxynucleotidyl transferase establishes and broadens antiviral CD8+ T cell immunodominance hierarchies.* J Immunol, 2008. **181**(1): p. 649-59.
36. Keck, S., et al., *Antigen affinity and antigen dose exert distinct influences on CD4 T cell differentiation.* Proc Natl Acad Sci U S A, 2014. **111**(41): p. 14852-7.
37. Hwang, S., et al., *TCR ITAM multiplicity is required for the generation of follicular helper T cells.* Nat Commun, 2015. **6**: p. 6982.
38. Burgueno-Bucio, E., C.A. Mier-Aguilar, and G. Soldevila, *The multiple faces of CD5.* J Leukoc Biol, 2019. **105**(5): p. 891-904.
39. Azzam, H.S., et al., *CD5 expression is developmentally regulated by T cell receptor (TCR) signals and TCR avidity.* J Exp Med, 1998. **188**(12): p. 2301-11.
40. Mandl, J.N., et al., *T cell-positive selection uses self-ligand binding strength to optimize repertoire recognition of foreign antigens.* Immunity, 2013. **38**(2): p. 263-274.
41. Stebegg, M., et al., *Regulation of the Germinal Center Response.* Front Immunol, 2018. **9**: p. 2469.
42. Moon, J.J., et al., *Naive CD4(+) T cell frequency varies for different epitopes and predicts repertoire diversity and response magnitude.* Immunity, 2007. **27**(2): p. 203-13.
43. Matsui, K., et al., *Kinetics of T cell receptor binding to peptide/I-Ek complexes: correlation of the dissociation rate with T cell responsiveness.* Proc Natl Acad Sci U S A, 1994. **91**(26): p. 12862-6.
44. Boyton, R.J., et al., *CD4 T cells selected by antigen under Th2 polarizing conditions favor an elongated TCR alpha chain complementarity-determining region 3.* J Immunol, 2002. **168**(3): p. 1018-27.
45. Reynolds, C., et al., *Elongated TCR alpha chain CDR3 favors an altered CD4 cytokine profile.* BMC Biol, 2014. **12**: p. 32.
46. Cook, K.D., et al., *T Follicular Helper Cell-Dependent Clearance of a Persistent Virus Infection Requires T Cell Expression of the Histone Demethylase UTX.* Immunity, 2015. **43**(4): p. 703-14.

47. Greczmiel, U., et al., *Sustained T follicular helper cell response is essential for control of chronic viral infection.* Sci Immunol, 2017. **2**(18).
48. Yamano, T., et al., *Thymic B Cells Are Licensed to Present Self Antigens for Central T Cell Tolerance Induction.* Immunity, 2015. **42**(6): p. 1048-61.
49. Perera, J., et al., *Autoreactive thymic B cells are efficient antigen-presenting cells of cognate self-antigens for T cell negative selection.* Proc Natl Acad Sci U S A, 2013. **110**(42): p. 17011-6.
50. Frommer, F. and A. Waisman, *B cells participate in thymic negative selection of murine auto-reactive CD4+ T cells.* PLoS One, 2010. **5**(10): p. e15372.
51. Rother, M.B., et al., *The Human Thymus Is Enriched for Autoreactive B Cells.* J Immunol, 2016. **197**(2): p. 441-8.
52. Joao, C., et al., *B cell-dependent TCR diversification.* J Immunol, 2004. **172**(8): p. 4709-16.
53. Weber, J.P., et al., *ICOS maintains the T follicular helper cell phenotype by down-regulating Kruppel-like factor 2.* J Exp Med, 2015. **212**(2): p. 217-33.
54. Crotty, S., *T follicular helper cell differentiation, function, and roles in disease.* Immunity, 2014. **41**(4): p. 529-42.

Chapter 4 Supplemental Figures

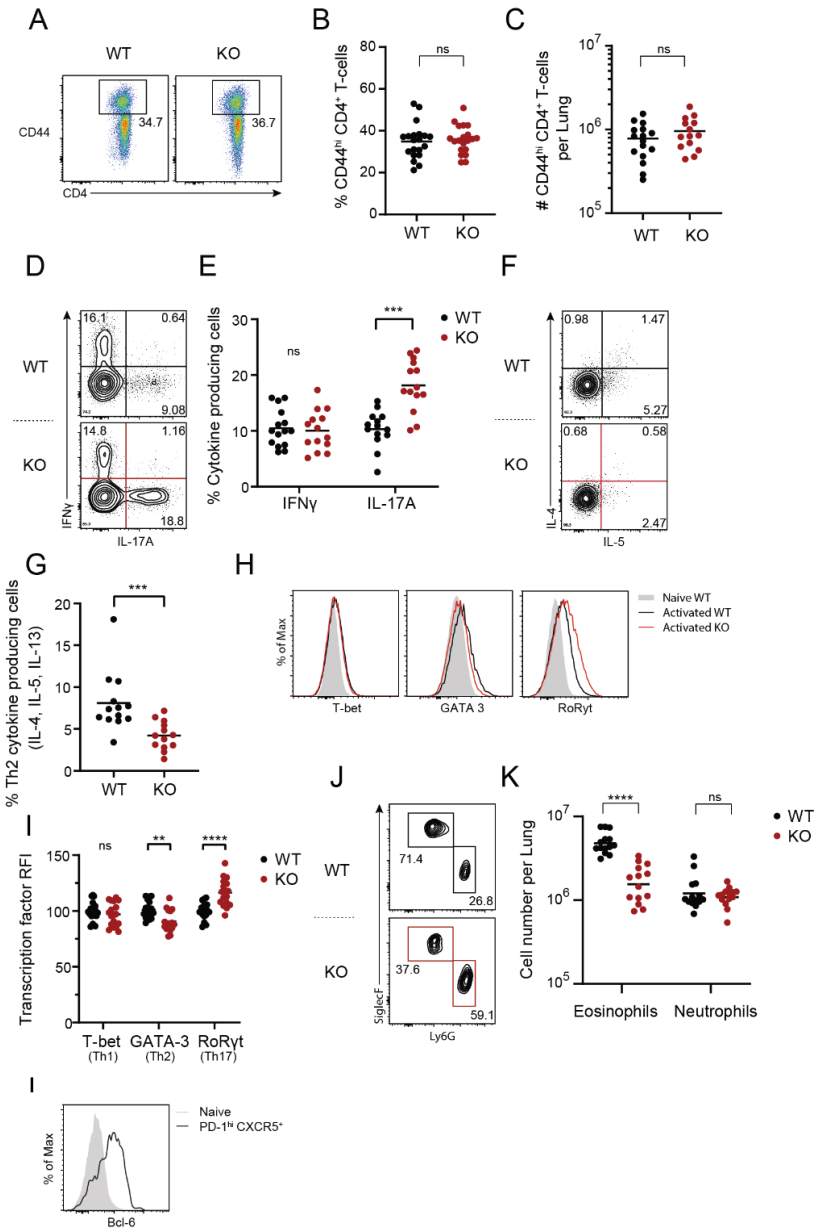

Supplemental Figure 1. Altered CD4 T cell differentiation in TdTKO mice during *C. neoformans infection.* *$CD4^+$ T cell differentiation was assessed at 20 days post infection **A,B,C**. Representative flow cytometry plots (gated on $CD4^+$ $FoxP3^-$) of CD44 expression in the lung **(A)**, summary of percent $CD44^{hi}$ CD4 T cells **(B)**, summary of the number of CD44hi CD4 T cells in the lung **(C)**. **D,E.** Representative flow cytometry plots (gated on CD4+ FoxP3- $CD44^{hi}$) of IFNγ and IL-17A expression **(D)**, summary of cytokine expression from 4 experiments **(E)**. **F,G.** Representative flow cytometry plots (gated on $CD4^+$ $FoxP3^-$ $CD44^{hi}$) of IL-4 and IL-5 expression **(F)**, summary of cytokine expression from 4 experiments **(G)**. **H,I.** Representative flow cytometry histograms (gated on $CD4^+$ $FoxP3^-$ $CD44^{hi}$) of RoRγt, T-bet, and GATA-3 transcription factors **(H)**, summary of expression from 4 experiments **(I)**. **J,K.** Representative flow cytometry plots (gated on $CD11b^+$ $CD11c^+$ $CD68^+$) of eosinophils ($SiglecF^+$ $Ly6G^-$) and neutrophils (SiglecF- Ly6G+) **(J)**, summary of eosinophil and neutrophil numbers from 4 experiments **(K)**. **L,** Representative flow cytometry plot of Bcl-6 expression on naïve (CD44-) CD4+ T cells versus Tfh (CXCR5+ PD-1hi) cells.*

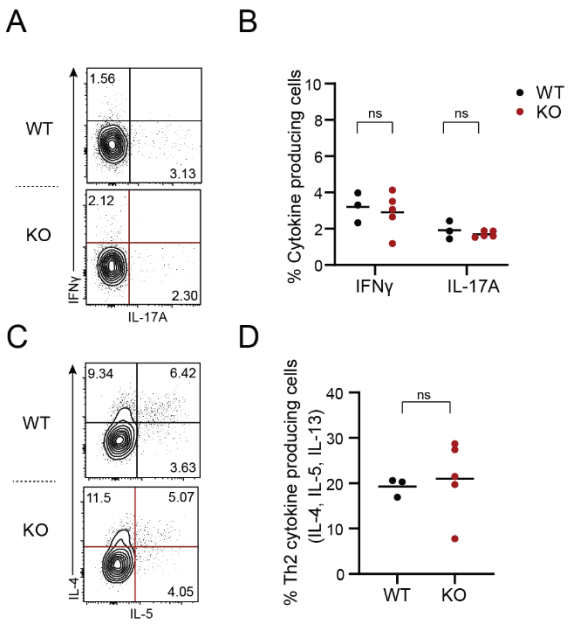

Supplemental Figure 2. No difference in Th2 or Th17 differentiation in TdTKO mice during *H. polygyrus* infection. *$CD4^+$ T cell differentiation was assessed in WT versus KO mice at 14 days post infection with H. polygyrus.* ***A,B.*** *Representative flow cytometry plots (gated on $CD4^+$ $FoxP3^-$ $CD44^{hi}$) of IFNγ and IL-17A expression* ***(A)****, summary of cytokine expression from 1 experiment* ***(B). C,D.*** *Representative flow cytometry plots (gated on $CD4^+$ $FoxP3^-$ $CD44^{hi}$) of IL-4 and IL-5 expression* ***(C)****, summary of cytokine expression from 1 experiment* ***(D)****.*

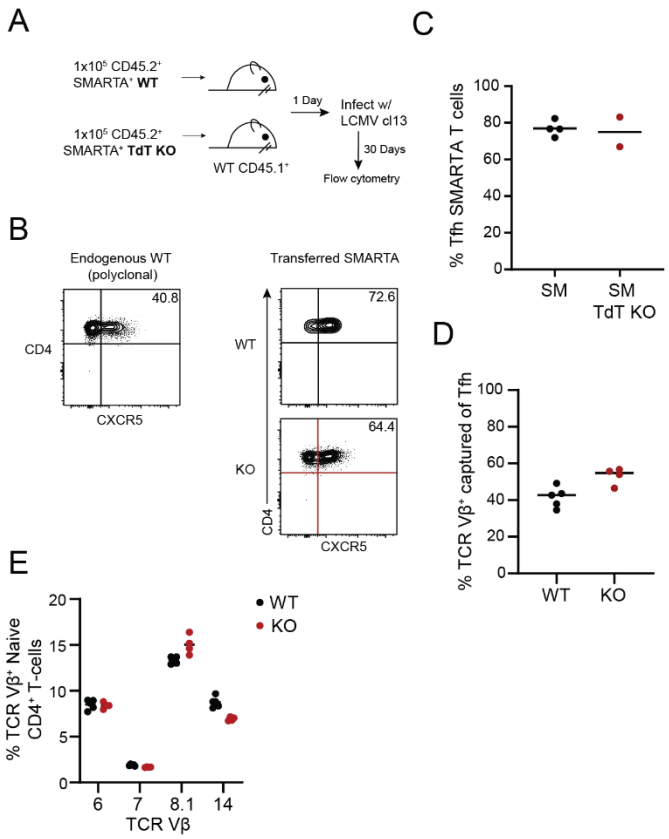

Supplemental Figure 3. Increased Tfh differentiation in TdTKO mice is TCR intrinsic. ***A.*** *Experimental setup for SMARTA T cell adoptive transfer and LCMV cl13 infection.* ***B,C.*** *Gating strategy for GC-Tfh cells (CXCR5⁺) with endogenous wildtype cells (CD45.1⁺ CD4⁺ FoxP3⁻ CD44^{hi}) on the left, and transferred (CD45.2⁺ CD4⁺ FoxP3⁻ CD44^{hi}) cells on the right* ***(B)****, summary of GC-Tfh cells from 1 experiment* ***(C)****.* ***D.*** *Sum of the percentage of GC-Tfh cells expressing TCR Vβ6, Vβ7, Vβ8.1, and Vβ14 from Day 30 of LCMV cl13 infection in wildtype versus TdT KO mice.* ***e,*** *Summary of TCR Vβ expression in naïve CD4⁺ T cells from Day 30 LCMV cl13 infected mice.*

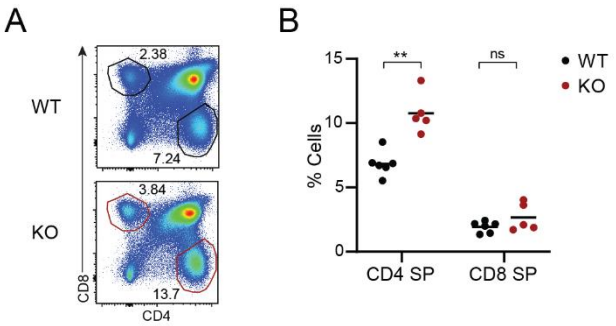

Supplemental Figure 4. Increased CD4 SP and CD8 SP thymocytes in TdTKO mice. ***A.*** *Representative flow cytometry plots (gated on live, singlets, lymphocytes) of 4SP and 8SP gating. 4SP cells were further gated on CD25$^-$ cells (not shown).* ***B.*** *Summary of the frequency of 4SP and 8SP populations from 2 experiments.*

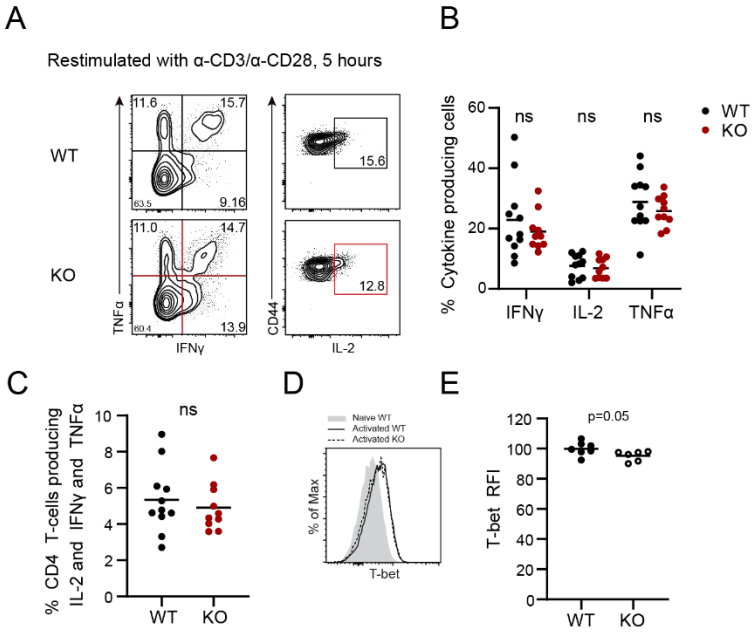

Supplemental Figure 5. Unaltered cytokine production in TdTKO mice during LCMV cl13 infection. ***A,B.*** *Representative flow cytometry plots (gated on CD4$^+$ FoxP3$^-$ CD44^{hi}) of IFNγ, TNFα, and IL-2 expression 30 Days post LCMV cl13 infection* ***(A)****, summary of cytokine expression from 3 experiments* ***(B).*** ***C.*** *Summary of cells expressing all three cytokines (Boolean gating).* ***D,E.*** *Representative flow cytometry histogram of T-bet expression* ***(D)****, summary from 2 experiments* ***(E)****.*

Chapter 5: Discussion

The work in this thesis investigated different mechanisms controlling the selection of an effective T cell repertoire. The primary focus was on how the environmental factor vitamin D controls mTEC function and differentiation, and thymic organogenesis. This work was undertaken based on clinical data that linked vitamin D deficiency early in life to increased risk of developing autoimmunity, suggesting that vitamin D may play a role in the negative selection of T cells in the thymus. I also investigated how the action of a highly conserved thymic DNA polymerase, TdT, regulates the diversity of $CD4^+$ effector T cell differentiation during infection.

The presence of the VDR in the thymus was recognized as early as 1984, as calf thymus extracts were used as a source of VDR for competitive binding assays for 1,25D [175]. VDR expression in the thymus was also confirmed later by other groups [176]. In 1987, a study found that rats fed a vitamin D-deficient diet and later injected with radio-labeled 1,25D (^3H) had retained radioactivity in the nucleus of reticular cells, but not lymphocytes, of the thymic cortex and medulla [177]. This was abrogated when rats were first injected with excess unlabeled 1,25D [177], thus providing strong evidence for the presence of the VDR and active vitamin D signaling in rat thymi. However, the thymic cell types expressing the VDR and the potential role for 1,25D signaling in the thymus were not investigated until much later. A study published in 2022 using a tdTomato-reporter, labeling cells with past or current Vdr expression, found that the Vdr was expressed in all major subsets of conventional thymocytes, notably being highly expressed in DP cells [178]. Basic phenotypic analyses of lymphocyte populations in the thymus of Vdr-deficient mice did not reveal substantial alterations in the frequency of conventional thymocyte populations [179]. However, the thymic development iNKT cell and $CD8\alpha\alpha^+$ intraepithelial cells were shown to be defective in *Vdr* KO mice [180, 181]. To our knowledge, the thymic phenotype of *Cyp27b1*

KO mice had not been studied prior to our investigations. Moreover, alterations in thymic populations in Vdr-deficient mice thus far have been restricted to the phenotype of hematopoietic cells, despite evidence of Vdr expression in critical stromal cell types.

Consistent with previous studies, we found that the Vdr was expressed in thymocytes. Furthermore, we demonstrated that the Vdr is expressed in both cortical and medullary TECs (reticular cells) using specific markers, and that it is also present in hematopoietic thymic APCs such as DCs and B cells. The presence of nuclear Vdr staining in whole thymus by IF was suggestive of active vitamin D signaling, consistent with our findings of the presence of *Cyp24a1* transcripts in RNA sequencing data of mouse and human TECs. Confirmation of signaling was obtained by *Cyp24a1* induction in 1,25D-treated thymic slices (2–10-fold) and sorted TECs (50–100-fold). We further demonstrated that 1,25D regulates the induction of Aire mRNA and protein expression in mTECs, and the absence of 1,25D in *Cyp27b1* KO mice resulted in impaired $Aire^+$ mTEC differentiation. The relatively higher induction of *Cyp24a1* in TECs, relative to thymic slices, indicated that TECs are more sensitive to 1,25D than thymocytes, which make up ~98% of thymic slices. This is supported by observations from our imaging data from whole thymi, which showed that the Vdr was generally nuclear in mTECs but cytoplasmic in thymocytes.

Aire expression and mTEC differentiation is crucially dependent on NF-κB signaling following engagement of RANK with its ligand RANKL, which is provided primarily by positively selected 4SP thymocytes in adult mice [150]. We have preliminary data not included in this thesis that 1,25D treatment upregulates the expression of *Rankl* mRNA in thymic slices. Additionally, we found that *Rankl* mRNA and protein was decreased in *Cyp27b1* KO thymocytes. Therefore, in order to clarify the TEC-intrinsic role of 1,25D in $Aire^+$ TEC maturation, it will be necessary to generate TEC-specific conditional KO mice. We demonstrated that nearly all thymic

cell types express Cyp27b1 and could theoretically produce 1,25D. Furthermore, renal-derived 1,25D may enter the thymus through the circulation. Therefore, TEC-specific deletion of *Cyp27b1* may not prevent Vdr activation in TECs due to paracrine 1,25D signaling. To address this question, analysis of the thymic phenotypes in $Vdr^{fl/fl}$ x $FoxN1^{cre}$ mice would be critical. This includes investigating potential defects in $Aire^{+}$ mTEC maturation, TRA expression, and thymic cellularity and involution. Important controls to include would be $Vdr^{fl/fl}$ x $FoxN1^{cre-}$ mice and $Vdr^{fl/fl}$ x $Cd4^{cre}$ mice to study potential T cell intrinsic roles. For preliminary studies, it would also be important to include full *Vdr* KO controls, because of known phenotypic differences with *Cyp27b1* KO mice, such as alopecia in *Vdr* but not *Cyp27b1* KO mice [61]. In the event that the *Vdr* KO does not phenocopy the *Cyp27b1* KO thymic phenotype, other conditional KO models to target 1,25D signaling in TECs without targeting the Vdr may be necessary. Furthermore, if this is the case, the roles of 1,25D-independent actions of the Vdr on Aire expression would merit further investigation.

RNA sequencing studies with Aire KO and control TECs demonstrated that Aire regulates the expression of more than 3,200 genes in mTECs [182-184], representing transcriptional control of ~21% of the 15,000 expressed genes in mTECs [184]. However, the mechanisms by which AIRE is recruited to its target genes in humans and mice, and regulates transcriptional activity are still under investigation. The PHD1 domain of AIRE binds hypomethylated lysine 4 residues on histone H3 tails (H3K4me0)[132, 185], a histone mark associated with transcriptionally inactive genes. The range of genes targeted by Aire was unaltered in mice expressing a PHD1 domain mutant (D299A) that decreased the affinity of Aire for H3 tails by 15- to 30-fold [186]. However, the impact of Aire on transcription was globally diminished [186]. Furthermore, these mice had similar autoimmune disease to Aire KO mice, indicating that recognition of H3K4 marks by Aire

are important for central tolerance. However, overexpression of a H3K4-specific demethylase in *in vitro* experiments did not alter the transcriptional range or activity of Aire, collectively suggesting that while binding of Aire to H3K4me0 marks with its PHD1 domain is essential for central tolerance, these marks are not a targeting mechanism by which Aire is recruited to chromatin. Another study proposed that Aire is recruited to chromatin via interactions of its SAND domain with transcriptionally silent genes by the methyl CpG-binding protein 1-activating transcription factor 7-interacting protein (MBD1-ATFip) complex, which binds methylated CpG islands [187]. MBD1 KO mice had aberrant T cell infiltration into salivary and lacrimal glands. However, comparison of TRA gene expression in MBD1 and Aire KO mice revealed that MBD1 targets differed from those of Aire. Moreover, the effect on Aire-dependent gene expression in MBD1 KO mice was minor [187]. Therefore, association of Aire to its target genes via MBD1-ATFip does not appear to be the principal mechanism by which Aire is recruited. Overall, evidence for the precise mechanism by which Aire is recruited and recognizes its target genes is lacking.

The observation that mouse and human AIRE contain 4 LXXLL motifs traces back to a the original paper describing the cloning of the mouse *Aire* gene in 1997 [137], a finding that was noted in subsequent publications but never further investigated by the field. (Note that the original paper describing the cloning of the mouse *Aire* gene described only 3 LXXLL motifs [137]). As mentioned above, LXXLL motifs are critical for recruitment of cofactors to agonist-bound nuclear receptors, such as the VDR. Through co-IP experiments in transfected HEK293 cells, we found that the VDR and AIRE were interacting partners, and this interaction was enhanced by the presence of 1,25D. ChIP and re-ChIP assays confirmed the simultaneous presence of the VDR and AIRE on a *CYP24A1* VDRE in transfected 1,25D-treated HEK293 cells. We further confirmed the presence of the Vdr and Aire on VDREs adjacent to the *Cyp24a1* and *Rnase1* genes in sorted

primary mouse mTECs. Finally, using HEK293 cells transfected with a construct containing a minimal promoter composed of two VDRE's and a TATA box driving the expression of a luciferase reporter, we found that transfecting increasing concentrations of an *AIRE* expression vector enhanced VDR-dependent transcription in a 1,25D dependent manner. These results suggest that binding of AIRE to ligand-bound nuclear receptors such as the VDR may be a targeting mechanism by which AIRE is recruited to target genes. The VDR regulates the expression of thousands of genes. Our analysis of expression profiles showed that, in addition to the VDR, there are several other nuclear receptors expressed in mTECs. Collectively, these results suggest that recruitment of AIRE by the VDR and other nuclear receptors to DNA may contribute substantially to the breadth of AIRE target genes *in vivo*.

In addition to differences in the epigenetic landscapes, differences in nuclear receptor expression or function in different cell types may explain why the targets of AIRE differ when transfected into different cell types. Our finding that AIRE is a coactivator of the VDR is consistent with previous ideas that AIRE appears to enhance transcription [188]. Recruitment of AIRE to VDR target genes, including some TRA genes, may be a mechanism to enhance the transcription of rare TRA's. Future ChIP-seq studies of $mTEC^{hi}$ cells to determine the 1,25D-dependent genome-wide (co)distribution of Aire and the Vdr would address multiple aspects of these hypotheses. In the absence of 1,25D, the range of genes with chromatin-associated Aire protein would be expected to be decreased compared to $mTEC^{hi}$ cells isolated from whole thymus. Increases in the range of TRA genes bound by Aire in the presence of 1,25D, particularly when co-occupying sites with the Vdr, by directed ChIP/re-ChIP would convincingly demonstrate that the Vdr recruits Aire to TRA genes to regulate TRA production. Investigating whether 1,25D signaling enhances the transcription of rare TRA genes by scRNAseq may be complicated by the

fact that only the most abundant transcripts are amplified. An alternative may be to perform a comprehensive analysis of TRA gene expression levels in bulk RNAseq samples from highly pure sorted wildtype and *Cyp27b1* KO mTEC^{hi} cells, in addition to wildtype mTEC^{hi} cells treated with or without 1,25D.

We observed that 1,25D-treatment upregulated *Aire* mRNA in thymic slices, but it is unclear whether this regulation is direct, i.e., through binding of 1,25D-Vdr to putative *Aire* VDRE(s). This may be addressed by screening for Vdr binding in the vicinity of the *Aire* gene and validation by directed ChIP assays. It is also important to determine whether or not the absence of 1,25D signaling in the thymus specifically has an impact on the incidence or severity of autoimmunity in mouse models. Autoimmune infiltration into the salivary gland of *Aire* KO mice can be detected starting at 9 weeks of age, however, immune infiltration in most other organs is more readily observable between 20–35 weeks of age [189]. Histological examination of these target organs in *Cyp27b1* KO in a similar time window would be of interest. To distinguish potential thymic contributions to autoimmunity from peripheral 1,25D signaling, inclusion of conditional KO (*Vdr*$^{fl/fl}$ x *FoxN1*^{cre} or *Cd4*^{cre}) mice will be critical.

While relatively little was known about vitamin D signaling in the mouse thymus prior to our studies, even less is known about vitamin D action in the human thymus. We analyzed published single cell RNA sequencing data derived from the thymi of two 10-month-old children and found *VDR* transcripts. We additionally found *CYP27B1*- and *CYP24A1*-positive TECs, providing evidence for the presence of 1,25D and active vitamin D signaling in human TECs. Mapping vitamin D signaling experimentally with human thymic samples would be necessary to translate our findings from mice. It would be fascinating to compare scRNAseq data from human thymic samples derived from healthy and vitamin D deficient or rachitic donors to assess whether

vitamin D in humans influences TEC differentiation and thymic organ development. However, it would be extremely unlikely to have access to such samples.

Our work has provided ample evidence that Aire^{+} TEC differentiation and TRA gene expression was impaired in *Cyp27b1* KO mice. The impact on negative selection was assessed indirectly by quantifying the frequency of Helios^{+} 4SP thymocytes and the number of apoptotic thymocytes in the thymic medulla. Helios is downregulated in positively selected thymocytes, and upregulated in negatively selected thymocytes, and is thus a marker of autoreactive T cells in the thymus [190]. Our finding that the frequency of Helios^{+} FoxP3^{-} 4SP thymocytes was halved in *Cyp27b1* KO thymi may be explained by decreased Helios induction due to decreased negative selection, or by enhanced positive selection. We found no significant difference in the expression of TCRβ, CD69, or CD5, which are markers associated with positively selected thymocytes. This makes it unlikely that positive selection is more efficient in *Cyp27b1* KO thymi and provides little explanation for the decreased Helios expression observed. The decreased number of cleaved-caspase-3^{+} thymocytes in the *Cyp27b1* KO medulla supports the hypothesis of decreased negative selection. Furthermore, the frequency of Helios^{+} FoxP3^{-} 4SP thymocytes was reduced in other knockout mouse models with impaired negative selection [191]. Nonetheless, while suggestive of impaired negative selection, more rigorous validation of the role of 1,25D signaling in negative selection is merited. This can be addressed by treating thymic slices with or without 1,25D and assessing antigen-specific T cell fates. Tetramer staining to investigate this in a polyclonal repertoire is challenging due to the rarity of tetramer-specific cells and the low number of cells that can be extracted from thymic slices. An alternative method would be to utilize INS2-USA Tg mice, which have a modified OVA gene at the start codon of the *Ins2* gene that contains other epitopes including gp33, LCMV gp66, and 2W. Since *Ins2* transcription is highly Aire-dependent,

the expression of the USA is also Aire-dependent in this model. Antigen-specific tolerance can be assessed using 1,25D or vehicle treated thymic slices generated from INS2-USA transgenic (Tg) on wildtype or *Cyp27b1* KO backgrounds, overlayed with CFSE-labeled USA-specific TCR Tg thymocytes from OT-I Rag2 KO (OVA-specific) or SMARTA Rag1 KO (LCMV gp66-specific) TCR Tg mice.

Unexpectedly, we found that thymic involution was accelerated in *Cyp27b1* KO mice. A previous study from 1985 demonstrated that aged nephritic rats had a ~40% reduction in thymic weight wet compared to normal rats [192]. Importantly, treatment with vitamin D or its metabolites, such as 1,25D, moderately or completely restored thymic weight in nephritic rats to control levels [192]. We've extended these findings on multiple levels. First, the presence of 1,25D does not appear to affect thymic organogenesis in young mice, less than 4 weeks of age. Rather, it appears to delay the age-associated decline in thymic cellularity that occurs after the thymus reaches its peak size. Second, 1,25D signaling controls TEC proliferation and the gene expression of various pro-thymic cytokines, including *Fgf21*, *Igf1*, and *Fgf7*. We also found that the number of splenic T cells was reduced in *Cyp27b1* KO mice. This may be due to decreased thymic output, altered peripheral T cell homeostasis, or both. Recent thymic emigrants (RTE's) can be quantified by enumerating the amount of signal joint T cell receptor excision circles (sjTRECs), which are DNA sequences generated in thymocytes during thymic development that are not passed on during cell division [193, 194]. Quantifying sjTREC numbers in wildtype and *Cyp27b1* KO mice and comparing splenic T cell numbers in 4-week-old mice, when there is no difference in thymic size between control and KO mice, would illustrate the contribution of the thymic defect to the peripheral lymphopenia observed in 6–10-week-old *Cyp27b1* KO mice.

B cell numbers were also reduced systemically in *Cyp27b1* KO mice. Because B cells are

thymic APCs that express Aire, with non-overlapping roles in negative selection with mTECs, it is likely that their reduced numbers in *Cyp27b1* KO mice have deleterious effects for T cell selection. However, unlike mTECs, Aire expression in B cells was unaltered in *Cyp27b1* KO mice, suggesting that Aire expression in these two cell types may be regulated differently. Our data suggested that B cell development in the bone marrow of *Cyp27b1* KO mice was deficient. Mechanistically, this may be due to defects in RANKL expression in the absence of 1,25D, which we demonstrated to be downregulated in the thymus of *Cyp27b1* KO mice. Global mouse knockouts for RANK and RANKL result in a systemic 50% decrease in B cell numbers [195, 196]. However, B cell-specific RANK deficiency does not alter their maturation [197], suggesting an indirect role of RANKL deficiency in B cell development. We also examined the frequency of thymic DCs, which are critical for T cell selection. Total DC ($CD11c^+$ $MHC\text{-}II^+$) frequencies were unaltered in *Cyp27b1* KO thymi, however, the frequencies of pDC, and cDC $SIRP\alpha^+$ or $CD8\alpha^+$ DCs were not analyzed individually. Since 1,25D signaling in peripheral DCs inhibits antigen presentation [198], and most negative selection is thought to occur in the cortex through interactions with DCs expressing peptides derived from $Aire^+$ mTECs [199, 200], it would be of interest to further investigate the role of 1,25D on thymic DC function. Prior to the findings established in this thesis, our knowledge of how vitamin D shapes the T cell repertoire was limited. These results show that vitamin D regulates the development and function of mTECs, which are critical for enforcing a self-tolerant T cell repertoire and open the path for important future studies.

T cells bearing TCRs with high avidity for self-pMHC are removed from the repertoire during negative selection. Furthermore, T cells with high avidity for self-pMHC also have high avidity for foreign pMHC [201], and highly reactive T cells dominate the immune response during infection [201-203]. Therefore, the trade-off for generating a self-tolerant T cell repertoire is

sacrificing some T cells with high TCR affinity, thus limiting the host's ability to detect and vigorously respond to infection and cancer. This compromise has been evolutionarily determined to be beneficial to the host. Therefore, T cell selection is optimized to generate a repertoire containing the most beneficial TCRs. However, precisely how individual TCR sequences correlate with antigen specificity, T cell function, and host protection remains unclear. This is challenging to investigate due to the massive diversity of the T cell repertoire and expressed MHC alleles, within and between individuals. However, advances have been made in identifying the determinants of TCR specificity and avidity for pMHC.

Observations that TCRs from T cells with the same specificity often share conserved TCR sequences lead to an analysis of 10 epitope-specific repertoires. This study demonstrated that each epitope-specific repertoire contained TCRs with core sequence similarities, but with diverse outlier TCR sequences [204]. They further developed a TCR classifier that could predict the TCR specificity of the tested repertoires with 72–80% accuracy. Another study developed an algorithm called GLIPH (**g**rouping of **l**ymphocyte **i**nteractions **b**y **p**aratope **h**otspots) based on TCR structural data and sequencing data from pMHC-tetramer sorted T cells [205]. This algorithm clusters TCRs based on their probability of sharing specificity, as a function of CDR3 sequences and other conserved motifs. GLIPH was able to group TCRs from different blood donors, illustrating that conserved CDR3 motifs participated to define TCR specificity. Importantly, TCRαβ sequencing from 22 donors with latent *M.tb* infection and GLIPH analysis allowed them to accurately identify pMHC ligands for *M.tb*. Furthermore, they used GLIPH to predict the specificity of new TCRs, not seen in donors, to the *M.tb*. antigen Rv1195. Interestingly, these TCRs had similar or improved antigen-specific activation compared to naturally occurring TCRs derived from one of their donors. These findings have enormous implications for cancer T cell

therapies, which rely on the identification of tumor-pMHC ligands and adoptive transfer of autologous tumor-specific T cells [206].

A challenge in designing such T cell therapies is the selection of TCRs bearing high reactivity for the tumor-antigens of interest. This has been addressed by genetic engineering of TCR affinity enhanced T cells [206]. However, modifying T cell receptor affinity without altering specificity is challenging, and while often effective at providing anti-tumor immunity, has also resulted in off-target attack of self-tissues [207-209]. Therefore, identifying and utilizing highly specific TCRs within the naturally occurring T cell repertoire with high pMHC avidity is prudent. Cell surface markers such as CD5 are excellent readouts of TCR reactivity, but varies even within the monoclonal repertoires of TCR transgenic mice [201]. Therefore, it remains important to understand what structural elements of the TCR govern pMHC reactivity. Two TCR transgenic mice specific for the same HSV glycoprotein B epitope had equal tetramer binding strength and proliferation after *in vitro* stimulation, demonstrating that not all structural differences in the TCR result in functional differences [210]. Like TCR specificity, this suggests that there may be certain motifs of the TCR that are important to mediate reactivity. Whether or not these potential motifs are conserved between TCRs or whether they vary between TCR-pMHC combinations is under investigation. One study found that hydrophobic amino acids at positions 6 and 7 of the CDR3β chain conferred higher reactivity for self-pMHC, regardless of MHC haplotype tested [211]. This indicates that hydrophobicity at these residues may confer higher pMHC reactivity as a general rule of the repertoire.

We investigated how the loss of TCRs containing N-nucleotides affects pathogen resistance and the functional diversity of $CD4^+$ T cells, using TdT KO mice. Our data demonstrated that $CD4^+$ T cell differentiation was altered in TdT KO mice. GC-Tfh differentiation was increased in

TdT KO mice in three models of chronic infection, including *C. neoformans*(fungus), *H. polygyrus* (parasite), and LCMV cl13 (virus). This suggests that the bias in GC-Tfh differentiation is a general property of the germline encoded repertoire. Furthermore, Th17 cell differentiation was increased and Th2 differentiation was decreased in *TdT* KO mice during *C. neoformans*, but not *H. polygyrus*, infection. This may represent a specific bias in the TCRs involved during the response to *C. neoformans*. Th1 and Th17 cytokine profiles were reported to be enriched in cells with shorter CDR3α lengths, whereas Th2 cells had longer CDR3α lengths [212]. Another study also demonstrated that Th2 cells had longer CDR3α sequences than their Th1 counterparts [213]. Additionally, *in vivo* polarized antigen specific Tfh cells had short CDR3α and CDR3β sequences [214]. The Tfh, Th17, and Th2 CDR3 length data are consistent with the TCRs generated in *TdT* KO mice, which lack N-nucleotides and have short CDR3 sequences.

Th1 differentiation is favored by higher affinity TCRs [29], but was unaltered in TdT KO mice in all infection models tested. The explanation for this is unclear. However, the increase in Th17 and GC-Tfh cells, and decrease in Th2 cells, is consistent with a repertoire enriched for higher affinity TCRs [29]. This is also supported by our data of increased PD-1 MFI and elevated LCMV gp66 tetramer binding strength in *TdT* KO T cells during chronic LCMV infection. Collectively, our data that T cells lacking N-region diversity may be enriched for higher avidity TCRs and are predisposed towards GC-Tfh differentiation. These findings may have uses in the clinical setting, specifically, for the selection and usage of T cell clones with short CDR3 sequences for anti-cancer therapy. Furthermore, vaccination strategies aimed at inducing GC-Tfh cells may benefit from targeting Vβ6^{+} T cells with short CDR3 sequences.

A recent study demonstrated that T cells with shorter CDR3β chains are enriched for during thymic selection and antigen-driven expansion [215]. This provides evidence that T cells with

TCRs bearing less N-nucleotides have a selective advantage and may be better adapted for and have higher reactivity for pMHC. In such a case, the addition of non-templated "random" nucleotides by TdT may generate TCRs less well-suited to bind pMHC. Interestingly, the CDR3β chain is primarily encoded by Dβ gene segments and N-nucleotides [216]. Therefore, it would be interesting to investigate whether *TdT* KO TCR sequences encode less hydrophobic amino acids in positions 6 and 7 of the CDR3β compared to germline sequences, as a potential mechanism of lowering TCR reactivity. While TdT-mediated nucleotide additions are non-templated, germline encoded TCRs may be evolutionarily optimized to generate TCRs with hydrophobic residues at these positions at higher frequencies. The evidence that the expression of TdT is tightly regulated in a temporal and spatial manner, across multiple species, implies that it has some kind of advantage for the host. However, a defect in pathogen control was only observed in T cell specific TdT KO mice during chronic LCMV infection. This is unlikely to be related to the increase in GC-Tfh differentiation, which is protective in LCMV. Further investigation with T cell-specific conditional TdT KO mice in infectious or autoimmune models driven by Th2 or Th17 responses, respectively, may reveal a rationale for the host to generate TdT-dependent TCRs.

Summary and Conclusions

Chapter 2: My aim was to determine whether vitamin D signaling was active in the thymus and investigate its potential roles in the process of central tolerance. I demonstrated that the Vdr and Cyp27b1 are expressed in both stromal and hematopoietic thymic cell types, and that vitamin D signaling is active in the thymus. I further found that 1,25D regulates the expression of the critical transcription factor Aire, and Aire-dependent TRA gene expression. Finally, we demonstrated that Aire interacts with the Vdr, and is a coactivator of Vdr-dependent gene transcription. These findings provide a potential mechanism by which Aire is recruited to DNA, and for the first time reveal a role for vitamin D signaling in thymic processes essential for central tolerance.

Chapter 3: Our aim was to investigate thymic development in the absence of 1,25D signaling. I found that *Cyp27b1* KO mice were lymphopenic, and that age-associated thymic involution was markedly accelerated. Aire$^+$ mTEC differentiation and TRA gene expression was impaired in KO mice, consistent with our previous findings that 1,25D augments Aire expression. We further investigated TEC phenotypes using scRNAseq and found that *Ccl21a*$^+$ mTECs were increased in KO mice at the expense of Aire$^+$ cells. RNA velocity analysis indicated that the Ccl21a$^+$ cells were not precursors of Aire$^+$ mTECs, suggesting that 1,25D regulates another precursor TEC population. Ingenuity pathway analysis revealed that *Cyp27b1* KO TECs have a gene signature associated with aging thymi. We found that the expression of various pro-thymic longevity factors was reduced in sorted KO TECs. Furthermore, fewer KO TECs were actively cycling, and there were fewer Ki67$^+$ TECs in KO thymi. Collectively, these data demonstrate that 1,25D regulates TEC development, notably of Aire$^+$ TECs, and slows age-related thymic involution.

Chapter 4: Here, I investigate whether T cell repertoire diversity impacts $CD4^+$ T cell differentiation using TdT deficient mice. I found that GC-Tfh responses were increased in TdT KO mice in response to genetically diverse pathogens in a TCR-intrinsic manner. The Vβ repertoire of responding T cells was altered in TdT KO mice, favoring T cells expressing TCRs with Vβ6 segments. CD5 expression in pre-selection KO thymocytes was significantly increased, supporting previous data that TdT KO TCRs may bind pMHC more efficiently. Furthermore, PD-1 expression was increased on non-GC-Tfh KO $CD4^+$ T cells and KO T cells had higher GP66 tetramer binding strength during persistent LCMV cl13 infection. Bone marrow chimera experiments restricting TdT deficiency to B or T cells, or both, demonstrated that there were both T cell- and B cell-intrinsic components to the increased GC-Tfh phenotype. Finally, viral loads were increased in T cell specific TdT deficient chimeras relative to wildtype or full KO chimeras, 30 days post infection with LCMV cl13. These data collectively show that the germline repertoire favors GC-Tfh differentiation, and that TCR diversification generated by TdT may serve to diversify effector T cell responses to infection.

References

1. Klimas, N., A.O. Koneru, and M.A. Fletcher. 2008. *Overview of HIV.* Psychosom Med. **70**(5): p. 523-30.
2. Fischer, A., L.D. Notarangelo, B. Neven, M. Cavazzana, and J.M. Puck. 2015. *Severe combined immunodeficiencies and related disorders.* Nat Rev Dis Primers. **1**: p. 15061.
3. Hossain, Z., A. Reza, W.A. Qasem, J.K. Friel, and A. Omri. 2022. *Development of the immune system in the human embryo.* Pediatr Res. **92**(4): p. 951-955.
4. Rieger, M.A. and T. Schroeder. 2012. *Hematopoiesis.* Cold Spring Harb Perspect Biol. **4**(12).
5. Pinho, S. and P.S. Frenette. 2019. *Haematopoietic stem cell activity and interactions with the niche.* Nat Rev Mol Cell Biol. **20**(5): p. 303-320.
6. Marshall, J.S., R. Warrington, W. Watson, and H.L. Kim. 2018. *An introduction to immunology and immunopathology.* Allergy Asthma Clin Immunol. **14**(Suppl 2): p. 49.
7. Schleimer, R.P., A. Kato, R. Kern, D. Kuperman, and P.C. Avila. 2007. *Epithelium: at the interface of innate and adaptive immune responses.* J Allergy Clin Immunol. **120**(6): p. 1279-84.
8. Italiani, P. and D. Boraschi. 2014. *From Monocytes to M1/M2 Macrophages: Phenotypical vs. Functional Differentiation.* Front Immunol. **5**: p. 514.
9. Vivier, E., D. Artis, M. Colonna, A. Diefenbach, J.P. Di Santo, G. Eberl, S. Koyasu, R.M. Locksley, A.N.J. McKenzie, R.E. Mebius, F. Powrie, and H. Spits. 2018. *Innate Lymphoid Cells: 10 Years On.* Cell. **174**(5): p. 1054-1066.
10. Ivashkiv, L.B. 2018. *IFNgamma: signalling, epigenetics and roles in immunity, metabolism, disease and cancer immunotherapy.* Nat Rev Immunol. **18**(9): p. 545-558.
11. Goswami, R. and A. Awasthi. 2020. *Editorial: T Cell Differentiation and Function in Tissue Inflammation.* Front Immunol. **11**: p. 289.
12. Mogensen, T.H. 2009. *Pathogen recognition and inflammatory signaling in innate immune defenses.* Clin Microbiol Rev. **22**(2): p. 240-73, Table of Contents.
13. Boparai, J.K. and P.K. Sharma. 2020. *Mini Review on Antimicrobial Peptides, Sources, Mechanism and Recent Applications.* Protein Pept Lett. **27**(1): p. 4-16.
14. Jung, Y., B. Kong, S. Moon, S.H. Yu, J. Chung, C. Ban, W.J. Chung, S.G. Kim, and D.H. Kweon. 2019. *Envelope-deforming antiviral peptide derived from influenza virus M2 protein.* Biochem Biophys Res Commun. **517**(3): p. 507-512.
15. Huan, Y., Q. Kong, H. Mou, and H. Yi. 2020. *Antimicrobial Peptides: Classification, Design, Application and Research Progress in Multiple Fields.* Front Microbiol. **11**: p. 582779.
16. Scott, M.G., D.J. Davidson, M.R. Gold, D. Bowdish, and R.E. Hancock. 2002. *The human antimicrobial peptide LL-37 is a multifunctional modulator of innate immune responses.* J Immunol. **169**(7): p. 3883-91.
17. Akira, S. and K. Takeda. 2004. *Toll-like receptor signalling.* Nat Rev Immunol. **4**(7): p. 499-511.
18. Kawai, T. and S. Akira. 2007. *Signaling to NF-kappaB by Toll-like receptors.* Trends Mol Med. **13**(11): p. 460-9.
19. Boraschi, D. 2022. *What Is IL-1 for? The Functions of Interleukin-1 Across Evolution.* Front Immunol. **13**: p. 872155.
20. Velazquez-Salinas, L., A. Verdugo-Rodriguez, L.L. Rodriguez, and M.V. Borca. 2019. *The Role of Interleukin 6 During Viral Infections.* Front Microbiol. **10**: p. 1057.
21. Pollard, A.J. and E.M. Bijker. 2021. *A guide to vaccinology: from basic principles to new developments.* Nat Rev Immunol. **21**(2): p. 83-100.
22. Cyster, J.G. and C.D.C. Allen. 2019. *B Cell Responses: Cell Interaction Dynamics and Decisions.* Cell. **177**(3): p. 524-540.

23. Surh, C.D. and J. Sprent. 2008. *Homeostasis of naive and memory T cells.* Immunity. **29**(6): p. 848-62.
24. Sheu, T.T. and B.L. Chiang. 2021. *Lymphopenia, Lymphopenia-Induced Proliferation, and Autoimmunity.* Int J Mol Sci. **22**(8).
25. Golubovskaya, V. and L. Wu. 2016. *Different Subsets of T Cells, Memory, Effector Functions, and CAR-T Immunotherapy.* Cancers (Basel). **8**(3).
26. Saravia, J., N.M. Chapman, and H. Chi. 2019. *Helper T cell differentiation.* Cell Mol Immunol. **16**(7): p. 634-643.
27. Zhu, J. 2018. *T Helper Cell Differentiation, Heterogeneity, and Plasticity.* Cold Spring Harb Perspect Biol. **10**(10).
28. Crotty, S. 2014. *T follicular helper cell differentiation, function, and roles in disease.* Immunity. **41**(4): p. 529-42.
29. Bhattacharyya, N.D. and C.G. Feng. 2020. *Regulation of T Helper Cell Fate by TCR Signal Strength.* Front Immunol. **11**: p. 624.
30. Hegazy, A.N., M. Peine, C. Helmstetter, I. Panse, A. Frohlich, A. Bergthaler, L. Flatz, D.D. Pinschewer, A. Radbruch, and M. Lohning. 2010. *Interferons direct Th2 cell reprogramming to generate a stable GATA-3(+)T-bet(+) cell subset with combined Th2 and Th1 cell functions.* Immunity. **32**(1): p. 116-28.
31. MacDonald, A.S., E.A. Patton, A.C. La Flamme, M.I. Araujo, C.R. Huxtable, B. Bauman, and E.J. Pearce. 2002. *Impaired Th2 development and increased mortality during Schistosoma mansoni infection in the absence of CD40/CD154 interaction.* J Immunol. **168**(9): p. 4643-9.
32. Oh, D.Y. and L. Fong. 2021. *Cytotoxic CD4(+) T cells in cancer: Expanding the immune effector toolbox.* Immunity. **54**(12): p. 2701-2711.
33. Rezk, S.A., B.N. Nathwani, X. Zhao, and L.M. Weiss. 2013. *Follicular dendritic cells: origin, function, and different disease-associated patterns.* Hum Pathol. **44**(6): p. 937-50.
34. Lucas, E.D. and B.A.J. Tamburini. 2019. *Lymph Node Lymphatic Endothelial Cell Expansion and Contraction and the Programming of the Immune Response.* Front Immunol. **10**: p. 36.
35. Bouillon, R., C. Marcocci, G. Carmeliet, D. Bikle, J.H. White, B. Dawson-Hughes, P. Lips, C.F. Munns, M. Lazaretti-Castro, A. Giustina, and J. Bilezikian. 2019. *Skeletal and Extraskeletal Actions of Vitamin D: Current Evidence and Outstanding Questions.* Endocr Rev. **40**(4): p. 1109-1151.
36. Ginde, A.A., P. Blatchford, K. Breese, L. Zarrabi, S.A. Linnebur, J.I. Wallace, and R.S. Schwartz. 2017. *High-Dose Monthly Vitamin D for Prevention of Acute Respiratory Infection in Older Long-Term Care Residents: A Randomized Clinical Trial.* J Am Geriatr Soc. **65**(3): p. 496-503.
37. Mailhot, G. and J.H. White. 2020. *Vitamin D and Immunity in Infants and Children.* Nutrients. **12**(5).
38. Cooper, J.D., D.J. Smyth, N.M. Walker, H. Stevens, O.S. Burren, C. Wallace, C. Greissl, E. Ramos-Lopez, E. Hypponen, D.B. Dunger, T.D. Spector, W.H. Ouwehand, T.J. Wang, K. Badenhoop, and J.A. Todd. 2011. *Inherited variation in vitamin D genes is associated with predisposition to autoimmune disease type 1 diabetes.* Diabetes. **60**(5): p. 1624-31.
39. Afzal, S., P. Brondum-Jacobsen, S.E. Bojesen, and B.G. Nordestgaard. 2014. *Vitamin D concentration, obesity, and risk of diabetes: a mendelian randomisation study.* Lancet Diabetes Endocrinol. **2**(4): p. 298-306.
40. Viatte, S., A. Yarwood, K. McAllister, S. Al-Mudhaffer, B. Fu, E. Flynn, D.P. Symmons, A. Young, and A. Barton. 2014. *The role of genetic polymorphisms regulating vitamin D levels in rheumatoid arthritis outcome: a Mendelian randomisation approach.* Ann Rheum Dis. **73**(7): p. 1430-3.

41. Mokry, L.E., S. Ross, O.S. Ahmad, V. Forgetta, G.D. Smith, D. Goltzman, A. Leong, C.M. Greenwood, G. Thanassoulis, and J.B. Richards. 2015. *Vitamin D and Risk of Multiple Sclerosis: A Mendelian Randomization Study.* PLoS Med. **12**(8): p. e1001866.
42. Rhead, B., M. Baarnhielm, M. Gianfrancesco, A. Mok, X. Shao, H. Quach, L. Shen, C. Schaefer, J. Link, A. Gyllenberg, A.K. Hedstrom, T. Olsson, J. Hillert, I. Kockum, M.M. Glymour, L. Alfredsson, and L.F. Barcellos. 2016. *Mendelian randomization shows a causal effect of low vitamin D on multiple sclerosis risk.* Neurol Genet. **2**(5): p. e97.
43. Christakos, S., P. Dhawan, A. Verstuyf, L. Verlinden, and G. Carmeliet. 2016. *Vitamin D: Metabolism, Molecular Mechanism of Action, and Pleiotropic Effects.* Physiol Rev. **96**(1): p. 365-408.
44. Ross, A.C. 2011. *The 2011 report on dietary reference intakes for calcium and vitamin D.* Public Health Nutr. **14**(5): p. 938-9.
45. Holick, M.F., N.C. Binkley, H.A. Bischoff-Ferrari, C.M. Gordon, D.A. Hanley, R.P. Heaney, M.H. Murad, C.M. Weaver, and S. Endocrine. 2011. *Evaluation, treatment, and prevention of vitamin D deficiency: an Endocrine Society clinical practice guideline.* J Clin Endocrinol Metab. **96**(7): p. 1911-30.
46. Calvo, M.S., S.J. Whiting, and C.N. Barton. 2004. *Vitamin D fortification in the United States and Canada: current status and data needs.* Am J Clin Nutr. **80**(6 Suppl): p. 1710S-6S.
47. Bikle, D.D., S. Patzek, and Y. Wang. 2018. *Physiologic and pathophysiologic roles of extra renal CYP27b1: Case report and review.* Bone Rep. **8**: p. 255-267.
48. Bikle, D. and S. Christakos. 2020. *New aspects of vitamin D metabolism and action - addressing the skin as source and target.* Nat Rev Endocrinol. **16**(4): p. 234-252.
49. Ismailova, A. and J.H. White. 2022. *Vitamin D, infections and immunity.* Rev Endocr Metab Disord. **23**(2): p. 265-277.
50. Adams, J.S. and M.A. Gacad. 1985. *Characterization of 1 alpha-hydroxylation of vitamin D3 sterols by cultured alveolar macrophages from patients with sarcoidosis.* J Exp Med. **161**(4): p. 755-65.
51. Burke, R.R., B.A. Rybicki, and D.S. Rao. 2010. *Calcium and vitamin D in sarcoidosis: how to assess and manage.* Semin Respir Crit Care Med. **31**(4): p. 474-84.
52. Wei, R. and S. Christakos. 2015. *Mechanisms Underlying the Regulation of Innate and Adaptive Immunity by Vitamin D.* Nutrients. **7**(10): p. 8251-60.
53. Lindner, J., S. Rausch, S. Treptow, K. Geldmeyer-Hilt, T. Krause, R. St-Arnaud, A. Arabian, A. Radbruch, S. Hartmann, M. Worm, and G. Heine. 2017. *Endogenous Calcitriol Synthesis Controls the Humoral IgE Response in Mice.* J Immunol. **199**(12): p. 3952-3958.
54. Verstuyf, A., G. Carmeliet, R. Bouillon, and C. Mathieu. 2010. *Vitamin D: a pleiotropic hormone.* Kidney Int. **78**(2): p. 140-5.
55. Shaffer, P.L. and D.T. Gewirth. 2002. *Structural basis of VDR-DNA interactions on direct repeat response elements.* EMBO J. **21**(9): p. 2242-52.
56. Klopot, A., K.W. Hance, S. Peleg, J. Barsony, and J.C. Fleet. 2007. *Nucleo-cytoplasmic cycling of the vitamin D receptor in the enterocyte-like cell line, Caco-2.* J Cell Biochem. **100**(3): p. 617-28.
57. Ekimoto, T., T. Kudo, T. Yamane, and M. Ikeguchi. 2021. *Mechanism of Vitamin D Receptor Ligand-Binding Domain Regulation Studied by gREST Simulations.* J Chem Inf Model. **61**(7): p. 3625-3637.
58. Willems, H.M., E.G. van den Heuvel, G. Carmeliet, A. Schaafsma, J. Klein-Nulend, and A.D. Bakker. 2012. *VDR dependent and independent effects of 1,25-dihydroxyvitamin D3 on nitric oxide production by osteoblasts.* Steroids. **77**(1-2): p. 126-31.
59. Demay, M.B., P.N. MacDonald, K. Skorija, D.R. Dowd, L. Cianferotti, and M. Cox. 2007. *Role of the vitamin D receptor in hair follicle biology.* J Steroid Biochem Mol Biol. **103**(3-5): p. 344-6.

60. Malloy, P.J. and D. Feldman. 2011. *The role of vitamin D receptor mutations in the development of alopecia.* Mol Cell Endocrinol. **347**(1-2): p. 90-6.
61. Bouillon, R., G. Carmeliet, L. Verlinden, E. van Etten, A. Verstuyf, H.F. Luderer, L. Lieben, C. Mathieu, and M. Demay. 2008. *Vitamin D and human health: lessons from vitamin D receptor null mice.* Endocr Rev. **29**(6): p. 726-76.
62. Miksza, K.F., F.M. Brenner, G.M. Andreola, and P.H. Sakiyama. 2017. *Alopecia in patients with vitamin D-resistant rickets type-II.* An Bras Dermatol. **92**(2): p. 286-287.
63. Thompson, C.C. 2009. *Hairless is a nuclear receptor corepressor essential for skin function.* Nucl Recept Signal. **7**: p. e010.
64. Bikle, D.D., H. Elalieh, S. Chang, Z. Xie, and J.P. Sundberg. 2006. *Development and progression of alopecia in the vitamin D receptor null mouse.* J Cell Physiol. **207**(2): p. 340-53.
65. Bikle, D.D. 2014. *Vitamin D metabolism, mechanism of action, and clinical applications.* Chem Biol. **21**(3): p. 319-29.
66. Cui, A., T. Zhang, P. Xiao, Z. Fan, H. Wang, and Y. Zhuang. 2023. *Global and regional prevalence of vitamin D deficiency in population-based studies from 2000 to 2022: A pooled analysis of 7.9 million participants.* Front Nutr. **10**: p. 1070808.
67. Webb, A.R., L. Kline, and M.F. Holick. 1988. *Influence of season and latitude on the cutaneous synthesis of vitamin D3: exposure to winter sunlight in Boston and Edmonton will not promote vitamin D3 synthesis in human skin.* J Clin Endocrinol Metab. **67**(2): p. 373-8.
68. Bach, J.F. 2018. *The hygiene hypothesis in autoimmunity: the role of pathogens and commensals.* Nat Rev Immunol. **18**(2): p. 105-120.
69. Munger, K.L., L.I. Levin, B.W. Hollis, N.S. Howard, and A. Ascherio. 2006. *Serum 25-hydroxyvitamin D levels and risk of multiple sclerosis.* JAMA. **296**(23): p. 2832-8.
70. Munger, K.L., J. Aivo, K. Hongell, M. Soilu-Hanninen, H.M. Surcel, and A. Ascherio. 2016. *Vitamin D Status During Pregnancy and Risk of Multiple Sclerosis in Offspring of Women in the Finnish Maternity Cohort.* JAMA Neurol. **73**(5): p. 515-9.
71. Mathieu, C., C. Gysemans, A. Giulietti, and R. Bouillon. 2005. *Vitamin D and diabetes.* Diabetologia. **48**(7): p. 1247-57.
72. Manousaki, D., T. Dudding, S. Haworth, Y.H. Hsu, C.T. Liu, C. Medina-Gomez, T. Voortman, N. van der Velde, H. Melhus, C. Robinson-Cohen, D.L. Cousminer, M. Nethander, L. Vandenput, R. Noordam, V. Forgetta, C.M.T. Greenwood, M.L. Biggs, B.M. Psaty, J.I. Rotter, B.S. Zemel, J.A. Mitchell, B. Taylor, M. Lorentzon, M. Karlsson, V.V.W. Jaddoe, H. Tiemeier, N. Campos-Obando, O.H. Franco, A.G. Utterlinden, L. Broer, N.M. van Schoor, A.C. Ham, M.A. Ikram, D. Karasik, R. de Mutsert, F.R. Rosendaal, M. den Heijer, T.J. Wang, L. Lind, E.S. Orwoll, D.O. Mook-Kanamori, K. Michaelsson, B. Kestenbaum, C. Ohlsson, D. Mellstrom, L. de Groot, S.F.A. Grant, D.P. Kiel, M.C. Zillikens, F. Rivadeneira, S. Sawcer, N.J. Timpson, and J.B. Richards. 2017. *Low-Frequency Synonymous Coding Variation in CYP2R1 Has Large Effects on Vitamin D Levels and Risk of Multiple Sclerosis.* Am J Hum Genet. **101**(2): p. 227-238.
73. Munger, K.L., L.I. Levin, J. Massa, R. Horst, T. Orban, and A. Ascherio. 2013. *Preclinical serum 25-hydroxyvitamin D levels and risk of type 1 diabetes in a cohort of US military personnel.* Am J Epidemiol. **177**(5): p. 411-9.
74. Hyppönen, E., E. Läärä, A. Reunanen, M.-R. Järvelin, and S.M. Virtanen. 2001. *Intake of vitamin D and risk of type 1 diabetes: a birth-cohort study.* The Lancet. **358**(9292): p. 1500-1503.
75. Vargas Buonfiglio, L.G., O.G. Vanegas Calderon, M. Cano, J.E. Simmering, P.M. Polgreen, J. Zabner, A.K. Gerke, and A.P. Comellas. 2020. *Seasonal Antimicrobial Activity of the Airway: Post-Hoc Analysis of a Randomized Placebo-Controlled Double-Blind Trial.* Nutrients. **12**(9).
76. Vargas Buonfiglio, L.G., M. Cano, A.A. Pezzulo, O.G. Vanegas Calderon, J. Zabner, A.K. Gerke, and A.P. Comellas. 2017. *Effect of vitamin D(3) on the antimicrobial activity of human airway surface*

liquid: preliminary results of a randomised placebo-controlled double-blind trial. BMJ Open Respir Res. **4**(1): p. e000211.
77. Gombart, A.F., N. Borregaard, and H.P. Koeffler. 2005. *Human cathelicidin antimicrobial peptide (CAMP) gene is a direct target of the vitamin D receptor and is strongly up-regulated in myeloid cells by 1,25-dihydroxyvitamin D3.* FASEB J. **19**(9): p. 1067-77.
78. Wang, T.T., F.P. Nestel, V. Bourdeau, Y. Nagai, Q. Wang, J. Liao, L. Tavera-Mendoza, R. Lin, J.W. Hanrahan, S. Mader, and J.H. White. 2004. *Cutting edge: 1,25-dihydroxyvitamin D3 is a direct inducer of antimicrobial peptide gene expression.* J Immunol. **173**(5): p. 2909-12.
79. Raftery, T., A.R. Martineau, C.L. Greiller, S. Ghosh, D. McNamara, K. Bennett, J. Meddings, and M. O'Sullivan. 2015. *Effects of vitamin D supplementation on intestinal permeability, cathelicidin and disease markers in Crohn's disease: Results from a randomised double-blind placebo-controlled study.* United European Gastroenterol J. **3**(3): p. 294-302.
80. Dimitrov, V. and J.H. White. 2016. *Species-specific regulation of innate immunity by vitamin D signaling.* J Steroid Biochem Mol Biol. **164**: p. 246-253.
81. Oberg, F., J. Botling, and K. Nilsson. 1993. *Functional antagonism between vitamin D3 and retinoic acid in the regulation of CD14 and CD23 expression during monocytic differentiation of U-937 cells.* J Immunol. **150**(8 Pt 1): p. 3487-95.
82. Wang, T.T., B. Dabbas, D. Laperriere, A.J. Bitton, H. Soualhine, L.E. Tavera-Mendoza, S. Dionne, M.J. Servant, A. Bitton, E.G. Seidman, S. Mader, M.A. Behr, and J.H. White. 2010. *Direct and indirect induction by 1,25-dihydroxyvitamin D3 of the NOD2/CARD15-defensin beta2 innate immune pathway defective in Crohn disease.* J Biol Chem. **285**(4): p. 2227-31.
83. Deretic, V. 2016. *Autophagy in leukocytes and other cells: mechanisms, subsystem organization, selectivity, and links to innate immunity.* J Leukoc Biol. **100**(5): p. 969-978.
84. Bhutia, S.K. 2022. *Vitamin D in autophagy signaling for health and diseases: Insights on potential mechanisms and future perspectives.* J Nutr Biochem. **99**: p. 108841.
85. Dimitrov, V., C. Barbier, A. Ismailova, Y. Wang, K. Dmowski, R. Salehi-Tabar, B. Memari, E. Groulx-Boivin, and J.H. White. 2021. *Vitamin D-regulated Gene Expression Profiles: Species-specificity and Cell-specific Effects on Metabolism and Immunity.* Endocrinology. **162**(2).
86. Verway, M., M. Bouttier, T.T. Wang, M. Carrier, M. Calderon, B.S. An, E. Devemy, F. McIntosh, M. Divangahi, M.A. Behr, and J.H. White. 2013. *Vitamin D induces interleukin-1beta expression: paracrine macrophage epithelial signaling controls M. tuberculosis infection.* PLoS Pathog. **9**(6): p. e1003407.
87. Khoo, A.L., L.Y. Chai, H.J. Koenen, M. Oosting, A. Steinmeyer, U. Zuegel, I. Joosten, M.G. Netea, and A.J. van der Ven. 2011. *Vitamin D(3) down-regulates proinflammatory cytokine response to Mycobacterium tuberculosis through pattern recognition receptors while inducing protective cathelicidin production.* Cytokine. **55**(2): p. 294-300.
88. Zhang, Y., D.Y. Leung, B.N. Richers, Y. Liu, L.K. Remigio, D.W. Riches, and E. Goleva. 2012. *Vitamin D inhibits monocyte/macrophage proinflammatory cytokine production by targeting MAPK phosphatase-1.* J Immunol. **188**(5): p. 2127-35.
89. Deniz, G., G. Erten, U.C. Kucuksezer, D. Kocacik, C. Karagiannidis, E. Aktas, C.A. Akdis, and M. Akdis. 2008. *Regulatory NK cells suppress antigen-specific T cell responses.* J Immunol. **180**(2): p. 850-7.
90. Adorini, L. and G. Penna. 2009. *Dendritic cell tolerogenicity: a key mechanism in immunomodulation by vitamin D receptor agonists.* Hum Immunol. **70**(5): p. 345-52.
91. E, L.B., A. Ismailova, S. Dimeloe, M. Hewison, and J.H. White. 2021. *Vitamin D and Immune Regulation: Antibacterial, Antiviral, Anti-Inflammatory.* JBMR Plus. **5**(1): p. e10405.

92. von Essen, M.R., M. Kongsbak, P. Schjerling, K. Olgaard, N. Odum, and C. Geisler. 2010. *Vitamin D controls T cell antigen receptor signaling and activation of human T cells.* Nat Immunol. **11**(4): p. 344-9.
93. Chen, J., D. Bruce, and M.T. Cantorna. 2014. *Vitamin D receptor expression controls proliferation of naive CD8+ T cells and development of CD8 mediated gastrointestinal inflammation.* BMC Immunol. **15**: p. 6.
94. Rigby, W.F., T. Stacy, and M.W. Fanger. 1984. *Inhibition of T lymphocyte mitogenesis by 1,25-dihydroxyvitamin D3 (calcitriol).* J Clin Invest. **74**(4): p. 1451-5.
95. Bener, A., M.S. Ehlayel, H.Z. Bener, and Q. Hamid. 2014. *The impact of Vitamin D deficiency on asthma, allergic rhinitis and wheezing in children: An emerging public health problem.* J Family Community Med. **21**(3): p. 154-61.
96. Heine, G., C. Tabeling, B. Hartmann, C.R. Gonzalez Calera, A.A. Kuhl, J. Lindner, A. Radbruch, M. Witzenrath, and M. Worm. 2014. *25-hydroxvitamin D3 promotes the long-term effect of specific immunotherapy in a murine allergy model.* J Immunol. **193**(3): p. 1017-23.
97. Bruce, D., S. Yu, J.H. Ooi, and M.T. Cantorna. 2011. *Converging pathways lead to overproduction of IL-17 in the absence of vitamin D signaling.* Int Immunol. **23**(8): p. 519-28.
98. Lemire, J.M. and D.C. Archer. 1991. *1,25-dihydroxyvitamin D3 prevents the in vivo induction of murine experimental autoimmune encephalomyelitis.* J Clin Invest. **87**(3): p. 1103-7.
99. Mayne, C.G., J.A. Spanier, L.M. Relland, C.B. Williams, and C.E. Hayes. 2011. *1,25-Dihydroxyvitamin D3 acts directly on the T lymphocyte vitamin D receptor to inhibit experimental autoimmune encephalomyelitis.* Eur J Immunol. **41**(3): p. 822-32.
100. Vidyarani, M., P. Selvaraj, M.S. Jawahar, and P.R. Narayanan. 2007. *1, 25 Dihydroxyvitamin D3 modulated cytokine response in pulmonary tuberculosis.* Cytokine. **40**(2): p. 128-34.
101. O'Kelly, J., J. Hisatake, Y. Hisatake, J. Bishop, A. Norman, and H.P. Koeffler. 2002. *Normal myelopoiesis but abnormal T lymphocyte responses in vitamin D receptor knockout mice.* J Clin Invest. **109**(8): p. 1091-9.
102. Cantorna, M.T., C.E. Hayes, and H.F. DeLuca. 1998. *1,25-Dihydroxycholecalciferol inhibits the progression of arthritis in murine models of human arthritis.* J Nutr. **128**(1): p. 68-72.
103. Watson, M.L., J.K. Rao, G.S. Gilkeson, P. Ruiz, E.M. Eicher, D.S. Pisetsky, A. Matsuzawa, J.M. Rochelle, and M.F. Seldin. 1992. *Genetic analysis of MRL-lpr mice: relationship of the Fas apoptosis gene to disease manifestations and renal disease-modifying loci.* J Exp Med. **176**(6): p. 1645-56.
104. Lemire, J.M., A. Ince, and M. Takashima. 1992. *1,25-Dihydroxyvitamin D3 attenuates the expression of experimental murine lupus of MRL/l mice.* Autoimmunity. **12**(2): p. 143-8.
105. Chen, Y.G., C.E. Mathews, and J.P. Driver. 2018. *The Role of NOD Mice in Type 1 Diabetes Research: Lessons from the Past and Recommendations for the Future.* Front Endocrinol (Lausanne). **9**: p. 51.
106. Mathieu, C., M. Waer, J. Laureys, O. Rutgeerts, and R. Bouillon. 1994. *Prevention of autoimmune diabetes in NOD mice by 1,25 dihydroxyvitamin D3.* Diabetologia. **37**(6): p. 552-8.
107. Giulietti, A., C. Gysemans, K. Stoffels, E. van Etten, B. Decallonne, L. Overbergh, R. Bouillon, and C. Mathieu. 2004. *Vitamin D deficiency in early life accelerates Type 1 diabetes in non-obese diabetic mice.* Diabetologia. **47**(3): p. 451-462.
108. Gysemans, C., E. van Etten, L. Overbergh, A. Giulietti, G. Eelen, M. Waer, A. Verstuyf, R. Bouillon, and C. Mathieu. 2008. *Unaltered diabetes presentation in NOD mice lacking the vitamin D receptor.* Diabetes. **57**(1): p. 269-75.
109. Wang, Y., D. He, C. Ni, H. Zhou, S. Wu, Z. Xue, and Z. Zhou. 2016. *Vitamin D induces autophagy of pancreatic beta-cells and enhances insulin secretion.* Mol Med Rep. **14**(3): p. 2644-50.

110. Romano, R., L. Palamaro, A. Fusco, G. Giardino, V. Gallo, L. Del Vecchio, and C. Pignata. 2013. *FOXN1: A Master Regulator Gene of Thymic Epithelial Development Program.* Front Immunol. **4**: p. 187.
111. Rothenberg, E.V. 2011. *T cell lineage commitment: identity and renunciation.* J Immunol. **186**(12): p. 6649-55.
112. Simpson, E. 1992. *Positive and negative selection of the T cell repertoire: role of MHC and other ligands.* Int Rev Immunol. **8**(4): p. 269-77.
113. Klein, L., B. Kyewski, P.M. Allen, and K.A. Hogquist. 2014. *Positive and negative selection of the T cell repertoire: what thymocytes see (and don't see).* Nat Rev Immunol. **14**(6): p. 377-91.
114. Shichkin, V.P. and M. Antica. 2022. *Key Factors for Thymic Function and Development.* Front Immunol. **13**: p. 926516.
115. Schatz, D.G. and Y. Ji. 2011. *Recombination centres and the orchestration of V(D)J recombination.* Nat Rev Immunol. **11**(4): p. 251-63.
116. Dupic, T., Q. Marcou, A.M. Walczak, and T. Mora. 2019. *Genesis of the alphabeta T-cell receptor.* PLoS Comput Biol. **15**(3): p. e1006874.
117. Roth, D.B. 2014. *V(D)J Recombination: Mechanism, Errors, and Fidelity.* Microbiol Spectr. **2**(6).
118. Motea, E.A. and A.J. Berdis. 2010. *Terminal deoxynucleotidyl transferase: the story of a misguided DNA polymerase.* Biochim Biophys Acta. **1804**(5): p. 1151-66.
119. Chang, H.H.Y., N.R. Pannunzio, N. Adachi, and M.R. Lieber. 2017. *Non-homologous DNA end joining and alternative pathways to double-strand break repair.* Nat Rev Mol Cell Biol. **18**(8): p. 495-506.
120. Cabaniols, J.P., N. Fazilleau, A. Casrouge, P. Kourilsky, and J.M. Kanellopoulos. 2001. *Most alpha/beta T cell receptor diversity is due to terminal deoxynucleotidyl transferase.* J Exp Med. **194**(9): p. 1385-90.
121. Dutta, A., B. Zhao, and P.E. Love. 2021. *New insights into TCR beta-selection.* Trends Immunol. **42**(8): p. 735-750.
122. Xing, Y., S.C. Jameson, and K.A. Hogquist. 2013. *Thymoproteasome subunit-beta5T generates peptide-MHC complexes specialized for positive selection.* Proc Natl Acad Sci U S A. **110**(17): p. 6979-84.
123. Karimi, M.M., Y. Guo, X. Cui, H.A. Pallikonda, V. Horkova, Y.F. Wang, S.R. Gil, G. Rodriguez-Esteban, I. Robles-Rebollo, L. Bruno, R. Georgieva, B. Patel, J. Elliott, M.H. Dore, D. Dauphars, M.S. Krangel, B. Lenhard, H. Heyn, A.G. Fisher, O. Stepanek, and M. Merkenschlager. 2021. *The order and logic of CD4 versus CD8 lineage choice and differentiation in mouse thymus.* Nat Commun. **12**(1): p. 99.
124. Klein, L., M. Hinterberger, G. Wirnsberger, and B. Kyewski. 2009. *Antigen presentation in the thymus for positive selection and central tolerance induction.* Nat Rev Immunol. **9**(12): p. 833-44.
125. Irla, M., G. Hollander, and W. Reith. 2010. *Control of central self-tolerance induction by autoreactive CD4+ thymocytes.* Trends Immunol. **31**(2): p. 71-9.
126. Hadeiba, H., K. Lahl, A. Edalati, C. Oderup, A. Habtezion, R. Pachynski, L. Nguyen, A. Ghodsi, S. Adler, and E.C. Butcher. 2012. *Plasmacytoid dendritic cells transport peripheral antigens to the thymus to promote central tolerance.* Immunity. **36**(3): p. 438-50.
127. Perniola, R. 2018. *Twenty Years of AIRE.* Front Immunol. **9**: p. 98.
128. Yamano, T., J. Nedjic, M. Hinterberger, M. Steinert, S. Koser, S. Pinto, N. Gerdes, E. Lutgens, N. Ishimaru, M. Busslinger, B. Brors, B. Kyewski, and L. Klein. 2015. *Thymic B Cells Are Licensed to Present Self Antigens for Central T Cell Tolerance Induction.* Immunity. **42**(6): p. 1048-61.
129. Ferre, E.M.N., M.M. Schmitt, and M.S. Lionakis. 2021. *Autoimmune Polyendocrinopathy-Candidiasis-Ectodermal Dystrophy.* Front Pediatr. **9**: p. 723532.

130. Ramsey, C., O. Winqvist, L. Puhakka, M. Halonen, A. Moro, O. Kampe, P. Eskelin, M. Pelto-Huikko, and L. Peltonen. 2002. *Aire deficient mice develop multiple features of APECED phenotype and show altered immune response.* Hum Mol Genet. **11**(4): p. 397-409.
131. Purohit, S., P.G. Kumar, M. Laloraya, and J.X. She. 2005. *Mapping DNA-binding domains of the autoimmune regulator protein.* Biochem Biophys Res Commun. **327**(3): p. 939-44.
132. Org, T., F. Chignola, C. Hetenyi, M. Gaetani, A. Rebane, I. Liiv, U. Maran, L. Mollica, M.J. Bottomley, G. Musco, and P. Peterson. 2008. *The autoimmune regulator PHD finger binds to non-methylated histone H3K4 to activate gene expression.* EMBO Rep. **9**(4): p. 370-6.
133. Mathis, D. and C. Benoist. 2009. *Aire.* Annu Rev Immunol. **27**: p. 287-312.
134. Derbinski, J., S. Pinto, S. Rosch, K. Hexel, and B. Kyewski. 2008. *Promiscuous gene expression patterns in single medullary thymic epithelial cells argue for a stochastic mechanism.* Proc Natl Acad Sci U S A. **105**(2): p. 657-62.
135. Villasenor, J., W. Besse, C. Benoist, and D. Mathis. 2008. *Ectopic expression of peripheral-tissue antigens in the thymic epithelium: probabilistic, monoallelic, misinitiated.* Proc Natl Acad Sci U S A. **105**(41): p. 15854-9.
136. Liston, A., D.H. Gray, S. Lesage, A.L. Fletcher, J. Wilson, K.E. Webster, H.S. Scott, R.L. Boyd, L. Peltonen, and C.C. Goodnow. 2004. *Gene dosage--limiting role of Aire in thymic expression, clonal deletion, and organ-specific autoimmunity.* J Exp Med. **200**(8): p. 1015-26.
137. Nagamine, K., P. Peterson, H.S. Scott, J. Kudoh, S. Minoshima, M. Heino, K.J. Krohn, M.D. Lalioti, P.E. Mullis, S.E. Antonarakis, K. Kawasaki, S. Asakawa, F. Ito, and N. Shimizu. 1997. *Positional cloning of the APECED gene.* Nat Genet. **17**(4): p. 393-8.
138. Lee, T.I. and R.A. Young. 2013. *Transcriptional regulation and its misregulation in disease.* Cell. **152**(6): p. 1237-51.
139. Abuhashem, A., V. Garg, and A.K. Hadjantonakis. 2022. *RNA polymerase II pausing in development: orchestrating transcription.* Open Biol. **12**(1): p. 210220.
140. Oven, I., N. Brdickova, J. Kohoutek, T. Vaupotic, M. Narat, and B.M. Peterlin. 2007. *AIRE recruits P-TEFb for transcriptional elongation of target genes in medullary thymic epithelial cells.* Mol Cell Biol. **27**(24): p. 8815-23.
141. Giraud, M., H. Yoshida, J. Abramson, P.B. Rahl, R.A. Young, D. Mathis, and C. Benoist. 2012. *Aire unleashes stalled RNA polymerase to induce ectopic gene expression in thymic epithelial cells.* Proc Natl Acad Sci U S A. **109**(2): p. 535-40.
142. Yoshida, H., K. Bansal, U. Schaefer, T. Chapman, I. Rioja, I. Proekt, M.S. Anderson, R.K. Prinjha, A. Tarakhovsky, C. Benoist, and D. Mathis. 2015. *Brd4 bridges the transcriptional regulators, Aire and P-TEFb, to promote elongation of peripheral-tissue antigen transcripts in thymic stromal cells.* Proc Natl Acad Sci U S A. **112**(32): p. E4448-57.
143. Gordon, J. and N.R. Manley. 2011. *Mechanisms of thymus organogenesis and morphogenesis.* Development. **138**(18): p. 3865-78.
144. Rodewald, H.R. 2008. *Thymus organogenesis.* Annu Rev Immunol. **26**: p. 355-88.
145. Gray, D.H., N. Seach, T. Ueno, M.K. Milton, A. Liston, A.M. Lew, C.C. Goodnow, and R.L. Boyd. 2006. *Developmental kinetics, turnover, and stimulatory capacity of thymic epithelial cells.* Blood. **108**(12): p. 3777-85.
146. Alawam, A.S., G. Anderson, and B. Lucas. 2020. *Generation and Regeneration of Thymic Epithelial Cells.* Front Immunol. **11**: p. 858.
147. Ohigashi, I., S. Zuklys, M. Sakata, C.E. Mayer, S. Zhanybekova, S. Murata, K. Tanaka, G.A. Hollander, and Y. Takahama. 2013. *Aire-expressing thymic medullary epithelial cells originate from beta5t-expressing progenitor cells.* Proc Natl Acad Sci U S A. **110**(24): p. 9885-90.

148. Lee, E.N., J.K. Park, J.R. Lee, S.O. Oh, S.Y. Baek, B.S. Kim, and S. Yoon. 2011. *Characterization of the expression of cytokeratins 5, 8, and 14 in mouse thymic epithelial cells during thymus regeneration following acute thymic involution.* Anat Cell Biol. **44**(1): p. 14-24.
149. Xing, Y. and K.A. Hogquist. 2014. *Isolation, identification, and purification of murine thymic epithelial cells.* J Vis Exp(90): p. e51780.
150. Zhu, M. and Y. Fu. 2010. *The complicated role of NF-kappaB in T-cell selection.* Cell Mol Immunol. **7**(2): p. 89-93.
151. Wells, K.L., C.N. Miller, A.R. Gschwind, W. Wei, J.D. Phipps, M.S. Anderson, and L.M. Steinmetz. 2020. *Combined transient ablation and single-cell RNA-sequencing reveals the development of medullary thymic epithelial cells.* Elife. **9**.
152. Dhalla, F., J. Baran-Gale, S. Maio, L. Chappell, G.A. Hollander, and C.P. Ponting. 2020. *Biologically indeterminate yet ordered promiscuous gene expression in single medullary thymic epithelial cells.* EMBO J. **39**(1): p. e101828.
153. Bornstein, C., S. Nevo, A. Giladi, N. Kadouri, M. Pouzolles, F. Gerbe, E. David, A. Machado, A. Chuprin, B. Toth, O. Goldberg, S. Itzkovitz, N. Taylor, P. Jay, V.S. Zimmermann, J. Abramson, and I. Amit. 2018. *Single-cell mapping of the thymic stroma identifies IL-25-producing tuft epithelial cells.* Nature. **559**(7715): p. 622-626.
154. Michelson, D.A., K. Hase, T. Kaisho, C. Benoist, and D. Mathis. 2022. *Thymic epithelial cells co-opt lineage-defining transcription factors to eliminate autoreactive T cells.* Cell. **185**(14): p. 2542-2558 e18.
155. Effros, R.B. 2004. *T cell replicative senescence: pleiotropic effects on human aging.* Ann N Y Acad Sci. **1019**: p. 123-6.
156. Liang, Z., X. Dong, Z. Zhang, Q. Zhang, and Y. Zhao. 2022. *Age-related thymic involution: Mechanisms and functional impact.* Aging Cell. **21**(8): p. e13671.
157. Gui, J., X. Zhu, J. Dohkan, L. Cheng, P.F. Barnes, and D.M. Su. 2007. *The aged thymus shows normal recruitment of lymphohematopoietic progenitors but has defects in thymic epithelial cells.* Int Immunol. **19**(10): p. 1201-11.
158. Mackall, C.L., J.A. Punt, P. Morgan, A.G. Farr, and R.E. Gress. 1998. *Thymic function in young/old chimeras: substantial thymic T cell regenerative capacity despite irreversible age-associated thymic involution.* Eur J Immunol. **28**(6): p. 1886-93.
159. Zhu, X., J. Gui, J. Dohkan, L. Cheng, P.F. Barnes, and D.M. Su. 2007. *Lymphohematopoietic progenitors do not have a synchronized defect with age-related thymic involution.* Aging Cell. **6**(5): p. 663-72.
160. Oh, J., W. Wang, R. Thomas, and D.M. Su. 2020. *Thymic rejuvenation via FOXN1-reprogrammed embryonic fibroblasts (FREFs) to counteract age-related inflammation.* JCI Insight. **5**(18).
161. Bousso, P., V. Wahn, I. Douagi, G. Horneff, C. Pannetier, F. Le Deist, F. Zepp, T. Niehues, P. Kourilsky, A. Fischer, and G. de Saint Basile. 2000. *Diversity, functionality, and stability of the T cell repertoire derived in vivo from a single human T cell precursor.* Proc Natl Acad Sci U S A. **97**(1): p. 274-8.
162. Nikolich-Zugich, J., M.K. Slifka, and I. Messaoudi. 2004. *The many important facets of T-cell repertoire diversity.* Nat Rev Immunol. **4**(2): p. 123-32.
163. Kikly, K. and G. Dennert. 1992. *Evidence for a role for T cell receptors (TCR) in the effector phase of acute bone marrow graft rejection. TCR V beta 5 transgenic mice lack effector cells able to cause graft rejection.* J Immunol. **149**(11): p. 3489-94.
164. Nanda, N.K., R. Apple, and E. Sercarz. 1991. *Limitations in plasticity of the T-cell receptor repertoire.* Proc Natl Acad Sci U S A. **88**(21): p. 9503-7.

165. Messaoudi, I., J.A. Guevara Patino, R. Dyall, J. LeMaoult, and J. Nikolich-Zugich. 2002. *Direct link between mhc polymorphism, T cell avidity, and diversity in immune defense.* Science. **298**(5599): p. 1797-800.
166. Wallace, M.E., R. Keating, W.R. Heath, and F.R. Carbone. 1999. *The cytotoxic T-cell response to herpes simplex virus type 1 infection of C57BL/6 mice is almost entirely directed against a single immunodominant determinant.* J Virol. **73**(9): p. 7619-26.
167. Gilfillan, S., M. Bachmann, S. Trembleau, L. Adorini, U. Kalinke, R. Zinkernagel, C. Benoist, and D. Mathis. 1995. *Efficient immune responses in mice lacking N-region diversity.* Eur J Immunol. **25**(11): p. 3115-22.
168. Haeryfar, S.M., H.D. Hickman, K.R. Irvine, D.C. Tscharke, J.R. Bennink, and J.W. Yewdell. 2008. *Terminal deoxynucleotidyl transferase establishes and broadens antiviral CD8+ T cell immunodominance hierarchies.* J Immunol. **181**(1): p. 649-59.
169. Gilfillan, S., C. Waltzinger, C. Benoist, and D. Mathis. 1994. *More efficient positive selection of thymocytes in mice lacking terminal deoxynucleotidyl transferase.* Int Immunol. **6**(11): p. 1681-6.
170. Virgin, H.W., E.J. Wherry, and R. Ahmed. 2009. *Redefining chronic viral infection.* Cell. **138**(1): p. 30-50.
171. Kassiotis, G., R. Zamoyska, and B. Stockinger. 2003. *Involvement of avidity for major histocompatibility complex in homeostasis of naive and memory T cells.* J Exp Med. **197**(8): p. 1007-16.
172. Vrisekoop, N., P. Artusa, J.P. Monteiro, and J.N. Mandl. 2017. *Weakly self-reactive T-cell clones can homeostatically expand when present at low numbers.* Eur J Immunol. **47**(1): p. 68-73.
173. Bucks, C.M., J.A. Norton, A.C. Boesteanu, Y.M. Mueller, and P.D. Katsikis. 2009. *Chronic antigen stimulation alone is sufficient to drive CD8+ T cell exhaustion.* J Immunol. **182**(11): p. 6697-708.
174. Xing, Y. and K.A. Hogquist. 2012. *T-cell tolerance: central and peripheral.* Cold Spring Harb Perspect Biol. **4**(6).
175. Reinhardt, T.A., R.L. Horst, J.W. Orf, and B.W. Hollis. 1984. *A microassay for 1,25-dihydroxyvitamin D not requiring high performance liquid chromatography: application to clinical studies.* J Clin Endocrinol Metab. **58**(1): p. 91-8.
176. Froicu, M., Y. Zhu, and M.T. Cantorna. 2006. *Vitamin D receptor is required to control gastrointestinal immunity in IL-10 knockout mice.* Immunology. **117**(3): p. 310-8.
177. Stumpf, W.E. and T.W. Downs. 1987. *Nuclear receptors for 1,25(OH)2 vitamin D3 in thymus reticular cells studied by autoradiography.* Histochemistry. **87**(4): p. 367-9.
178. Arora, J., J. Wang, V. Weaver, Y. Zhang, and M.T. Cantorna. 2022. *Novel insight into the role of the vitamin D receptor in the development and function of the immune system.* J Steroid Biochem Mol Biol. **219**: p. 106084.
179. Mathieu, C., E. Van Etten, C. Gysemans, B. Decallonne, S. Kato, J. Laureys, J. Depovere, D. Valckx, A. Verstuyf, and R. Bouillon. 2001. *In vitro and in vivo analysis of the immune system of vitamin D receptor knockout mice.* J Bone Miner Res. **16**(11): p. 2057-65.
180. Yu, S. and M.T. Cantorna. 2008. *The vitamin D receptor is required for iNKT cell development.* Proc Natl Acad Sci U S A. **105**(13): p. 5207-12.
181. Bruce, D. and M.T. Cantorna. 2011. *Intrinsic requirement for the vitamin D receptor in the development of CD8alphaalpha-expressing T cells.* J Immunol. **186**(5): p. 2819-25.
182. Passos, G.A., C.A. Speck-Hernandez, A.F. Assis, and D.A. Mendes-da-Cruz. 2018. *Update on Aire and thymic negative selection.* Immunology. **153**(1): p. 10-20.
183. Meredith, M., D. Zemmour, D. Mathis, and C. Benoist. 2015. *Aire controls gene expression in the thymic epithelium with ordered stochasticity.* Nat Immunol. **16**(9): p. 942-9.

184. St-Pierre, C., A. Trofimov, S. Brochu, S. Lemieux, and C. Perreault. 2015. *Differential Features of AIRE-Induced and AIRE-Independent Promiscuous Gene Expression in Thymic Epithelial Cells.* J Immunol. **195**(2): p. 498-506.
185. Koh, A.S., A.J. Kuo, S.Y. Park, P. Cheung, J. Abramson, D. Bua, D. Carney, S.E. Shoelson, O. Gozani, R.E. Kingston, C. Benoist, and D. Mathis. 2008. *Aire employs a histone-binding module to mediate immunological tolerance, linking chromatin regulation with organ-specific autoimmunity.* Proc Natl Acad Sci U S A. **105**(41): p. 15878-83.
186. Koh, A.S., R.E. Kingston, C. Benoist, and D. Mathis. 2010. *Global relevance of Aire binding to hypomethylated lysine-4 of histone-3.* Proc Natl Acad Sci U S A. **107**(29): p. 13016-21.
187. Waterfield, M., I.S. Khan, J.T. Cortez, U. Fan, T. Metzger, A. Greer, K. Fasano, M. Martinez-Llordella, J.L. Pollack, D.J. Erle, M. Su, and M.S. Anderson. 2014. *The transcriptional regulator Aire coopts the repressive ATF7ip-MBD1 complex for the induction of immunotolerance.* Nat Immunol. **15**(3): p. 258-65.
188. Patricio Artusa, M.-È.L., Camille Barbier, Babak Memari, Reyhaneh Salehi-Tabar, Sophia Karabatsos, Aiten Ismailova, Heather J. Melichar, John H. White. 2023. *Aire is a coactivator of the vitamin D receptor.* J. Immunol. **In press**.
189. Anderson, M.S., E.S. Venanzi, L. Klein, Z. Chen, S.P. Berzins, S.J. Turley, H. von Boehmer, R. Bronson, A. Dierich, C. Benoist, and D. Mathis. 2002. *Projection of an immunological self shadow within the thymus by the aire protein.* Science. **298**(5597): p. 1395-401.
190. Daley, S.R., D.Y. Hu, and C.C. Goodnow. 2013. *Helios marks strongly autoreactive CD4+ T cells in two major waves of thymic deletion distinguished by induction of PD-1 or NF-kappaB.* J Exp Med. **210**(2): p. 269-85.
191. McCarron, M.J., M. Irla, A. Serge, S.M. Soudja, and J.C. Marie. 2019. *Transforming Growth Factor-beta signaling in alphabeta thymocytes promotes negative selection.* Nat Commun. **10**(1): p. 5690.
192. Norman, A., *Vitamin D. Chemical, Biochemical and Clinical Update*. Vitamin D. Chemical, Biochemical and Clinical Update, ed. A.W. Norman, et al. 1985, Berlin, Boston: De Gruyter.
193. Sodora, D.L., D.C. Douek, G. Silvestri, L. Montgomery, M. Rosenzweig, T. Igarashi, B. Bernacky, R.P. Johnson, M.B. Feinberg, M.A. Martin, and R.A. Koup. 2000. *Quantification of thymic function by measuring T cell receptor excision circles within peripheral blood and lymphoid tissues in monkeys.* Eur J Immunol. **30**(4): p. 1145-53.
194. Lynch, H.E. and G.D. Sempowski. 2013. *Molecular measurement of T cell receptor excision circles.* Methods Mol Biol. **979**: p. 147-59.
195. Kong, Y.Y., H. Yoshida, I. Sarosi, H.L. Tan, E. Timms, C. Capparelli, S. Morony, A.J. Oliveira-dos-Santos, G. Van, A. Itie, W. Khoo, A. Wakeham, C.R. Dunstan, D.L. Lacey, T.W. Mak, W.J. Boyle, and J.M. Penninger. 1999. *OPGL is a key regulator of osteoclastogenesis, lymphocyte development and lymph-node organogenesis.* Nature. **397**(6717): p. 315-23.
196. Dougall, W.C., M. Glaccum, K. Charrier, K. Rohrbach, K. Brasel, T. De Smedt, E. Daro, J. Smith, M.E. Tometsko, C.R. Maliszewski, A. Armstrong, V. Shen, S. Bain, D. Cosman, D. Anderson, P.J. Morrissey, J.J. Peschon, and J. Schuh. 1999. *RANK is essential for osteoclast and lymph node development.* Genes Dev. **13**(18): p. 2412-24.
197. Perlot, T. and J.M. Penninger. 2012. *Development and function of murine B cells lacking RANK.* J Immunol. **188**(3): p. 1201-5.
198. Barragan, M., M. Good, and J.K. Kolls. 2015. *Regulation of Dendritic Cell Function by Vitamin D.* Nutrients. **7**(9): p. 8127-51.
199. Gallegos, A.M. and M.J. Bevan. 2004. *Central tolerance to tissue-specific antigens mediated by direct and indirect antigen presentation.* J Exp Med. **200**(8): p. 1039-49.

200. McCaughtry, T.M., T.A. Baldwin, M.S. Wilken, and K.A. Hogquist. 2008. *Clonal deletion of thymocytes can occur in the cortex with no involvement of the medulla.* J Exp Med. **205**(11): p. 2575-84.
201. Mandl, J.N., J.P. Monteiro, N. Vrisekoop, and R.N. Germain. 2013. *T cell-positive selection uses self-ligand binding strength to optimize repertoire recognition of foreign antigens.* Immunity. **38**(2): p. 263-274.
202. Fulton, R.B., S.E. Hamilton, Y. Xing, J.A. Best, A.W. Goldrath, K.A. Hogquist, and S.C. Jameson. 2015. *The TCR's sensitivity to self peptide-MHC dictates the ability of naive CD8(+) T cells to respond to foreign antigens.* Nat Immunol. **16**(1): p. 107-17.
203. Persaud, S.P., C.R. Parker, W.L. Lo, K.S. Weber, and P.M. Allen. 2014. *Intrinsic CD4+ T cell sensitivity and response to a pathogen are set and sustained by avidity for thymic and peripheral complexes of self peptide and MHC.* Nat Immunol. **15**(3): p. 266-74.
204. Dash, P., A.J. Fiore-Gartland, T. Hertz, G.C. Wang, S. Sharma, A. Souquette, J.C. Crawford, E.B. Clemens, T.H.O. Nguyen, K. Kedzierska, N.L. La Gruta, P. Bradley, and P.G. Thomas. 2017. *Quantifiable predictive features define epitope-specific T cell receptor repertoires.* Nature. **547**(7661): p. 89-93.
205. Glanville, J., H. Huang, A. Nau, O. Hatton, L.E. Wagar, F. Rubelt, X. Ji, A. Han, S.M. Krams, C. Pettus, N. Haas, C.S.L. Arlehamn, A. Sette, S.D. Boyd, T.J. Scriba, O.M. Martinez, and M.M. Davis. 2017. *Identifying specificity groups in the T cell receptor repertoire.* Nature. **547**(7661): p. 94-98.
206. Yang, J.C. and S.A. Rosenberg. 2016. *Adoptive T-Cell Therapy for Cancer.* Adv Immunol. **130**: p. 279-94.
207. Udyavar, A., R. Alli, P. Nguyen, L. Baker, and T.L. Geiger. 2009. *Subtle affinity-enhancing mutations in a myelin oligodendrocyte glycoprotein-specific TCR alter specificity and generate new self-reactivity.* J Immunol. **182**(7): p. 4439-47.
208. Campillo-Davo, D., D. Flumens, and E. Lion. 2020. *The Quest for the Best: How TCR Affinity, Avidity, and Functional Avidity Affect TCR-Engineered T-Cell Antitumor Responses.* Cells. **9**(7).
209. Alli, R., Z.M. Zhang, P. Nguyen, J.J. Zheng, and T.L. Geiger. 2011. *Rational design of T cell receptors with enhanced sensitivity for antigen.* PLoS One. **6**(3): p. e18027.
210. Mueller, S.N., W. Heath, J.D. McLain, F.R. Carbone, and C.M. Jones. 2002. *Characterization of two TCR transgenic mouse lines specific for herpes simplex virus.* Immunol Cell Biol. **80**(2): p. 156-63.
211. Stadinski, B.D., K. Shekhar, I. Gomez-Tourino, J. Jung, K. Sasaki, A.K. Sewell, M. Peakman, A.K. Chakraborty, and E.S. Huseby. 2016. *Hydrophobic CDR3 residues promote the development of self-reactive T cells.* Nat Immunol. **17**(8): p. 946-55.
212. Reynolds, C., D. Chong, E. Raynsford, K. Quigley, D. Kelly, J. Llewellyn-Hughes, D. Altmann, and R. Boyton. 2014. *Elongated TCR alpha chain CDR3 favors an altered CD4 cytokine profile.* BMC Biol. **12**: p. 32.
213. Boyton, R.J., N. Zaccai, E.Y. Jones, and D.M. Altmann. 2002. *CD4 T cells selected by antigen under Th2 polarizing conditions favor an elongated TCR alpha chain complementarity-determining region 3.* J Immunol. **168**(3): p. 1018-27.
214. Fazilleau, N., L.J. McHeyzer-Williams, H. Rosen, and M.G. McHeyzer-Williams. 2009. *The function of follicular helper T cells is regulated by the strength of T cell antigen receptor binding.* Nat Immunol. **10**(4): p. 375-84.
215. Hou, X., P. Zeng, X. Zhang, J. Chen, Y. Liang, J. Yang, Y. Yang, X. Liu, and H. Diao. 2019. *Shorter TCR beta-Chains Are Highly Enriched During Thymic Selection and Antigen-Driven Selection.* Front Immunol. **10**: p. 299.
216. Davis, M.M. and P.J. Bjorkman. 1988. *T-cell antigen receptor genes and T-cell recognition.* Nature. **334**(6181): p. 395-402.